The molecular role of Bicaudal-C in *Drosophila* oogenesis

Jarred Chicoine

Department of Biology

McGill University

Montréal, Québec, Canada

December 2006

A thesis submitted to the Faculty of Graduate Studies and Research in partial fulfillment of the requirements for the degree of Doctor of Philosophy

Your file Votre référence
ISBN: 978-0-494-32165-2
Our file Notre référence
ISBN: 978-0-494-32165-2

Abstract

Bicaudal-C (*Bic-C*) encodes a KH-type RNA binding protein required maternally for anterior patterning of the *Drosophila* oocyte and correct migration of the centripetal follicle cells. In *Drosophila*, premature translation of the germ-plasm determinant Oskar in *Bic-C* mutant oocytes suggests a function for Bic-C in post-transcriptional gene regulation.

Purification and microarray analysis of Bic-C containing ribonucleoprotein complexes revealed that Bic-C associates with multiple transcripts encoding functionally-related components of the Wnt/Frizzled/Dishevelled signaling pathway that regulate actin dynamics, in addition to its own mRNA. Using transgenic reporter constructs, Bic-C was demonstrated to destabilize its own mRNA via *cis*-acting 5' UTR elements. When auto-regulation was bypassed and Bic-C was over-expressed in the female germline, premature cytoplasmic streaming was induced, disrupting axial patterning through displacement of both Gurken (Grk) and *oskar*. These phenotypes can also be induced by disruption of the actin cytoskeleton with pharmacological agents and are similar to those described for hypomorphic mutant alleles of *orb*, which encodes a CPEB-like protein that promotes polyadenylation of target mRNAs. The Bic-C overexpression phenotypes require its RNA binding activity, are substantially enhanced by mutations affecting *orb* and *poly(A) polymerase*, and are suppressed by mutations affecting the deadenylase CCR4 and its accessory protein NOT3. Co-immunoprecipitation experiments demonstrate that Bic-C associates with components of the deadenylase complex and with components of an ER-associated RNP complex that includes Me31B, PABP and Trailer-

hitch. The latter complex is involved in Grk exocytosis. Accordingly, Grk secretion is defective in Bic-C mutants.

Taken together, these results support a model whereby Bic-C antagonizes Orb function by negatively regulating the expression of Orb target mRNAs, through recruitment of the deadenylase machinery, that are involved in coordinating cytoplasmic movements. Furthermore, this work identifies a novel function of Bic-C in dorsal/ventral patterning by promoting Grk secretion.

Résumé

Le gène *Bicaudal-C* (*Bic-C*) encode une protéine liant l'ARN de type KH. Chez la Drosophile, cette protéine doit être contribuée maternellement pour le modelage antérieur de l'oocyte ainsi que la migration des cellules folliculaires centripètes. La traduction prématurée du déterminant du plasma-germinale, Oskar, dans des oocytes mutants *Bic-C* suggère que Bic-C joue un rôle dans la régulation post-transcriptionelle de certains gènes.

L'analyse par puce d'ADN de complexes ribonucléoprotéiques purifiés contenant Bic-C nous a révélé que celle-ci était associée avec son propre ARN messager, ainsi qu'avec de multiples ARNms encodants des composantes d'une voie de signalisation apparenté à la voie Wnt/Frizzled/Dishevelled, régulant les dynamiques de l'actine. A l'aide de transgènes, nous avons démontré que Bic-C déstabilise son propre ARNm via des éléments présents dans la région non-traduite en 5'. Lorsque l'autorégulation fut contournée par la surexpression de Bic-C dans les cellules germinales femelles, le coulage cytoplasmique fut induit prématurément, perturbant le modelage axial en déplaçant Gurken (Grk) et *oskar*. Ces phénotypes peuvent aussi être induits en perturbant le cytosquelette d'actine avec des agents pharmacologiques, et sont similaires à ceux décrit pour l'allèle mutante hypomorphique d'*orb*, qui encode une protéine qui s'apparente à CPEB impliqué dans la polyadénylation d'ARNms. Les phénotypes de surexpression de Bic-C requières sa capacité de lier l'ARN, sont augmentés par des mutations affectant *orb* et *poly(A) polymerase* et sont supprimés par des mutations affectant la déadénylase CCR4 et sa protéine accessoire NOT3. Des expériences de co-immunoprécipitation démontrent que Bic-C est associée avec des composantes du

complexe de déadénylation et des composantes d'un complexe RNP associé au RE qui inclut Me31b, PABP et Trailer Hitch. Ce dernier complexe est impliqué dans l'exocytose de Grk et conséquemment, l'exocytose de Grk est défectueux dans les mutants de Bic-C.

Globalement, ces résultats soutiennent un modèle où Bic-C oppose la fonction d'Orb en contrecarrant l'expression des ARNms ciblé par Orb importants pour coordonner les déplacements cytoplasmique, en recrutant la machinerie de déadénylation. De plus, nous avons identifié un rôle nouveau de Bic-C dans la sécrétion de Grk lors du modelage dorsal/ventral.

Forward

The following statements have been included in accordance with thesis specifications outlined in "Guidelines for thesis preparation".

Candidates have the option of including part of the thesis, the text of a paper(s) submitted or to be submitted for publication, or the clearly duplicated text of a published paper(s). These texts must be bound as an integral part of the thesis.

If this option is chosen, connecting texts that provide logical bridges between the different papers are mandatory. The thesis must be written in such a way that it is more than a mere collection of manuscripts; in other words, results of a a series of papers must be integrated.

The thesis must still conform to all other requirements of the "Guidelines for Thesis Preparation". The thesis must include: A Table of Contents, an abstract in English and French, an introduction which clearly states the rationale and objectives of the study, a comprehensive review of the literature, a final conclusion and summary, and a thorough bibliography or reference list.

Additional material must be provided where appropriate (e.g. in appendices) and in sufficient detail to allow a clear and precise judgment to be made of the importance and originality of the research in the thesis.

In the case of manuscripts co-authored by the candidate and others, **the candidate is required to make explicit statement in the thesis as to who contributed to such work and to what extent.** Supervisors must attest to the accuracy of such statements at the doctoral defense. Since the task of the examiners is made more difficult in these cases, it is in the candidate's interest to make perfectly clear the responsibilities of all the authors and co-authors of the papers. **Under no circumstances can a co-author of such a thesis serve as an examiner of that thesis.**

Preface

The work presented in this thesis is my own, with the following exceptions:

Section 3, Chapter 1

The α-Myst Western blot was performed by Mathieu Miron, using samples that I had prepared.

Probe labeling, hybridization to Affymetrix™ microarrays and analysis were technical services provided by Dr. Robert Sladek at the McGill University and Genome Quebec Innovation Center, microarray platform.

Section 3, Chapter 5

The phosphoamino acid analysis of Bic-C was performed by Dr. Brian Raught, in the laboratory of Dr. Nahum Sonenberg, using protein that I labeled and purified.

The Bic-C rescue constructs (*Bic-C*^{WT} and *Bic-C*^{Y822F}) used to test Tyr822 functionality, were both generated by Dr. Ruben Khechumyan, in the laboratory of Dr. Paul Lasko.

Table of Contents

List of Figures and Tables

Section 3.1

Section 3.2

Section 3.3

Section 3.4

Section 3.5

Section 4

List of Abbreviations

Ago	Argonaute
A/P	anterior / posterior
ARE	AU-rich element
Arm	Armitage
Aub	Aubergine
β-Gal	beta-galatosidase
Bcd	Bicoid
Bic-C	Bicaudal-C
BRE	Bruno Response Elelments
Bru	Bruno
Cad	Caudal
Capu	Cappuccino
CCR4	Carbon Catabolite Repression 4
Cic	Capicua
Cni	Cornichon
CP18	Chorion Protein 18
CPEB	Cytoplasm Polyadenylation Element Binding Protein
CPSF	Cleavage and Polyadenylation Specificity Factor
DAAM	Dishevelled-Associated Activator of Morphogenesis
DAPI	4',6-Diamidino-2-phenylindole
DCP	Decapping Protein
Dgo	Diego
DNA	deoxyribonucleic acid
DPP	Decapentaplegic
DROK	*Drosophila* Rho-Associated Kinase
DTT	Dithiothrietol
D/V	dorsal / ventral
Dsh	Dishevelled
ECM	extracellular matrix
EDTA	Ethylenediaminetetraacetic acid
EGFR	Epidermal Growth Factor Receptor
eIF	eukaryotic Initiation Factor
Exu	Exuperantia
FBF	Fem-3 Binding Factor
FMR1	Fragile-X Mental Retardation 1
Ftz	Fushi Tarazu
Fz	Frizzled
GFP	Green Fluorescent Protein
GLD	Germline development Defective
Grk	Gurken
GST	Glutathione S-Transferase
Hb	Hunchback
Hrg	Hiiragi
IP	Immunoprecipitation

Kek	Kekkon
KH	hnRNP-K Homology
KHC	Kinesin Heavy Chain
MBP	Maltose Binding Protein
Me31b	Maternal Expression at 31b
miRNA	microRNA
Mirr	Mirror
Nos	Nanos
OreR	Oregon-R
Osk	Oskar
Otu	Ovarian Tumor
PABP	Poly(A) Binding Protein
PAN	Poly(A)-binding protein-dependent poly(A) riboNuclease
PARN	Poly(A)-Specific Nuclease
PCP	Planar Cell Polarity
PMSF	Phenylmethylsulfonyl fluoride
Pop2	PGK promoter directed OverProduction 2
PUF	Pumilio and FBF
Pum	Pumilio
RNA	Ribonucleic acid
RNP	Ribonucleoprotein
SAM	Sterile Alpha Motif
SH2	Src-Homolgy 2
Smg	Smaug
Spir	Spire
Spn-E	Spindle-E
Sqh	Spaghetti Squash
Stau	Staufen
Swa	Swallow
TGF	Transforming Growth Factor
TOR	Target of Rapamycin
Tral	Trailer Hitch
Tsc	Tuberous sclerosis
TTP	Tristetraprolin
UAS	Upstream Activating Sequence
UTR	Untranslated Region
Vas	Vasa
Wnt	Wingless and Int
YPS	Ypsilon Schachtel
ZBP	Zipcode Binding Protein

Acknowledgements

I am deeply grateful to my supervisor, Dr. Paul Lasko, for his guidance, support and patience throughout this seemingly unending process. His trust has granted me an exceptional degree of academic freedom, allowing me to develop a sense of independence and self-confidence as a researcher, while his generosity has granted me the opportunity to share my work and interact with the *Drosophila* research community at various conferences in North America and Europe. These rich experiences have reinforced my sense of purpose in research and have provided me with many treasured memories. Thanks Paul. Thanks also go to the members of my supervisory committee, Dr. Richard Roy and Dr. Nahum Sonenberg, for their time, advice and encouragement.

I would like to thank Ngan Nguey Lee, Beili Hu, Dr. Hong Han and Dr. Robert Sladek for excellent technical assistance, as well as Dr. Howard Lipshitz, Dr. Craig Smibert and Dr. Martine Simonelig for providing me with the *UASP-CCR4-HA*, *UASP-Pop2-HA*, *ccr4/twin* and *pap/hiragi* fly lines. Thanks also go to the Perrimon laboratory for *UASP-Grk* flies. I am grateful to Dr. David Dansereau, Travis Thomson and all of the members of the Lasko, Nilson and Schöck Laboratories (past and present) for useful discussions and advice. I would also like to thank Dr. Nahum Sonenberg for providing my first experience in research and the former members of his laboratory, Drs. Brian Raught, Anne-Claude Gingras, Mathieu Miron and especially Francis Poulin, for their patience and generosity of time while training me, and Colin Lister for his encyclopedic knowledge, which he is always willing to share. I am grateful to Lucia Caceres for

generating the *kekkon-lacZ* /grk^{HK} flies and for providing technical assistance with simultaneous *in situ* hybridization/immuno-fluorescence experiments.

I was supported in part by a graduate fellowship from the Fonds pour la Formation de Chercheurs et l'Aide a la Recherche (FCAR) and by McGill Major awards. This research was supported by an operating grant to Dr. Paul Lasko from the National Cancer Institute of Canada with funds from the Canadian Cancer Society.

Without the support of my wife, Dominique Anzellotti, I may not have had the will (or organizational skills) to achieve what I have. Her support has, and continues to be a vital component of any success I dare to claim. I thank my family and friends for enriching my life and helping me to maintain perspective at difficult times. Finally, I thank my mother, whose unwavering faith in me has provided the most precious gift anyone can receive, a belief in oneself. This work is dedicated to her memory.

Section 1: Literature Review

1.1 Overview

The fundamental goal of developmental biology is to understand the molecular processes that transform a single cell into a highly complex and integrated multi-cellular organism. The entire genetic blueprint of any multi-cellular organism is contained within a single nucleus at some point during its development. This blueprint, stored as DNA, must be duplicated, transcribed into a more dynamic form (RNA) and ultimately translated into proteins, which perform an incredibly diverse array of functions. The general questions put forth in developmental biology are not new. However, recent advances in molecular biology and biochemical techniques have allowed us to address many of these questions in greater detail than ever before but as the limits of our knowledge recede, more questions inevitably surface.

Model organisms, such as the common fruit fly *Drosophila melanogaster*, have been instrumental in our study of development. The historical evolution of life on this planet tells us that all organisms are fundamentally connected. Although humans may look very different from a mouse or a fly, many of the molecules and processes that underlie our development are similar. Research on *Drosophila* has greatly advanced our understanding of the genetic pathways that shape life on a cellular and organismal level and have provided much of the ground work responsible for our current understanding of human diseases at the molecular level.

Drosophila oogenesis has been a particularly fertile (pun intended) area of research. Through the study of mutants affecting axial patterning in the oocyte and early

embryo, a great deal of information regarding post-transcriptional control of gene expression and intercellular signaling has been gathered. Dynamic control of mRNA localization, stability and translation are all employed to specify both the anterior/posterior (A/P) and dorsal/ventral (D/V) axes.

The following literature review will summarize some of the post-transcriptional control mechanisms that govern mRNA translation and stability during metazoan development. It will also provide a general description of *Drosophila* oogenesis, the mechanisms that establish axial patterning and the key genes that regulate these processes. A synopsis of the literature regarding *Bicaudal-C*, the subject of this thesis, is also presented along with a description of the *Bicaudal-C* homologues that have been studied in other model organisms. Finally, a brief summary of the KH domain and how it functions in some extensively studied RNA-binding proteins is included.

1.2 Post-transcriptional gene regulation in development

1.2.1 Closed-loop model of translation

As initiation is the rate limiting step of translation, many forms of translational control have evolved that target this process. All eukaryotic mRNAs transcribed in the nucleus possess a 5' cap structure consisting of a methylated guanosine (m^7GpppN, where N is any nucleotide). The cap structure is important for a number of aspects of mRNA metabolism including translation initiation. The initiation factor eIF4E binds to the 5' cap, where it recruits the 40S ribosomal subunit via an interaction with eIF4G (Gingras et al., 1999). eIF4G does this through an interaction with eIF3, which binds directly to the 40S ribosomal subunit (Hinton et al., 2006). eIF4G also binds the RNA

helicase eIF4A, that, together with eIF4B, is believed to unwind secondary structure in the 5' UTR (Hinton et al., 2006). This enables binding and progression of the 40S ribosomal subunit along the mRNA until it encounters the first AUG start codon. The complex of eIF4E, eIF4G and eIF4A is collectively referred to as eIF4F. Another important function of eIF4G stems from its interaction with the poly(A) binding protein (PABP) (Tarun and Sachs, 1996; Imataka et al., 1998). As its name implies, PABP binds to the poly(A) tail present at the 3' end of most eukaryotic mRNAs. The interaction between eIF4G and PABP links the 5' cap structure to the 3' end, causing transcripts to circularize. Transcript circularization, which has been visualized by electron microscopy (Christensen et al., 1987), results in a synergistic enhancement of translational efficiency (Gallie, 1991; Iizuka et al., 1994). The exact mechanism underlying this enhancement is unclear but it may involve stabilization of the eIF4F complex on the 5' cap by PABP, or, as evidence in yeast suggests, PABP may promote joining of the 60S ribosomal subunit (Wei et al., 1998; Searfoss et al., 2001). Transcript circularization may also promote ribosomal "recycling" by guiding terminating ribosomes back to the 5' end of a transcript. Since transcript circularization requires that an mRNA be full-length, a selective advantage may be gained through this mechanism by discouraging the formation of truncated proteins that may produce dominant negative effects.

1.2.2 CPEB and cytoplasmic polyadenylation

Developmental regulation of poly(A) tail length provides an effective means of controlling the stability and translatability of specific mRNAs. This form of control is particularly crucial during oogenesis and early embryogenesis when, due to

transcriptional quiescence, many developmental events are orchestrated by the products of maternally inherited mRNAs. Our picture of developmentally regulated polyadenylation has largely been constructed by studies in *Xenopus* oocytes, where the Cytoplasmic Polyadenylation Element Binding protein (CPEB) controls the temporal expression of key maternal determinants through a combination of mRNA silencing and poly(A)-mediated activation (Mendez and Richter, 2001). Cytoplasmic polyadenylation requires two distinct 3'UTR sequence elements; the cytoplasmic polyadenylation element (CPE; UUUUUAU) that is bound by CPEB, and the AAUAAA hexanucleotide which is usually found 20-30 nucleotides downstream of the CPE (Mendez and Richter, 2001). These sequences can vary slightly from their canonical forms. Also, the relative position of these elements, copy number of the CPE, and neighbouring 3'UTR sequences are all variables that influence the regulation of a given transcript. CPEB can repress translation of some CPE containing mRNAs through an interaction with Maskin, which binds simultaneously to eIF4E and CPEB, preventing eIF4F assembly through competitive inhibition of eIF4G binding to eIF4E (de Moor and Richter, 1999). Before *Xenopus* oocytes can be fertilized, a process known as oocyte maturation must be initiated by exposure to progesterone. This leads to CPEB phosphorylation by Eg2, a member of the Aurora family of serine/threonine kinases. CPEB phosphorylation increases its affinity for the Cleavage and Polyadenylation Specificity Factor (CPSF) (Mendez et al., 2000b). CPSF binds to the AAUAAA element and in turn recruits a poly(A) polymerase, thereby promoting polyadenylation and consequently translation of target transcripts such as *c-mos* and *cyclin B* (Mendez et al., 2000a). This form of post-transcriptional regulation is not unique to *Xenopus*, as the mammalian homologue of CPEB performs similar

functions in mouse oocytes (Hodgman et al., 2001). Furthermore, a growing body of evidence indicates that regulated polyadenylation is not limited to early development, as synaptic plasticity and long-term memory have been linked to mammalian CPEB function in neurons (Wu et al., 1998; Huang et al., 2002).

1.2.3 mRNA deadenylation and degradation

In addition to its role in modulating the rate of translation of its cognate mRNA, the poly(A) tail plays a critical role in the control of mRNA stability, as its removal is a prerequisite for all general forms of mRNA degradation. Three distinct deadenylase complexes have been identified in eukaryotes. The CCR4/Pop2/NOT complex appears to be the predominant deadenylase complex in most eukaryotes (Parker and Song, 2004). Another complex consisting of the conserved proteins Pan2p/Pan3p (PAN) can serve as the predominant deadenylase complex in yeast when the CCR4/Pop2/NOT complex is inactivated by mutation (Parker and Song, 2004), although the initial shortening of poly(A) tails during mRNA maturation appears to be the primary function of the PAN complex (Uchida et al., 2004). Finally, the poly(A)-specific nuclease (PARN) is required for default deadenylation in *Xenopus* (Korner et al., 1998) and has also been implicated in nonsense-mediated decay in mammals (Lejeune et al., 2003). However, these functions may be limited to vertebrates, as PARN is not present in the genomes of *S. cerevisiae* and *D. melanogaster* (Parker and Song, 2004).

Once the poly(A) tail is shortened below a critical threshold, mRNAs can be degraded by one of two general decay pathways. The first consists of 3'-5' degradation by a large multi-protein complex called the exosome (Parker and Song, 2004). The

second pathway involves removal of the 5' cap structure by DCP1/DCP2 and subsequent 5'-3' digestion by the exonuclease XRN1 (known as PacMan in *D. melanogaster*). In yeast, this pathway degrades mRNA 2-5 fold faster than via the exosome, however, the predominant pathway is still unclear (Decker and Parker, 2002). It is likely that the interplay between *cis*-acting sequence elements and *trans*-acting factors governs the movement of individual transcripts into a given pathway. The exosome appears to be active throughout the cytoplasm, whereas the decapping and 5'-3' degradation factors are concentrated in discrete cytoplasmic foci called P bodies (Cougot et al., 2004).

1.2.4 P bodies

A major advance in our understanding of mRNA metabolism has come with the recent discovery that mRNA storage and decay occur in cytoplasmic RNP (ribonucleoprotein) granules called processing bodies (P bodies). P bodies are uniform spheroid particles that have been largely conserved from yeast to humans in both protein content and function (Cougot et al., 2004). These structures are defined by the absence of ribosomes and translation factors (with the exception of eIF4E) and the presence of several proteins involved in mRNA degradation (Anderson and Kedersha, 2006). These include the decapping factors DCP1 and DCP2, the 5'-3' exonuclease XRN1, the deadenylase CCR4 and the DEAD-box RNA helicase RCK/p54 (also known as Me31B in *Drosophila* and Dhh1p in yeast) (Anderson and Kedersha, 2006).

P bodies were initially considered as sites of mRNA decay, however recent evidence in yeast suggests that intact mRNAs can exit these structures and reinitiate translation (Brengues et al., 2005). In metazoans, several lines of evidence have

implicated P bodies in RNA silencing and degradation by miRNAs (Liu et al., 2005a; Behm-Ansmant et al., 2006). miRNAs are short (~21-23 nucleotides) noncoding single-stranded RNA molecules that mitigate translational repression when bound to target mRNAs with partial complementarity, or degradation when bound to targets with complete complementarity (Ambros, 2004). miRNA function is mediated by the Argonaute family of proteins that localize to mammalian P bodies in an miRNA dependent manner and physically interact with the P body components DCP1 and GW182 (Liu et al., 2005a; Behm-Ansmant et al., 2006). Furthermore, specific mRNAs have been shown to accumulate in P bodies when targeted by miRNAs (Liu et al., 2005b). GW182 is required for silencing and/or degradation of targeted mRNAs, while the activities of the CCR4/NOT deadenylase complex and the decapping factors DCP1/2 are only required for degradation (Behm-Ansmant et al., 2006).

One class of mRNAs that appear to be targeted to P bodies by miRNAs are those bearing AU-rich elements (AREs) in their 3' UTRs. AREs are found in a variety of short-lived mRNAs, such as those encoding proto-oncogenes or cytokines (van Hoof and Parker, 2002). Several ARE-binding proteins, including tristetraprolin (TTP), have been implicated in ARE-mediated mRNA degradation. This process was believed to occur primarily via 3'-5' degradation in the bulk cytoplasm by the exosome, however recent evidence suggests that 5'-3' degradation by XRN1 in P bodies may play a more significant role in this process (Stoecklin et al., 2006). TTP, which mediates ARE-dependent degradation of *TNF-α* mRNA and of its own transcript, localizes to P bodies where it physically interacts with the Argonaute family members Ago1 and Ago2 (Brooks et al., 2004; Jing et al., 2005). In addition to these proteins, ARE-mediated

degradation requires the activities of Dicer, which is involved in miRNA processing, and miRNAs that display complementarity to the AU-instability element (Jing et al., 2005). Such miRNAs have been identified in humans (miR16) and *Drosophila* (miR289) (Jing et al., 2005).

1.3 An introduction to *Drosophila* oogenesis

Drosophila oogenesis begins in a structure called the germarium, where the asymmetric division a stem cell produces another stem cell and a committed cystoblast. The cystoblast then undergoes four rounds of mitotic division with incomplete cytokinesis, producing a cyst of 16 interconnected cells. Before exiting the germarium, this cyst of germline cells will become encapsulated by a layer of somatically-derived follicle cells, producing a mature egg chamber. Oogenesis has been divided into 14 stages, based on the morphological characteristics of the egg chamber (King, 1970). One of the germline cells in the cyst migrates to the posterior of the egg chamber and becomes the oocyte, while the remaining 15 cells of the cyst adopt a supportive role as nurse cells.

The nurse cells produce most, if not all, of the RNAs and proteins required by the oocyte. These molecules are transferred to the oocyte through a series of cytoplasmic bridges called ring canals. From stages 1-7, transport into the oocyte is selective and dependent upon a polarized microtubule cytoskeleton (Theurkauf, 1994a). During these stages, microtubules emanate from a microtubule organizing center (MTOC) located near the posterior cortex of the oocyte. The plus-ends of these microtubules extend into the nurse cells through the ring canals, providing a means to transport specific mRNAs into the oocyte (Theurkauf, 1994a). At stage 6/7, a series of signaling events between the

oocyte and posterior-most follicle cells result in disassembly of the MTOC. The microtubule cytoskeleton then reorganizes into a gradient with highest concentrations of microtubules at the anterior cortex of the oocyte. Since the plus-end directed motor protein kinesin-1 transiently accumulates at the posterior cortex during stages 9-10 (Clark et al., 1994), it was believed that microtubule polarization was aligned with the A/P axis, such that their plus-ends extended towards the posterior of the oocyte. However, recent evidence suggests that microtubule plus-ends extend into the cytoplasm towards the center of the oocyte, driving Kinesin-1 and associated cargoes away from the cortex. (Cha et al., 2002). These complexes are believed to accumulate at the posterior by default, because this region of the cortex is relatively devoid of microtubules. This highly regulated cytoskeletal architecture permits posterior accumulation of the pole plasm, a specialized form of cytoplasm that ultimately directs abdomen and pole cell (i.e. germ cell) formation in the early embryo.

After stage 10, the microtubule cytoskeleton is uniformly concentrated around the entire oocyte cortex, while rapid cytoplasmic streaming mixes oocyte cytoplasm with incoming nurse cell cytoplasm during bulk cytoplasmic transfer (Theurkauf, 1994a). At the onset of embryogenesis, nuclear divisions take place without any corresponding cytoplasmic division, generating a multinucleate syncytial blastoderm. It is at this stage that opposing gradients of anterior and posterior morphogens establish the A/P axis and extra-cellular signaling initiates graded uptake of a transcription factor along the perpendicular axis to initiate embryonic D/V patterning.

1.3.1 Axis formation in *Drosophila* oogenesis

The dorsal/ventral and anterior/posterior axes of the oocyte and early embryo are initially established through the activities of the TGF-α homologue Gurken (Grk) and the pole plasm determinant Oskar (Osk) (Gonzalez-Reyes et al., 1995; Roth et al., 1995). During oogenesis, *osk* and *grk* mRNAs are localized to distinct regions of the oocyte cytoplasm in a microtubule-dependent manner, and their localization is dynamic, highly regulated, and essential for their developmental functions. Translation from both of these mRNAs is also under complex regulation (Wilhelm and Smibert, 2005).

1.3.2 Oskar

Oskar (Osk) is the key determinant in both pole plasm assembly and posterior somatic patterning as it is the first component of the pole plasm to become localized and because Osk can catalyze the assembly of functional pole plasm at ectopic sites (Kim-Ha et al., 1991; Ephrussi and Lehmann, 1992). Thus, translational repression of *osk* prior to posterior localization is essential. *osk* mRNA begins accumulating in the oocyte shortly after egg chamber formation. During the cytoskeletal rearrangements at stage 7, *osk* transiently accumulates at the anterior cortex of the oocyte before re-localizing to the posterior cortex from stage 8 onward. Upon posterior localization, *osk* is derepressed through a functional interaction between its 5' and 3' UTRs (Gunkel et al., 1998) and translation is activated by several factors including the double-stranded RNA-binding protein Staufen, the CPEB-like protein Orb, the DEAD-box RNA helicase Vasa and the eIF2C-related protein Aubergine (Micklem et al., 2000; Chang et al., 1999; Markussen et al., 1997; Harris and Macdonald, 2001). The exact mechanism governing this process is

unclear but it is believed to involve lengthening of the *osk* poly(A) tail by Orb (Castagnetti and Ephrussi, 2003). Once translated, phosphorylation by the Par-1 kinase stabilizes Osk protein (Riechmann et al., 2002), which is anchored to the posterior cortex through an actin-dependent mechanism (Erdelyi et al., 1995; Jankovics et al., 2002). *osk* mRNA is in turn anchored to the posterior cortex by Osk protein (Ephrussi et al., 1991; Kim-Ha et al., 1991).

Several observations suggest that translational repression of *osk* may be mediated by miRNA(s) and components of the RNAi machinery during stages 1-6. In mutants of *armitage (armi),* which encodes a putative RNA helicase that is related to the Silencing Defective 3 protein of Arabidopsis (Dalmay et al., 2001), Osk protein accumulates prematurely (Cook et al., 2004). Premature translation of Osk also occurs in mutants of *aubergine* (*aub*) and *spindle-E* (*spn-E*), which are required for RNAi in the embryo, and *maelstrom,* which is required for proper localization of the RNAi factors Dicer and Argonaute 2 (Cook et al., 2004; Kennerdell et al., 2002; Findley et al., 2003). This mechanism is consistent with the recent finding that translationally repressed *osk* mRNA is associated with polysomes (Braat et al., 2004), given that miRNA mediated silencing has been shown to block translation elongation but not initiation (Olsen and Ambros, 1999).

During stages 6-10, translational repression of un-localized *osk* occurs through an alternate mechanism involving interactions between factors bound to the 5' and 3' UTRs. The RRM-type RNA binding protein Bruno (Bru) binds directly to several *cis*-elements in the *osk* 3' UTR termed Bruno Response Elements (BREs) and represses Osk translation (Kim-Ha et al., 1995; Webster et al., 1997). Bruno has been shown to recruit

a 4E-T related protein called Cup to the mRNP complex where it simultaneously interacts with cap-bound eIF4E and Bruno, preventing assembly of the translation initiation machinery (Nakamura et al., 2004). This model is attractive because it explains how Bruno, bound to the 3' UTR, can influence events at the 5' end of *osk,* and how Cup can be recruited to bind eIF4E on a specific transcript. Bruno may also repress *osk* through another mechanism, as recent evidence indicates that Bruno can direct the assembly of *osk* mRNA into multimeric RNP particles, resembling P bodies, that render *osk* inaccessible to the translational machinery (Chekulaeva et al., 2006). Several other factors contribute to translational repression of *osk*, including Apontic, Hrp48, YPS and Bicaudal-C but the exact mechanisms by which these proteins suppress Osk production are still unclear (Lie and Macdonald, 1999; Yano et al., 2004; Mansfield et al., 2002; Saffman et al., 1998). Exactly how *osk* regulation is transferred from the early stage (1-6) to the late (stage 6-10) regulatory complexes is also an open question, however this remodeling may involve the RNA helicase Me31B. Me31B remains associated with *osk* during its transport from the nurse cells to the posterior cortex and forms an RNase sensitive complex with Cup, eIF4E and Bruno. Furthermore, Me31B is required for translational repression of *osk* during stage 6, when the mechanism of *osk* regulation is presumably being transferred (Nakamura et al., 2001; Nakamura et al., 2004).

A myriad of genes have been implicated in *osk* mRNA localization based on their mutant phenotypes but most of these mutants alter *osk* distribution through indirect effects on oocyte polarity. However, Staufen is directly involved in localizing *osk* to the posterior cortex, in addition to its role as a translational activator (St Johnston et al., 1991; Micklem et al., 2000). This dual role of Staufen may provide an additional

mechanism to prevent un-localized *osk* from being translated. *osk* localization is also linked to processing events in the nucleus, as Mago Nashi and Tsunagi, components of the exon-junction complex, remain associated with *osk* after nuclear export and are required for its posterior accumulation (Hachet and Ephrussi, 2001; Mohr et al., 2001). The first direct evidence linking translational repression of *osk* to its posterior localization was provided when Cup was shown to recruit Barentsz to the *osk* mRNP complex (Wilhelm et al., 2003). Barentsz is required for posterior accumulation of *osk*, presumably by coupling *osk* to the plus-end directed motor Kinesin-1, which is also required for *osk* localization (van Eeden et al., 2001; Brendza et al., 2000).

1.3.3 Me31B

Me31B (maternal expression at 31B) encodes a DDX6-like DEAD-box ATP-dependent RNA helicase (de Valoir et al., 1991). Homologues of Me31B have been identified in *S. cerevisiae* (Dhh1), *C. elegans* (CGH-1), *X. laevis* (Xp54) and mammals (RCK/p54), where they all associate with mRNA in various classes of mRNP particles and contribute to translational silencing of stored mRNAs (Weston and Sommerville, 2006).

In *Xenopus*, Xp54 physically interacts with CPEB and acts as a translational repressor of stored maternal mRNAs during early development, while in yeast, Dhh1p increases the efficiency of mRNA decapping in P bodies (Minshall et al., 2001). Dhh1p physically interacts with several proteins involved in mRNA degradation, including the decapping factor Dcp1p, the activators of decapping Lsm1p and Pat1p, as well as a component of the deadenylation complex, POP2p (Coller et al., 2001; Fischer and Weis,

2002). These interactions appear to be maintained in other species given that human RCK/p54 forms a complex with Dcp1/2 that co-localizes with the deadenylase CCR4 and the exonuclease Xrn1 in particles containing poly(A)$^+$ RNA (Fenger-Gron et al., 2005; Ferraiuolo et al., 2005; Brengues et al., 2005; Ingelfinger et al., 2002; Eystathioy et al., 2003; Cougot et al., 2004; Kedersha et al., 2005).

In *Drosophila*, Me31B is a component of maternal RNPs called sponge bodies, where it is required for translational silencing of un-localized *oskar* mRNA (Nakamura et al., 2001) and has recently been shown to co-localize with both Dcp1 and Dcp2 in cytoplasmic foci resembling P bodies (Lin et al., 2006). Surprisingly, Dcp1 is required for posterior localization of *oskar* mRNA and this function does not require its decapping activity (Lin et al., 2006). These findings raise the intriguing possibility that sponge bodies and polar granules may be closely related to P bodies, yet have adapted certain components to carry out novel functions. Me31B has also been identified as a component of the Trailer Hitch mRNP complex, which is required for proper maintenance of ER exit sites and normal exocytosis during oogenesis (Wilhelm et al., 2005). Me31B likely plays a critical role in this complex, as the *Me31B* null phenotypes closely resemble those described for the exocyst component Sec5. In both mutants, germline cells and ring canals aggregate due to collapse of cellular membranes (Nakamura et al., 2001; Murthy and Schwarz, 2004). Interestingly, all of the homologues of ME31B that have been tested associate with the corresponding Trailer Hitch homologue in each species (Weston and Sommerville, 2006). Furthermore, the human homologue of Trailer Hitch, RAP55, has also been detected in P bodies and has been shown to be a critical factor in their assembly (Yang et al., 2006). Similarly, Me31B and its homologues all share an

association with a conserved cold-shock domain RNA binding protein called Ypsilon Schachtel (YPS) in *Drosophila*, FRGY2 in *Xenopus* and MSY2 in mice (Weston and Sommerville, 2006). These striking commonalities suggest that Me31B, and its counterparts in other species, serve critical roles as post-transcriptional regulators in closely related mRNP complexes. Given its helicase activity, Me31B may contribute to mRNP remodeling by altering the complement of proteins bound to an mRNA, either through removal of bound proteins or by altering RNA structure such that new binding sites become accessible.

1.3.4 Orb

The *Drosophila* Oo18 RNA binding protein Orb is a maternally contributed RRM domain-containing protein with significant homology to *Xenopus* CPEB (Lantz et al., 1994; Hake and Richter, 1994). The similarity between Orb and CPEB is greatest in their RNA binding domains, suggesting that Orb, like CPEB, can specifically bind CPE-like sequences. Unlike CPEB however, Orb does not posses a Maskin-binding domain or the phosphorylation sites that regulate CPEB activity during egg activation (Mendez and Richter, 2001). *orb* activity is required at multiple points during oogenesis, beginning very early with the formation of the 16 cell cyst and establishment of the oocyte within this cluster (Lantz et al., 1994; Christerson and McKearin, 1994). In the *orb* null (orb^{F343}), oogenesis arrests before a 16 cell cyst is formed, while in the strong hypomorphic mutant (orb^{F303}), egg chambers are produced but the oocyte fails to migrate to their posterior and they are often incompletely surrounded by follicle cells (Lantz et al., 1994). These pseudo egg chambers degenerate shortly after exiting the germarium.

Weaker allelic combinations of *orb* (*orb*^{mel}/ *orb*^{F343} or *orb*^{mel}/ *orb*^{mel}), produce ventralized eggs with fused or missing dorsal appendages, which contain embryos with abdominal segment deletions (Christerson and McKearin, 1994). Consistently, these mutants also display defects in anterior/dorsal accumulation of *grk* mRNA and posterior localization of *osk* mRNA during oogenesis (Christerson and McKearin, 1994). These defects are accompanied by a substantial decrease in Grk and Osk protein production and a reduction in *osk* poly(A) tail length (Chang et al., 2001; Chang et al., 1999). In conjunction with observations that Orb associates with *osk* mRNA (Chang et al., 1999), these findings suggested that Orb may function similarly to CPEB in promoting translation of specific mRNAs by stimulating poly(A) tail lengthening. However, a recent study suggests that the effects on both Grk and Osk expression may be an indirect consequence of reorganization of the microtubule cytoskeleton and premature cytoplasmic streaming (Martin et al., 2003). Genetic assays and co-immunoprecipitation experiments suggest that the RNA binding proteins YPS and Bic-C both associate with Orb and antagonize its function (Mansfield et al., 2002; Castagnetti and Ephrussi, 2003).

1.3.5 Cytoplasmic streaming

Rapid circular streaming of the oocyte cytoplasm begins in late stage 10 and continues to stage 12, during which period the nurse cells transfer their cytoplasm into the oocyte (Theurkauf, 1994a). This microtubule-dependent process, driven by the motor activity of Kinesin Heavy Chain (KHC), is believed to be important for mixing the oocyte cytoplasm with incoming cytoplasm from the nurse cells (Palacios and St Johnston, 2002). Cytoplasmic streaming has been linked to *osk* localization, since disruption of this

event prevents anterior to posterior translocation of injected *osk* mRNA in stage 10b-11 oocytes (Glotzer et al., 1997). Furthermore, *Kinesin-1* mutants, blocked specifically in cytoplasmic streaming, display an abnormal persistence of *osk* in the center of stage 10 oocytes (Serbus et al., 2005). In stronger Kinesin-1 mutants, *osk* remains associated with the entire cortex where it is translated (Cha et al. 2002), indicating that the entire actin-rich cortex is capable of supporting Osk translation and demonstrating the importance of efficient posterior *osk* mRNA localization for proper embryonic patterning. Timing the onset of cytoplasmic streaming correctly is critical, since premature initiation disrupts local *grk* and *osk* accumulation, resulting in dorsal/ventral and posterior patterning defects. F-actin and the actin-associated proteins Chickadee (a profilin), Cappuccino (Capu; a formin homology protein) and Spire (Spir, a WASP-homology 2 domain containing protein) are all required to regulate the timing of cytoplasmic streaming (Theurkauf, 1994b; Manseau et al., 1996). Mutants in the corresponding genes commence cytoplasmic streaming as early as stage 8. Recent evidence indicates that Capu and a specific isoform of Spir (Spir C) restrict cytoplasmic streaming during stages 8-10b by crosslinking the actin and microtubule cytoskeletons together in response to Rho1 signaling (Rosales-Nieves et al., 2006). Mutations in *homeless* (*Spn-E*) and *orb*, both of which encode RNA-binding proteins, also initiate cytoplasmic streaming prematurely (Martin et al., 2003), suggesting that this process is subject to post-transcriptional regulation.

1.3.6 Gurken

The anterior/posterior (A/P) and dorsal/ventral (D/V) axes of the future embryo are both established during *Drosophila* oogenesis by signaling events between the oocyte and the overlying somatic follicle cells. These signals are mediated in part by the TGF-α homologue Grk, which is secreted from the oocyte to activate the follicle cell-bound EGF receptor (Gonzalez-Reyes et al., 1995). This initially occurs at stage 6, when activation of EGFR in a posterior group of follicle cells triggers the production of an unknown signal that establishes the A/P axis of the oocyte. Consequently, the microtubule cytoskeleton reorganizes within the oocyte such that patterning determinants, such as *osk* and *bcd*, localize to distinct subcellular domains. The oocyte nucleus, which is closely associated with *grk* mRNA throughout oogenesis, migrates to the anterior cortex in response to the cytoskeletal rearrangements at stage 7. Localized production of Grk then specifies the dorsal side of the oocyte through a second round of EGFR activation in the anterior/lateral follicle cells that happen to be closest to the oocyte nucleus (Neuman-Silberberg and Schupbach, 1993). A number of proteins, including the products of *K10* and *squid*, work in concert to restrict localization and translation of *grk* mRNA to the anterior/dorsal cortex (Kelley, 1993; Thio et al., 2000). Once translated, Grk is cleaved in the ER by the membrane-bound protease Rhomboid 2, producing its active, secreted form (Ghiglione et al., 2002; Guichard et al., 2000). Diffusion of the Grk cleavage product within the ER is prevented by Cornichon (Cni), a transmembrane protein that acts as a cargo receptor, binding to Grk and recruiting it into COP II-coated vesicles for rapid export (Bokel et al., 2006).

1.4 Patterning of the *Drosophila* egg and embryo

1.4.1 Dorsal appendage formation

EGFR activation in the anterior/dorsal follicle cells triggers a signaling cascade that specifies the formation of specialized egg shell structures called dorsal appendages, which are believed to mediate gas exchange between the embryo and its environment. The dorsal limits of these appendages are established through a self-amplifying/ inhibitory mechanism. The protease Rhomboid is expressed in response to EGFR activation, leading to autocrine production of Spitz, another activating ligand of EGFR (Wasserman and Freeman, 1998). Amplification of EGFR activation induces Argos expression along the dorsal mid-line, where the level of EGFR activation is highest. Argos antagonizes Spitz function, causing the domain of activated EGFR to split into two peaks, ultimately leading to the formation of two, symmetrically-positioned, dorsal appendages (Wasserman and Freeman, 1998). Positioning of these structures along the A/P axis is controlled by the TGF-β homologue *decapentaplegic* (*dpp*) (Peri and Roth, 2000). Dpp emanates from a group of follicle cells positioned along the nurse cell/oocyte border and has been proposed to activate expression of the homeodomain transcription factor *mirror* (*mirr*) in neighboring anterior follicle cells (Twombly et al., 1996; Atkey et al., 2006). Mirr is a critical determinant of dorsal appendage producing fates, although its mode of action is obscure and no specific transcriptional targets have been identified as yet (Zhao et al., 2000; Jordan et al., 2000). The ventral boundaries of the dorsal appendages are set by the transcriptional repressor Capicua (Cic), which restricts *mirr* expression to a patch of anterior/dorsal follicle cells (Atkey et al., 2006). Cic is

expressed in the ventral and lateral follicle cells but is excluded from dorsal follicle cells by EGFR activity (Goff et al., 2001; Atkey et al., 2006).

1.4.2 Dorsal/ventral patterning

EGFR activation also plays a crucial role in specifying the dorsal/ventral axis of the embryo by limiting *pipe* expression to the ventral 40% of the egg chamber circumference (Nilson and Schupbach, 1998; Sen et al., 1998). *pipe* encodes a heparin sulphate 2-O-sulphotransferase that is believed to modify components of the extracellular matrix (ECM) in the space between the oocyte and the follicle cells (Sen et al., 1998; Sen et al., 2000). After egg deposition, these ECM components, located between the embryo and the vitelline membrane, trigger a protease cascade that culminates in the activation of Spätzle, an activating ligand of the Toll receptor (Morisato and Anderson, 1994; Moussian and Roth, 2005). Spatial restriction of Spätzle is important, as Toll is uniformly distributed over the surface of the embryo (Hashimoto et al., 1991). Activation of Toll triggers a kinase cascade within the embryonic syncytial blastoderm that leads to local release of the NF-κB transcription factor Dorsal from Cactus, its cytoplasmic tether (Drier et al., 1999). This produces a ventral to dorsal gradient of nuclear Dorsal protein which activates multiple patterning genes in a concentration dependent manner (Stathopoulos and Levine, 2002).

1.4.3 Bicoid

The homeodomain transcription factor Bicoid (Bcd) is an anterior morphogen, required for the establishment of head and thoracic structures during *Drosophila*

embryogenesis (Driever and Nusslein-Volhard, 1989). A combination of mRNA localization and translational repression produces an anterior to posterior gradient of Bcd protein in the syncytial blastoderm. This gradient is ultimately translated into positional information through the stepwise activation of zygotically-expressed genes that pattern the embryo along the A/P axis. *bcd* mRNA localization is also a stepwise event that requires at least three *trans*-acting factors, Exuperantia (Exu), Swallow (Swa) and Staufen (Stau) (Ephrussi and St Johnston, 2004). Exu is involved in transporting *bcd* mRNA from the nurse cells into the oocyte, while Swa is required to restrict *bcd* to the anterior of the oocyte during oogenesis. Finally, Stau is needed to anchor the *bcd* transcript to the anterior of the egg, where its translation becomes activated by poly(A) tail lengthening at the onset of embryogenesis (Salles et al., 1994). Bcd performs dual roles as a transcriptional activator of zygotic *hunchback (hb)*, itself a transcription factor that is also important for specifying anterior fates, and as a translational repressor of the posterior determinant *caudal (cad)*. *cad* repression occurs through a novel mechanism involving the cap-binding protein 4EHP, which is recruited to *cad* mRNA through a direct interaction with Bcd (Cho et al., 2005). Bcd binds to elements in the 3' UTR of *cad*, while 4EHP presumably displaces eIF4E from the 5' cap structure, preventing assembly of the eIF4F initiation complex (Cho et al., 2005).

1.4.4 Nanos

Aside from its role in establishing the germline in each new generation, the pole plasm serves a critical role in abdomen formation, as it is required for the establishment of a posterior to anterior morphogen gradient of the posterior determinant Nanos (Nos) in

the syncytial blastoderm. Nos acts through the RNA-binding protein Pumilio (Pum) to repress translation of maternal *hunchback,* in part by promoting posterior deadenylation of *hb* mRNA (Wreden et al., 1997). Interestingly, Nos, Pum and a third protein called Brain Tumor (Brat) were recently shown to repress *hb* translation by recruiting 4EHP, using a similar mechanism as that employed by Bcd for *cad* repression (Cho et al., 2006).

As in the case of Bcd, establishment of the Nos gradient relies on a combination of mRNA localization and regulated translation. Posterior accumulation of *nos* mRNA begins at stage 12 of oogenesis, when rapid cytoplasmic streaming brings *nos* into contact with Osk and other pole plasm components that are anchored to the posterior cortex. This "local trapping" method of mRNA localization appears to be rather inefficient as only 4% of *nos* mRNA is estimated to concentrate at the posterior cortex (Bergsten and Gavis, 1999). It is therefore not surprising that unlocalized *nos* is subject to multiple forms of repression outside of the pole plasm. This repression is mediated in part by Smaug (Smg), which binds *nos* 3'UTR elements via its SAM domain (Aviv et al., 2003; Green et al., 2003; Smibert et al., 1996). Unexpectedly, Smg restricts Nos expression through two distinct mechanisms. It represses Nos translation through an interaction with the eIF4E interacting protein Cup (Nelson et al., 2004), and it promotes *nos* deadenylation and subsequent degradation by recruiting the CCR4/Pop2/NOT deadenylase complex (Zaessinger et al., 2006). Despite these mechanisms of repression, over 50% of *nos* is associated with polysomes, indicating that a third form of translational silencing may be at play (Clark et al., 2000). Accordingly, ectopic Nos translation is observed in mutants of *bicaudal,* which encodes a subunit of the Nascent polypeptide Associated Complex (NAC), suggesting that the nascent Nos polypeptide may be

targeted by Bicaudal in some way that stalls translation or prevents release of Nos from the ribosome (Markesich et al., 2000). During oogenesis, translational repression of *nos* is mediated by 3' UTR elements that are distinct from those bound by Smg. A protein called Glorund, with homology to mammalian hnRNPs F and H, has been shown to bind these elements and repress of *nos* translation late in oogenesis (Kalifa et al., 2006). The exact mechanism of *nos* translational de-repression in the pole plasm remains somewhat nebulous. However, it appears to involve displacement of Smg by Osk through a competitive interaction with the RNA-binding domain of Smg (Dahanukar et al., 1999; Zaessinger et al., 2006) and activation by the DEAD-box RNA-helicase Vasa (Gavis et al., 1996).

1.5 The CCR4 deadenylase complex in *Drosophila*

The CCR4/Pop2/NOT deadenylase complex is active during *Drosophila* oogenesis where its components are concentrated in cytoplasmic foci (Temme et al., 2004). Interestingly, hypomorphic alleles of *Drosophila ccr4* (also called *twin*) disrupt oogenesis without producing any obvious defects in the soma (Temme et al., 2004; Morris et al., 2005). Early in oogenesis, CCR4 is required to control the number and synchronicity of germline cyst divisions through regulation of *cyclinA* polyadenylation (Morris et al., 2005). CCR4 has also been implicated in *oskar* and *cyclinB* poly(A) tail regulation during oogenesis (Benoit et al., 2005). In early embryogenesis, the CCR4 complex is required to localize *hsp83* and *nanos* mRNAs to the posterior cortex through a combination of bulk cytoplasmic degradation and localized protection in the pole plasm (Semotok et al., 2005; Zaessinger et al., 2006). The CCR4 complex is specifically

recruited to these transcripts by the RNA-binding protein Smaug, which binds to *cis*-elements in their 3' UTRs (Semotok et al., 2005; Zaessinger et al., 2006). In the pole plasm, Osk protects *nanos* from degradation by abrogating the interaction between Smaug and *nanos* mRNA (Zaessinger et al., 2006). Given that Oskar interacts with the RNA-binding domain of Smaug, competitive binding is probably the mechanism by which *nanos* and *hsp83* are protected (Dahanukar et al., 1999).

1.6 Bic-C and related RNA binding proteins

1.6.1 Bic-C

In *D. melanogaster*, the *Bicaudal-C* (*Bic-C*) gene is required maternally for specifying anterior position during early development and for progression of oogenesis beyond stage 10 (Mohler and Wieschaus, 1986; Schupbach and Wieschaus, 1991; Mahone et al., 1995). The progeny of heterozygous *Bic-C* females display a variety of anterior patterning defects that are shared by mutants of *Bicaudal* and *Bicaudal-D* (Mohler and Wieschaus, 1986). These defects range in severity from reduced or missing mouth parts to bicaudal embryos, where the anterior half of the embryo is replaced by a mirror image duplication of the posterior half (Mohler and Wieschaus, 1986). Intermediate phenotypes include headless embryos or embryos possessing a disorganized array of denticle bands or segments with longitudinal strips having reversed or ambiguous polarity anterior to abdominal segment A4 (Mohler and Wieschaus, 1986). Additionally, an abundant class of these embryos fails to cellularize due to a developmental block in the later syncytial divisions (Mahone et al., 1995). Females heterozygous for chromosomal deletions that remove *Bic-C* produce similarly affected offspring, strongly suggesting that haplo-insufficiency is responsible for the dominant

maternal-effect phenotypes observed in *Bic-C* mutants (Mohler and Wieschaus, 1986). Consistent with the observed patterning defects, ectopic anterior accumulation of *oskar* and *nanos* transcripts have been detected in early cleavage embryos from Bic^{YC33} heterozygous females (Mahone et al., 1995). Furthermore, a portion of *osk* mRNA remains associated with the anterior cortex of the oocyte in stage 8-10 egg chambers from $Bic\text{-}C^{AA4}$ heterozygous females (Mahone et al., 1995). Premature translation of Osk has also been observed in stage 7-10 egg chambers of homozygous *Bic-C* females, where ectopic Osk protein accumulates in the anterior and central regions of the oocyte cytoplasm (Saffman et al., 1998).

In homozygous *Bic-C* females, oogenesis arrests at approximately stage 10, when the vast majority of egg chambers begin to degenerate. The few eggs that are produced by these females display an open-ended chorion phenotype because the centripetally migrating follicle cells fail to encapsulate the anterior of the oocyte at stage 10 of oogenesis. Some of the weaker allelic combinations are capable of producing eggs, many of which are flaccid and have fused dorsal appendages (Mahone, 1994).

The *Bic-C* gene encodes a 102 kDa protein, containing five KH domains in its N-terminal half (a.a. 96-524) and a SAM domain close to its C-terminus (a.a. 784-862) (Mahone et al., 1995). The KH domain is a single-stranded RNA and DNA binding motif, first identified in hnRNP K (Siomi et al., 1993). The SAM (Sterile Alpha Motif) domain is a protein interaction motif that, in some cases, has been shown to bind other SAM domains and SH2 domains (Burd and Dreyfuss, 1994; Schultz et al., 1997). However, more recent evidence indicates that some SAM domains can bind RNA as well (Aviv et al., 2003). Bic-C has been shown to bind RNA homopolymers *in vitro* and a

point mutation causing a glycine to arginine conversion in the third KH domain of the protein (G296R), results in substantially decreased RNA binding activity *in vitro* and a strong mutant phenotype *in vivo* (Saffman et al., 1998), suggesting that the RNA-binding activity of Bic-C is required for at least some aspects of its function *in vivo*.

A yeast two-hybrid screen for Bic-C interacting proteins has recently identified several proteins that have been implicated in translation control and/or RNA stability (Paliouras, M., Ph.D Thesis, 2005). These include Me31B, NOT3, a component of the CCR4 deadenylase complex (Temme et al., 2004), and Giant Nuclei, which has been implicated in maternal mRNA degradation (Tadros et al., 2003).

1.6.2 Bic-C homologues

Recent studies in *C. elegans, Xenopus*, mice and humans have revealed that *Bic-C* is a member of an evolutionarily conserved family of proteins. This protein family is characterized by a common structural architecture, consisting of five KH domains within the N-terminal portion and a sterile alpha motif (SAM) domain close to the C-terminus, separated by a serine/glycine-rich region. The *Xenopus*, mouse and human Bic-C orthologues are 44.7, 44.9 and 43.3% identical to the *D. melanogaster* Bic-C protein respectively; with the KH and SAM domains retaining the greatest degree of homology (Wessely et al., 2001).

Xenopus Bic-C (xBic-C) was isolated in a screen for maternal mRNAs that undergo poly(A) tail lengthening upon cortical rotation of the egg (Wessely and De Robertis, 2000). Overexpression of xBic-C or of a fragment of the protein containing the KH domains induces ectopic endoderm formation, while expression of a dominant-

negative version of the protein lacking the KH domains blocks both endoderm and mesoderm formation (Wessely and De Robertis, 2000). Given these observations and the fact that *xBic-C* mRNA is concentrated in the vegetal half of the egg/embryo, it was proposed that xBic-C may be a translational repressor of animal pole determinants, acting to sharpen morphogen gradients between the two hemispheres (Wessely and De Robertis, 2000).

The mouse orthologue of *Bic-C* (m*Bic-C*) is also provided maternally to the oocyte and is expressed in undifferentiated tissues such as Hensen's node and the developing mesenchyme during embryogenesis. Adult mice express *mBic-C* most abundantly in the heart and kidneys (Wessely et al., 2001). Mutations in *mBic-C* are responsible for both the *jcpk* and *bpk* mouse models of polycystic kidney disease (Cogswell et al., 2003). Homozygous *jcpk* mice develop numerous cysts in all parts of the nephron and die within 10 days of birth, while approximately 30% of *jcpk* heterozygotes develop a late-onset renal cystic disease, affecting only the glomeruli. Homozygous *bpk* mice die by four weeks of age due to cystic dilation of the renal collecting ducts and biliary dysgenesis. Polycystic kidney disease accounts for approximately 10% of all end-stage renal disease cases in humans and the inherited autosomal dominant form affects 1 in 1000 people (Cogswell et al., 2003).

Two genes related to *Bic-C, GLD-3* (germline development defective) and *BCC-1,* have been identified in *Caenorhabditis elegans* (Eckmann et al., 2002). Sequence comparisons indicate that both of these genes have diverged significantly from the other members of the *Bic-C* family (Eckmann et al., 2002). However BCC-1 is more closely related to Bic-C than GLD-3, which does not contain a SAM domain (Eckmann et al.,

2002). The function of BCC-1 is unknown, however, studies of GLD-3 indicate that it co-localizes with P granules (i.e. germ plasm) in early embryos and is required maternally for embryogenesis and germline survival (Eckmann et al., 2002). The zygotic requirements of GLD-3 have been studied in greater detail (Wang et al., 2002; Eckmann et al., 2002; Eckmann et al., 2004; Suh et al., 2006). In conjunction with the cytoplasmic poly(A) polymerase GLD-2, GLD-3 promotes a transition from mitosis to meiosis in the gonad by stabilizing *gld-1* mRNA and enhancing translation of GLD-1, which is a STAR/Quaking translational repressor (Eckmann et al., 2004; Suh et al., 2006). The *gld-1* and *gld-3* transcripts are both targeted by the translational repressor FBF (*fem-3* binding factor), a member of the PUF family of proteins. As its name implies, FBF also targets *fem-3* mRNA for translational repression, thereby promoting the switch from spermatogenesis to oogenesis in hermaphrodite worms (Zhang et al., 1997). Interestingly, the other zygotic function of GLD-3 is to promote spermatogenesis by binding directly to FBF and preventing *fem-3* repression (Eckmann et al., 2002; Eckmann et al., 2004). The region of GLD-3 required for FBF binding is not shared by Bic-C or its homologues. The complex regulatory relationships that have been discovered among these proteins highlight the importance of integrating multiple genetic pathways to achieve coordinated developmental events.

1.6.3 The KH domain

The KH-type RNA-binding domain is believed to have emerged relatively early in evolutionary history, as it is well represented in all of life's kingdoms. The heterogeneous nuclear ribonucleoprotein particle-K homology (KH) domain was first

recognized in heterogeneous nuclear ribonucleoprotein (hnRNP) K, to which it owes its name (Siomi et al., 1993). Sequence comparisons of multiple KH domain-containing proteins, including bacterial NusA, suggested that the domain spanned ~50 amino acids, with an overall βααββ topology. However, with the discovery of more KH proteins came the realization that most KH domains are actually ~70 amino acids long and consist of a βααββα topology (Adinolfi et al., 1999). These domains are characterized by their structure rather than primary sequence homology, of which they share very little. In fact, the only sequence within the domain that is absolutely conserved is a GxxG motif, located in the loop between the first and second α helices. Structural studies of the third KH domain of the neuronal splicing factor Nova-1, suggest that this loop forms part of the RNA-binding surface, acting as one arm of a molecular vice (Lewis et al., 2000). This vice brings the RNA bases into contact with amino acids in the first two α helices and the first β strand, providing the basis for sequence-specific RNA-binding (Lewis et al., 2000).

With the notable exception of the STAR (Signal Transduction and Activation of RNA) subfamily, most KH proteins contain multiple copies of the domain, which are thought to act cooperatively in RNA-binding. This is certainly the case for hnRNPK, which contains 3 KH domains that each bind to a short (6-7) stretch of nucleotides (Paziewska et al., 2004). Individually, these domains bind RNA promiscuously with reduced affinity, however, together they act synergistically to increase the strength and specificity of binding (Paziewska et al., 2004). This combinatorial effect is thought to restrict high-affinity binding to a discrete number of transcripts *in vivo*. The ability to dimerize is believed to be another common, yet not universal feature of KH domains,

which may also strengthen sequence-specific binding to RNA (Chen et al., 1997; Ramos et al., 2002).

Members of the STAR group of proteins contain a single KH domain, however flanking sequences also contribute to RNA-binding, creating an extended RNA-binding region referred to as the GSG (GRP33, Sam68, GLD-1) domain (Adinolfi et al., 1999). These proteins are also characterized by the presence of motifs that mediate functional regulation by signaling pathways. For example, one of the founding members of this group, Sam68 (Src-Associated Substrate during Mitosis of 68 kDa), contains proline-rich sequences that mediate binding to SH3 domains and a tyrosine-rich C-terminus that inhibits RNA-binding when phosphorylated (Lukong and Richard, 2003).

KH proteins are involved in virtually all aspects of RNA metabolism. For example, ZBP-1 (Zipcode-Binding Protein 1) is required for subcellular localization *of β-actin* mRNA to the leading edge of migrating fibroblasts (Ross et al., 1997), whereas Nova-1, the antigen targeted by auto-antibodies in patients with the neurodegenerative disease Paraneoplastic Opsoclonus Myoclonus Ataxia (POMA), regulates alternative splicing of inhibitory neurotransmitter receptor subunit pre-mRNAs (Jensen et al., 2000; Dredge and Darnell, 2003). hnRNPK has many functions but is probably best known for its role in repressing 15-lipoxygenase translation in erythroid cells (Ostareck et al., 2001).

The Fragile-X mental retardation protein (FMRP) is probably the most extensively studied KH domain protein, although despite considerable efforts, its molecular functions remain enigmatic. Mutations affecting this protein or its expression in the brain result in the Fragile X Syndrome, the most commonly inherited form of mental retardation in humans. Humans and mice with this disease have an increased

number of abnormally shaped dendritic spines, structures that regulate many of the neurochemical events that are involved in synaptic transmission (Comery et al., 1997; Irwin et al., 2001). FMRP has been implicated in a variety of post-transcriptional processes in neurons including nuclear export, subcellular mRNA transport, translational activation and repression and miRNA-mediated post-transcriptional silencing (Bagni and Greenough, 2005). A variety of techniques have been employed to identify RNA targets of FMRP but there has been relatively little overlap in the resulting candidates (Darnell et al., 2005). However, a commonality among putative targets has been mRNAs encoding regulators of neuronal maturation/function and synaptic plasticity, including the *MAP1B* mRNA which contains a G-quartet structure important for FMRP binding (Darnell et al., 2001). Interestingly, the synaptic hyperplasia phenotype observed upon mutating the *Drosophila* homologue of FMRP (dFmr1) can be fully rescued by a concomitant mutation in *futsch*, which encodes the *Drosophila* homologue of MAP1B (Zhang et al., 2001). dFmr1 is also important for gametogenesis and translational repression of *orb* mRNA (Zhang et al., 2004; Costa et al., 2005).

1.7 Research objectives and rationale for experimental design

When I began my graduate studies in the Lasko Lab, our shared objectives were much as they are today; to deepen our understanding of the post-transcriptional mechanisms that regulate growth, patterning and germline development in *Drosophila*. These objectives are motivated by a basic curiosity in the fundamental processes that shape life and have allowed it to develop into the astonishingly complex forms that exist today. Motivation also comes from the hope that our work will ultimately help to

improve the human condition, through an enhanced understanding of disease and its molecular roots.

At the onset of my work, the *Bic-C* gene had been identified and many aspects of the *Bic-C* mutant phenotype had been studied and described but very little was known about its molecular function. The presence of KH domains in the protein and premature translation of *osk* in the mutant suggested that Bic-C was a translational repressor, however, an association with *osk* or any other mRNA had not been demonstrated. Therefore, the initial primary objective of my project was to identify mRNAs that specifically interact with Bic-C. A number of techniques were considered for this task; however, after some experimentation with *in vitro* approaches, I decided to adopt a novel strategy based on a combination of immunoprecipitations and mRNA screening methods (first differential-display RT-PCR and later Affymetrix™ microarrays). I did not know it at the time but similar strategies were being developed independently by others and would later be termed Ribonomic Profiling.

This work identified *Bic-C* mRNA and several other transcripts, as putative regulatory targets of Bic-C. To determine if the association with its own mRNA reflected a biological function, I engineered a series of reporter constructs. This approach was taken because any analysis of endogenous Bic-C could be confounded by primary effects of the mutations affecting the gene. When this work suggested that *Bic-C* mRNA, and consequently protein levels, are regulated by an auto-repressive mechanism, I was struck by its implication; over-production of Bic-C must have deleterious consequences. To determine what these consequences might be and potentially gain further insight into Bic-C function, I employed the UASP/Gal4 system to overexpress Bic-C in the germline.

This inducible system was used because I anticipated (or perhaps just hoped) that it would not be feasible to maintain fly stocks constitutively overexpressing Bic-C.

Phenotypic analysis of Bic-C overexpressing flies indicated, for the first time, that Bic-C contributes to the regulation of cytoplasmic movements within the egg chamber and oocyte. Concurrent work by a colleague in the lab, Miltiadis Paliouras, suggested that Bic-C might physically interact with NOT3, a component of the CCR4 deadenylase complex. Bic-C overexpression provided a sensitized genetic background in which to test the biological relevance of this and other putative interactions. Co-immunoprecipitations were then performed to determine if genetic interactions were indicative of physical associations *in vivo*.

As an alternate approach to understanding Bic-C function, I also continued the phenotypic analysis of *Bic-C* mutants that had been initiated by my predecessors. Through this work I discovered that Gurken secretion and possibly exocytosis in general, is defective in *Bic-C* mutants.

In addition to this work, I have performed an initial characterization of Bic-C phosphorylation, in the hopes of elucidating the post-translational mechanisms regulating Bic-C function *in vivo*.

Section 2: Materials and Methods

2.1 α-Bic-C antibody production

An *Eco*RI fragment encompassing nucleotides 870-3624 of the *Bic-C* cDNA, containing the entire open reading frame, was subcloned into pGEX-3X (GE Healthcare) to produce a full-length GST-Bic-C fusion protein which was expressed in *E. coli* BL21 cells and purified from inclusion bodies as described in method 2 of (Sambrook et al., 1998). The purified fusion protein was injected subcutaneously into rabbits to generate α-Bic-C sera which were then affinity purified against full length GST-Bic-C coupled to AffiGel (BioRad).

2.2 Construction, expression and purification of MBP-Bic-C^{85-462}

To generate the MBP-Bic-C^{85-462} construct, a fragment of the Bic-C cDNA was amplified using *Pfu* DNA polymerase (Stratagene) using the following forward: 5'-TTCCGAATTCCTCCACACGGACACCATTCG-3' and reverse: 5'-CACTCTAGATCATGTGGCCAGGCGCAG -3' primers. These primers contain an *Eco*RI site and an *Xba*I site respectively. The resulting PCR product was digested with EcoR1 and *Xba*I and ligated into the same sites of the pMAL-C2 vector (New England Biolabs). The resulting construct was sequenced with the MAL-E primer (New England Biolabs) to verify that no mutations were introduced upon amplification. Proteins were expressed in *E. coli* BL21 cells and purified under native conditions as directed by the manufacturer (New England Biolabs).

2.3 *In vitro* RNA binding assay

Approximately 20 μg of purified MBP or MBP-Bic-C^{85-462} was incubated with 50μl of poly-G agarose beads (Sigma) or control agarose beads for 45 min at 4 °C in 1ml of binding/ wash buffer (25 mM Tris pH 7.5, 300 mM NaCl, 0.1% Triton-X-100). Beads were then rinsed five times with 1 ml of binding/ wash buffer before bound proteins were eluted by boiling in Laemmli sample buffer. Approximately 20% of each sample was loaded for SDS-PAGE. Proteins were visualized by staining gels with Gelcode reagent as instructed by the manufacturer (Pierce).

2.4 Ovarian mRNP isolation

Fattened 2-3 day old OreR females were hand-dissected in PBS and their ovaries were homogenized on ice in mRNP lysis buffer (20mM Hepes-KOH (pH 7.6), 150mM KCL, 1mM DTT, 0.25% NP-40). Extracts were incubated on ice for 5 min. then centrifuged at 10,000 rpm for 15 min in a microfuge at 4°C to remove debris. EDTA was then added to the cleared supernatant to a final concentration of 33mM and the mixture was incubated on ice for 20 min to dissociate polysomes. The supernatant was added to 50 μl of oligo-dT cellulose (Phamacia Biotech) which had been pre-washed with equilibration buffer (i.e. lysis buffer without NP-40). The slurry was incubated over-night at 4 °C (rotating) and then centrifuged at 3,000 rpm to remove the supernatant. The oligo-dT cellulose was then washed three times with 1 ml of equilibration buffer each time. Associated proteins were then eluted by boiling in SDS-PAGE (Laemmli) sample buffer, resolved by SDS-PAGE and analyzed by Western blotting.

2.5 Isolation of Bic-C associated mRNAs

Ovaries were hand-dissected from well-fed 2-3 day old Oregon-R females and homogenized in an equal volume of 2X lysis buffer (100mM Tris (pH 7.5), 500mM NaCl, 5mM $MgCl_2$, 4mM DTT, 2X complete protease inhibitor cocktail (Roche), 2mM PMSF, 2 U/µl RNA Guard (GE Healthcare) on ice. Extracts were centrifuged for 20 min at 13,000 rpm in a microfuge at 4°C. The supernatant was recovered and diluted to a final protein concentration of 1 mg/ml with ice-cold 1X lysis buffer containing 0.5% Triton-X-100, then divided into 1 ml aliquots for pre-clearing against 50µl of equilibrated protein-A-Sepharose (PAS; GE Healthcare) for 1 h at 4°C (rotating). After a brief centrifugation, supernatants were transferred to fresh tubes and mixed with 8 µl of either α-Bic-C or pre-immune sera and incubated at 4°C for 3 h (rotating). 30 µl of equilibrated PAS was then added to each sample and the incubation extended for another 3 h at 4°C. The samples were then centrifuged for 2 min (2000 rpm at 4°C) and the pellets were rinsed with 1 ml of ice-cold wash buffer (50 mM Tris (pH 7.5), 200-800mM NaCl, 0.5% Triton-X-100) and washed for 3X 15 min at 4°C with 1 ml of wash buffer containing 1 mg/ml heparin. The pellets were then rinsed another 3X with 1 ml of wash buffer, while removing as much buffer as possible between rinses with a bent 26 gauge needle, and then resuspended in 300 µl of RNase-free ddH_2O before phenol/chloroform extraction. 20 µg of glycogen and 0.1X volume of 3M sodium acetate (pH 5.2) were added to each sample before ethanol precipitation overnight at -20 °C. RNA samples were converted to single stranded DNA with $p(N)_6$ random primers using SuperScriptII RNase H^- reverse transcriptase (Invitrogen) as directed by the manufacturer. 10% of each sample served as template for Delta™ differential-display PCR reactions, following the manufacturer's

protocol (Clontech). Products of interest were excised from dried gels, re-amplified, cloned into the pGEMT vector (Promega) and sequenced. The fragment of Bic-C was amplified with a combination of P1 (5'-ATTAACCCTCACTAAATGCTGGGGA-3') and T8 (5'-CATTATGCTGAGTGATATCTTTTTTTTTGG-3') primers (Clontech). For analysis with transcript-specific primers, RNA was recovered from α-Bic-C and control IPs as described above, except the IP/wash buffer was modified (50mM Tris (pH 7.5), 250mM NaCl, 2.5mM $MgCl_2$, 0.5% Triton-X-100). Total (input) RNA was isolated from the ovarian lysate with Trizol (Invitrogen) following the manufacturer's instructions. RNA samples were reverse-transcribed as described above and 10% of each ssDNA sample served as template for PCR with *Bic-C* forward (5'-GACTTCGACATGAAACGG-3') and reverse (5'-GATACCCAGCTCCATCAG-3') primers or *cp18* forward (5'-ATCTGCCTCTGCGCCATC-3') and reverse (5'-CCTAGTTCCTTATTGGCAGG-3') primers. PCR conditions were as follows: 94°C for 3 min; 30 cycles of 94°C - 1 min, 54°C - 1 min, 72°C - 2 min; with a final extension of 72°C for 8 min. PCR products were resolved by electrophoresis on a 1.2% agarose gel and visualized by ethidium bromide staining.

2.6 Microarray analysis of Bic-C associated mRNAs

For microarray analysis, IPs and RNA recovery were performed essentially as described above, but with 8.75 ml of extract, containing 5 mg/ml of soluble protein, for each IP. 300 µl of affinity purified α-Bic-C and pre-immune sera (from rabbit 2428) or 560 µl of α-Bic-C or pre-immune sera (from rabbit 2429) were each pre-coupled to 70 µl or 200 µl of PAS respectively and washed extensively before use in subsequent IPs. For

Bruno mRNP isolation, 150 µl of α-Bruno sera (rabbit 1683) was coupled to 150 µl of PAS. IPs were incubated for 6 hrs at 4 °C in IP/wash buffer (50mM Tris (pH 7.5), 400mM NaCl, 2.5mM $MgCl_2$, 0.5% Triton-X-100 and 1 mM DTT) before beads were rinsed twice with 15ml of wash buffer and transferred to a 1.5 ml tubes. Beads were then washed 3 X 10 min with 1 ml of wash buffer + 1mg/ml heparin and then rinsed 2 more times with 1 ml of wash buffer. A final rinse was performed with wash buffer lacking Triton-X-100 before pellets were resuspended in 50 mM NaCl and phenol/chloroform extracted. All of the RNA recovered from each sample was processed and hybridized to GeneChip^R *Drosophila* genome arrays (Affymetrix) as described in (Bethin et al., 2003) and scanned images were analyzed using dChip analysis software (Zhong et al., 2003).

2.7 Generation of *Bic-C-lacZ* reporter constructs

To generate reporter constructs, the full-length *Bic-C* cDNA was subcloned into pGEX-5X-1 using its *Sal*I and *Not*I sites. The *Bic-C* ORF was then completely removed by digestion with *Kpn*I/*Sph*I, or partially removed with *Kpn*I/*Nhe*I or *Xho*I/*Nhe*I and replaced with the *β-gal* ORF, flanked by the same sites, to produce p*Bic-C-lacZ*-1, p*Bic-C-lacZ*-2 and p*Bic-C-lacZ*-4, respectively. The *β-gal* ORF inserts were produced by PCR amplification using pMC1871 (Pharmacia) as template with combinations of the following primers: Forward-*Xho*I: 5'-TACTCGAGGAATTCCCGGGGATCCC-3',
Forward-*Kpn*I: 5'-TTGGTACCATGGGAATTCCCGGGGATCCC-3',
Reverse-*Sph*I:5'-TTGCATGCTTATTTTTGACACCAGACCAACTG-3',
Reverse-*Nhe*I: 5'-TTGCTAGCTTATTTTTGACACCAGACCAACTG-3'.

To produce the *tub67C-Bic-C-lacZ* transgene, p*Bic-C-lacZ*-4 was digested with *Sal*I, blunt-ended, then digested with *Not*I. The resulting fragment was subcloned into a modified version of pDF313 (pDF313Δβ-gal, (Thio et al., 2000) that was cleaved with *NheI*, blunt-ended, and cleaved with *NotI*. To produce the *tub67C-Bic-C-lacZ*-Δ3'UTR transgene, p*Bic-C-lacZ*-4 was digested with *Sal*I, blunt-ended, and digested with *Nhe*I. The resulting fragment was subcloned into the *Pst*I (blunt-ended) and *Nhe*I sites of pDF313Δβ-gal.

p*Bic-C-lacZ*-2 was cleaved with *SalI/Nhe*I and the resulting fragment was subcloned into the *SalI/Xba*I sites of pBluescriptSK$^-$ (Stratagene) to produce p*Bic-C-lacZ*-2-Δ3'UTR, which was then cleaved with *Sal*I, blunt-ended, and cleaved with *Not*I. The resulting fragment was subcloned into the *HpaI/Not*I sites of pCOG to produce *otu-Bic-C-lacZ*-K10 3'UTR. p*Bic-C-lacZ*-2 was cleaved with *KpnI/Nhe*I and the resulting fragment was subcloned into the *KpnI/Spe*I sites of pBluescriptSK$^-$ to produce p*Bic-C-lacZ*-2-Δ5'/3'UTR, which was then cleaved with *Kpn*I, blunt-ended, and cleaved with *Not*I. The resulting fragment was subcloned into the *HpaI/Not*I sites of pCOG to produce *otu-Bic-C-lacZ*-K10 3'UTR-Δ5'UTR.

To produce *otu-Bic-C-lacZ* transgenes containing the *Bic-C* 3'UTR, the *K10* 3'UTR was removed from pCOG by digestion with *PstI/EcoR*I and replaced with a portion of the multiple cloning site from pSL1180 (GE Healthcare) flanked by *PstI/EcoR*I. I named the resulting plasmid pCOGΔK10. p*Bic-C-lacZ*-1 was cleaved with *Sal*I, blunt-ended, then cleaved with *Not*I. The resulting fragment was subcloned into the *HpaI/Not*I sites of pCOGΔK10 to produce the *otu-Bic-C-lacZ* transgene. To produce *otu-Bic-C-lacZ*-Δ5'UTR, p*Bic-C-lacZ*-1 was cleaved with *Kpn*I, blunt-ended, then cleaved

with *Not*I and the resulting fragment was subcloned into the *Hpa*I/*Not*I sites of pCOGΔK10.

The Δ1-196 *otu-Bic-C-lacZ*-1 transgene was generated by digesting p*Bic-C-lacZ*-1 with *Pmac*I and *Not*I and then sub-cloning the resulting fragment into the *Hpa*I/*Not*I sites of pCOGΔK10. To generate the Δ196-515 *otu-Bic-C-lacZ-1* transgene, p*Bic-C-lacZ*-1 was cleaved with *Pmac*I and *Sna*BI and then re-ligated to eliminate the intervening sequence. This construct was cleaved with *Sal*I, blunt-ended, then cleaved with *Not*I and the resulting fragment was subcloned into the *Hpa*I/*Not*I sites of pCOGΔK10. Finally, to generate the Δ515-789 *otu-Bic-C-lacZ-1* transgene, p*Bic-C-lacZ*-1 was digested with *Sna*BI and *Kpn*I, the *Kpn*I site was blunt-ended with the Klenow fragment and the construct was re-ligated, eliminating intervening sequences. This construct was then cleaved with *Sal*I, blunt-ended, then cleaved with *Not*I and the resulting fragment was subcloned into the *Hpa*I/*Not*I sites of pCOGΔK10.

2.8 X-gal stainings

Ovaries were hand-dissected from fattened 2-3 day old wild-type and *Bic-C*^{YC33} homozygous females, each bearing two copies of the respective *Bic-C-lacZ* transgenes. They were fixed for 10 min in buffered 1% glutaraldehyde, rinsed twice, and incubated at 37°C in staining solution (dissection buffer with 3 mM $K_3Fe(CN)_6$, 3mM $K_4Fe(CN)_6$ and 0.2% X-Gal) until color developed. In all cases where comparisons were made, control and mutant ovaries were developed for the same amount of time.

2.9 Western Blots

For Western analysis, samples were resolved on SDS-polyacrylamide gels and transferred to nitrocellulose membranes. Membranes were blocked overnight at 4°C in PBS + 0.1% Tween-20 + 5% skim milk powder, then probed with primary antibodies for 1.5 hrs at R.T. in PBS + 0.1% Tween-20 + 1% skim milk powder (this buffer was used in all subsequent steps). Membranes were then washed for 3 X 15 min at R.T. before probing with secondary antibodies (α-rabbit-HRP 1:5000 or α-mouse-HRP 1:3000, Amersham) for 45 min at R.T., followed by three 10 min washes. Proteins were then detected by chemiluminescence (NEN). Primary antibodies were used at: α-Bic-C 1:3000, α-Myst 1:1000, α-β-gal 1:1000 (Sigma), α-Grk 1:1000, α-alpha Tubulin 1:10,000 (DM1A, Sigma), α-deIF4A 1:2000, α-Orb 1:25 (clone 4H8, Developmental Studies Hybridoma Bank), α-NOT3 1:1000, α-HA 1:1000 (Sigma), α-GFP 1:1000 (clones 7.1/13.1, Roche), α-PABP 1:1000, α-Vasa 1:5000, α-Tral 1:1000.

2.10 Northern blots

Northern blots were prepared as described by (Fourney, 1988), using standard techniques. Briefly, total ovarian RNA was isolated using the RNeasy™ RNA extraction kit (Qiagen) and 15 μg of each sample was resolved on a 1% agarose, formaldehyde denaturing gel. RNA was then transferred O/N by capillary action to Hybond-N ™ membranes (Amersham) and auto-crosslinked in a UV Stratalinker™. The *β-gal* probe was generated by PCR from the pMC1871 plasmid (Pharmacia) using the following primers: forward: 5'-AATGGTCTGCTGCTGCTGAACG-3', reverse: 5'-ACATCCAGAGGCACTTCACC-3'. *otu* and R*pS15a* probes were generated from full-

length cDNAs. DNA probes were labeled with ^{32}P-dCTP using the Ready-To-Go DNA labeling kit (Amersham Biosciences) and unincorporated nucleotides were removed by passage through a G50 Sephadex column. Probes were diluted to a final activity of $1x10^6$ cpm/ ml in express-hyb™ buffer and all subsequent steps were carried out as instructed by the manufacturer (Clontech).

2.11 UASP-*Bic-C* constructs and Bic-C overexpression

To generate UASP-*Bic-C* constructs, both wild-type and Bic-C^{G296R} cDNAs were digested with *Eco*RI and the Bic-C ORF was subcloned into pBluescriptSK$^-$, and then into pUASP (Rorth, 1998) using flanking *Kpn*I and *Not*I sites. To achieve germline expression, flies were crossed to produce trans-heterozygous females bearing one copy of a UASP-*Bic-C* transgene and one copy of the *nosGal4::VP16* transgene (Van Doren et al., 1998).

2.12 Antibody stainings and *in situ* hybridizations

In situ hybridizations were performed as described by (Kobayashi, 1999) except that after initial fixation, samples were permeabilized and re-fixed as described in method A (without Proteinase K treatment) of (Nagaso et al., 2001). Antibody stainings were performed as described in (Hawkins et al., 1997) for Grk staining, except H_2O_2 treatment in methanol was omitted. Primary antibodies were used at the following concentrations: α-Bic-C, 1:1000; α-Grk, 1:1000; α-β-gal (Sigma), 1:1000; α-Orb (clone 4H8, Developmental Studies hybridoma bank), 1:25; α-Osk, 1:1000; α-Vas, 1:2000, α-Arm 1:1000. Primary antibodies were detected using Alexafluor-488 anti-mouse (1:500) and

Alexafluor-596 anti-rabbit (1:500) (Molecular Probes), after overnight pre-adsorption to wild-type ovaries. DNA was visualized by DAPI staining. Confocal images were acquired using a Zeiss LSM-510 microscope.

2.13 Fly strains and generation of transformants

Oregon-R (OreR) was the wild-type fly strain used. Transgenic flies were created by P-element mediated germline transformation of *yw* flies using either pUASP, DF313 or pCOG vectors, as described in (Spradling, 1986)

2.14 Genetic assays

To determine hatching frequencies and dorsal appendage numbers, virgin females of the genotypes of interest were mated to OreR males. For the first 36 hours, eggs were not counted. Eggs were then collected, counted and scored for dorsal appendage number and then allowed to incubate at 25 °C for 48 hours before being re-counted to determine the number of unhatched eggs.

2.15 Immunoprecipitations (co-IPs)

Immunoprecipitations and RNase treatments were performed essentially as described in Wilhelm et al., 2000, except that extracts were pre-cleared against protein-A Sepharose (Pharmacia) for 30-60 min at 4 °C, and after washing, bound proteins were eluted by boiling in Laemmli sample buffer. For every 10 mg of soluble ovarian protein extract, 80 µl of α-Bic-C sera or pre-immune sera (from the same rabbit) was used. For α-HA IPs, 30µl of α-HA resin (Sigma) was used for each IP.

2.16 Orthophosphate labeling and phosphoamino acid analysis

In vivo ^{32}P labeling of ovarian proteins, extract preparation and immunoprecipitations were carried out as described in (Lachance et al., 2002), with the exception that 20 µl of affinity purified α-Bic-C was used for immunoprecipitations. Subsequent phosphoamino acid analysis was performed as previously described (van der Geer and Hunter, 1994).

2.17 Generation of *Bic-C*^{WT} and *Bic-C*^{Y822F} rescue constructs

To generate the *Bic-C* mini-gene rescue constructs, a 1.9 Kb fragment of genomic DNA, starting at the first *Xba* I site upstream of the *Bic-C* gene and ending at a unique *Eco*RV in the *Bic-C* 5' UTR, was ligated to the same *Eco*RV site in the in the wild-type and Y822F *Bic-C* cDNAs. This sequence was cloned into the pCasper4 transformation vector using the *Xba*I site at the 5' end of the genomic fragment and the *Not*I site at the 3' end of the *Bic-C* cDNA.

2.18 Generation and purification of TAP-Bic-C

To generate the *UASP-TAP-Bic-C* construct, sequences encoding the TAP-tag were PCR-amplified from pZOME-N (Cellzome) and subcloned into the *Kpn*I site of *UASP-Bic-C* to produce an in-frame fusion with the *Bic-C* ORF. TAP-Bic-C expression was driven in ovaries using the *nos*Gal4::VP16 promoter and TAP-Bic-C was purified as described in Puig et al., 2001.

Section 3: Results

Chapter 1: Identification of Bic-C target mRNAs

3.1.1 Introduction

Since Bic-C contains five KH-type RNA-binding motifs and a point mutation in the third KH domain disrupts Bic-C function *in vivo* (Saffman et al., 1998), it is likely that the pleiotropic phenotypes observed in *Bic-C* mutants result from an inability to properly identify and regulate RNA substrates. To gain insight into the molecular nature of Bic-C function, I have sought to test whether Bic-C associates with mRNA *in vivo* and to identify specific mRNA targets.

3.1.2 The KH domains of Bic-C bind RNA directly and Bic-C is associated with ovarian mRNPs

Previous studies have shown that Bic-C, expressed in mouse tissue culture cells, associates with homopolymeric RNA *in vitro* (Saffman et al., 1998). However, Bic-C was not purified from whole cell lysates in these experiments. Therefore, direct binding to RNA was not definitively proven as this interaction could have been bridged by other RNA binding proteins (Chen et al., 1997). To establish clear evidence of direct RNA binding, a purified form of Bic-C is required. A major obstacle in characterizing the RNA-binding properties of Bic-C has been the inability to express and purify a soluble, recombinant full-length Bic-C protein. After experimenting with several different expression systems, I found that a fusion of the Maltose-Binding-Protein (MBP) to amino acids 85-462 of Bic-C (containing all 5 KH-domains; hereafter referred to as MBP-Bic-

C^{85-462}) allowed for sufficient recovery of pure protein from *E. coli (BL21)*. To determine whether the KH domains of Bic-C could bind RNA directly, MBP-Bic-C^{85-462} and MBP alone were incubated separately with either poly-G agarose beads or agarose beads as a negative control. After several washes, bound proteins were eluted by boiling in SDS sample buffer, resolved by SDS-PAGE and visualized in the gel by Gelcode™ staining (Fig. 3.1.1). MBP-Bic-C bound to poly-G agarose but not to agarose alone, indicating that binding was via poly-G and not a direct association with the matrix, whereas MBP did not demonstrate any binding, indicating that MBP-Bic-C^{85-462} binds to poly-G via moieties in Bic-C^{85-462} and not through MBP.

To determine if endogenous Bic-C associates with mRNA *in vivo*, mRNPs were isolated from ovarian lysates using oligo-dT cellulose after treatment with EDTA to dissociate polysomes (Spirin, 1986). mRNA and bound proteins are retained on the oligo-dT matrix via an interaction between the poly-A tails of mRNAs and oligo-dT. After several washes, bound proteins were eluted in SDS sample buffer, resolved by SDS-PAGE and analyzed by Western blotting (Fig. 3.1.2). This experiment demonstrates that Bic-C is enriched in the mRNP fraction, indicating an association (either direct or indirect) with mRNA *in vivo*. To ensure that this enrichment was not a general phenomenon, caused by non-specific binding, samples were also probed for an unrelated protein, CG2950, which we call Myst. Unlike Bic-C, this protein was not enriched in the mRNP fraction relative to the input sample (Fig. 3.1.2).

Figure 3.1.1 MBP-Bic-C$^{85-462}$ binds directly to homopolymeric RNA.

GelcodeTM staining of proteins resolved by SDS-PAGE (10 %) illustrate that the MBP-Bic-C$^{85-462}$ fusion protein binds homopolymeric RNA (poly-G), while MBP alone does not. Agarose beads were used as a negative control for poly-G-independent binding to the matrix. Input samples are equivalent to the total input added to each sample, while approximately 20% of each pull-down was loaded on the gel.

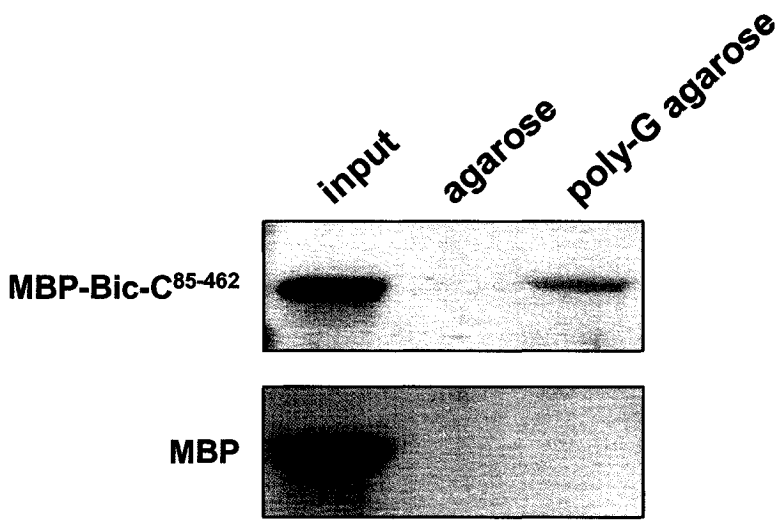
input
agarose
poly-G agarose
MBP-Bic-C85-462
MBP

Figure 3.1.2 Bic-C co-purifies with ovarian mRNPs.

Total ovarian proteins (input), the mRNP fraction (bound to oligo-dT cellulose) and a negative control (bound to cellulose alone) were analyzed by Western blotting with α-Bic-C and α-MYST antibodies. The amount of total protein (input) and of isolated mRNP samples (oligo-dT cellulose) were equivalent for both Western blots, indicating that Bic-C and not MYST is specifically enriched in the mRNP fraction.

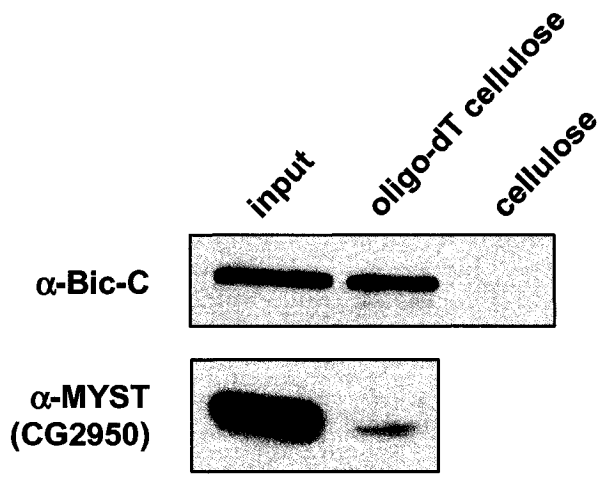
input
oligo-dT cellulose
cellulose
α-Bic-C
α-MYST
(CG2950)

3.1.3 Analysis of Bic-C-associated mRNAs by differential display RT-PCR

To identify potential mRNA targets of endogenous Bic-C *in vivo*, complexes containing Bic-C were isolated from ovarian extracts by immunoprecipitation (IP) using affinity-purified α-Bic-C. Co-precipitating mRNAs were identified by differential display reverse transcription PCR (DD-RT-PCR) with various combinations of primers that bind target sequences by chance homology. Pre-immune serum was used in parallel IPs as a control for non-specific binding. Through this work I recovered a fragment of the *Bic-C* 3' UTR (nucleotides 3640-3937) specifically from the Bic-C IP over a broad range of salt concentrations (Fig. 3.1.3-A). The association between Bic-C protein and mRNA was confirmed from independent α-BicC IPs using *Bic-C*-specific primers, while primers for the abundant *chorion protein 18 (cp18)* transcript controlled for non-specific binding (Fig. 3.1.3-B). The interaction was resistant to high concentrations of yeast tRNA competitor, and recovery of a PCR product required reverse transcriptase, demonstrating that the association was with RNA and not DNA. To ensure that co-precipitation of *Bic-C* mRNA was not a result of immunoprecipitating the nascent chain of Bic-C during translation, identical IPs were conducted where EDTA was added to lysates, IP buffers and washes, at a sufficient concentration (30 mM) to dissociate polysomes (Spirin, 1986). This treatment had no effect on the interaction (Fig. 3.1.4), indicating that this interaction is not dependent on an indirect association through the ribosome.

Figure 3.1.3 Bic-C protein associates with *Bic-C* mRNA *in vivo.*

(A) Radiolabeled RT-PCR products generated from Bic-C IPs (lanes 1, 3 and 5) or from pre-immune sera IPs (lanes 2, 4 and 6) with Clontech™ P1/T8 primers, isolated with 200mM (lanes 1, 2), 400mM (lanes 3, 4) or 800mM NaCl (lanes 5, 6) in the IP wash buffers. The marked band corresponds to nucleotides 3640-3937 of the *Bic-C* transcript.

(B) The presence of *Bic-C* mRNA within the Bic-C mRNP complex was confirmed with transcript-specific primers for *Bic-C*. The absence of *cp18* (an abundant ovarian transcript) in the complex demonstrates that Bic-C associates with a specific subset of mRNAs *in vivo*.

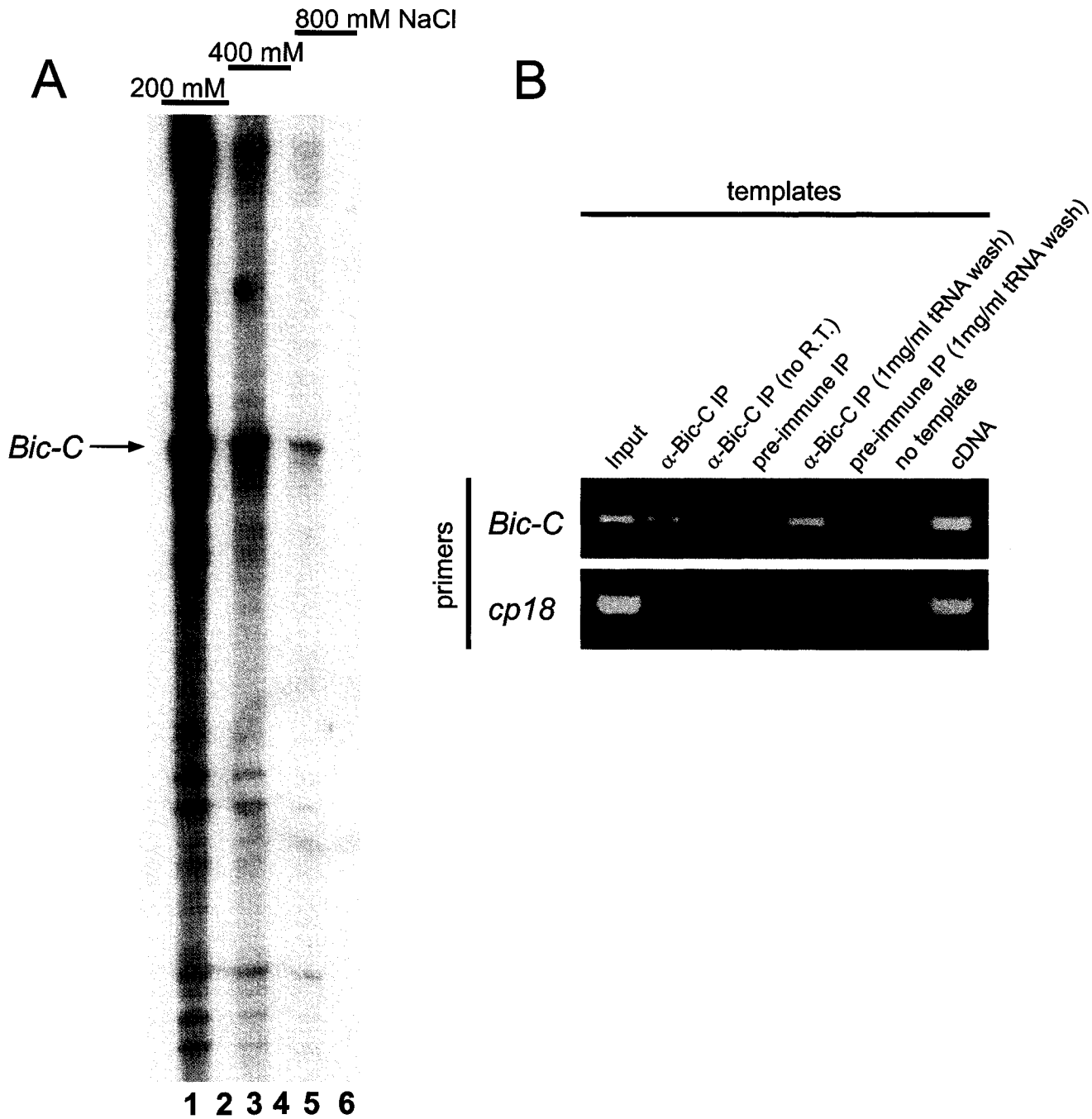
A
800 mM NaCl
400 mM
200 mM
Bic-C
1 2 3 4 5 6
B
templates
Input
α-Bic-C IP
α-Bic-C IP (no R.T.)
pre-immune IP
α-Bic-C IP (1mg/ml tRNA wash)
pre-immune IP (1mg/ml tRNA wash)
no template
cDNA
primers
Bic-C
cp18

Figure 3.1.4 The presence of *Bic-C* mRNA within the Bic-C mRNP complex is not dependent upon intact polysomes.

RT-PCR with transcript specific primers detects *Bic-C* mRNA in α-Bic-C immunoprecipitates (lane 2) but not in control IPs (lane 3). Treatment with 30 mM EDTA to dissociate polysomes does not disrupt this interaction (lane 4). Primers for *cp18* were used as a negative control for non-specific mRNA binding.

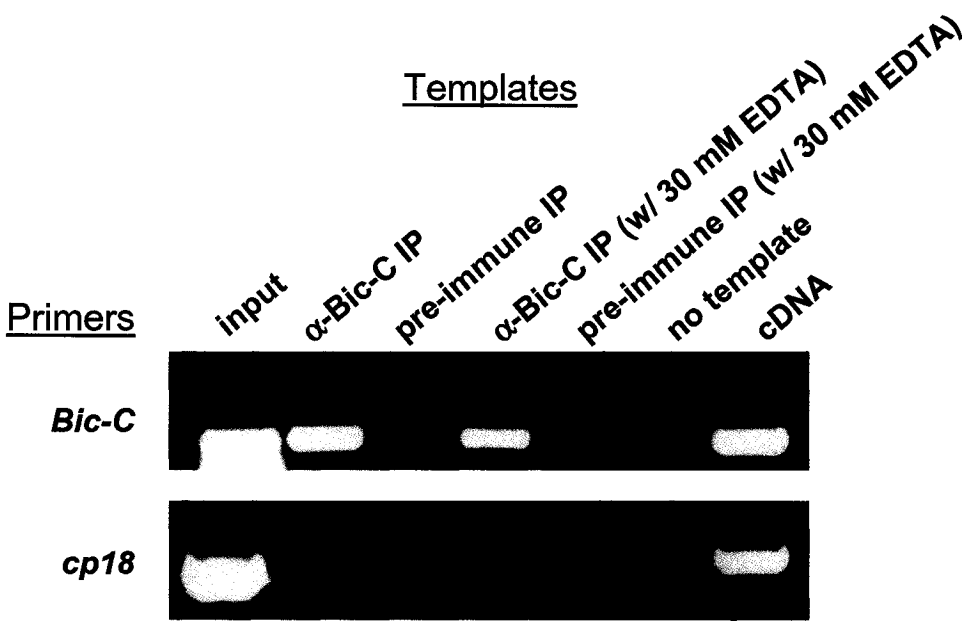
Templates
Primers
input
α-Bic-C IP
pre-immune IP
α-Bic-C IP (w/ 30 mM EDTA)
pre-immune IP (w/ 30 mM EDTA)
no template
cDNA
Bic-C
cp18

3.1.4 Identification of Bic-C associated mRNAs through interrogation of Affymetrix™ microarrays

A caveat of the differential display RT-PCR approach is that there is no way to be certain that the screen has been saturated, as well as the time-consuming and labor-intensive nature of the technique. Therefore, as the technology became available I expanded this line of experimentation to include a more comprehensive analysis of Bic-C-associated mRNAs using Affymetrix™ microarrays. Two independent α-Bic-C antibodies were used to isolate Bic-C-containing complexes from ovarian extracts and co-purifying mRNAs were identified by interrogating microarrays representing 13,500 different *Drosophila* genes. In these experiments, *Bic-C* mRNA displayed the highest average enrichment over pre-immune controls (93-fold), (Table 3.1.1). Remarkably, among the 53 most-highly enriched Bic-C associated mRNAs identified in this experiment, 7 have defined roles in the Wnt/Frizzled/Dishevelled signaling pathway (listed in bold). All transcripts found to be enriched 4 fold or greater in both experimental trials, relative to pre-immune controls, are listed in Table 3.1.1.

In a parallel experiment, Bruno-containing mRNP complexes were isolated and analyzed by a similar microarray-based comparison to a rabbit sera control IP (Table 3.1.2). A 5.25-fold enrichment of *osk* mRNA, a known target of Bruno (Kim-Ha et al., 1995), was observed in this experiment, indicating that this technique is suitable for detecting biologically relevant interactions. Furthermore, MEME sequence alignments (Bailey, 1994) identified Bruno response elements (BREs) in the 3' UTRs of several of the Bruno-associated transcripts, suggesting that Bruno may bind to these mRNAs directly (Fig. 3.1.5).

Table 3.1.1 Bic-C-associated mRNAs identified using Affymetrix microarrays.

IP/PI exp1	IP/PI exp2	Ave. enrich't over PI	Gene Name	Functional Data / Domains
73.71	112.47	93.09	*BicC*	anterior patterning determinant, KH-type RNA-binding protein
45.90	72.73	59.32	*CG10984*	N/A
39.30	36.17	37.73	*CG15199*	N/A
10.47	54.47	32.47	*CG11737*	N/A
16.58	44.17	30.38	*CG13016*	N/A
27.04	27.99	27.52	*CG9213*	N/A
32.51	20.54	26.53	*CG12112*	N/A
4.37	**47.50**	**25.94**	***par-1***	**Dishevelled-associated kinase, Microtubule polarity, Osk stabilization**
25.43	25.91	25.67	*CG3353*	N/A
29.36	14.88	22.12	*CG10476*	N/A
38.31	**5.75**	**22.03**	***diego (CG12342)***	**regulator of dishevelled**
6.12	37.63	21.88	*Hil*	regulator of neuronal cytokinesis and Septin function
4.70	38.18	21.44	*CG17293*	microtubule severing, WD40 domain
6.83	34.62	20.72	*CG3279*	vesicle mediated transport, V-snare domain
19.14	18.07	18.60	*CG13795*	neurotransmitter transport, Sodium neurotransmitter symporter domain
13.36	23.31	18.33	*MED17*	transcriptional co-activator, component of mediator complex
4.25	31.75	18.00	*Dip2 / Sip4*	Septin / Dorsal interacting protein
21.09	13.95	17.52	*Trypsin*	Protease
5.36	24.97	15.17	*CG4646*	DUF866 domain
5.38	24.60	14.99	*CG7082*	mRNA-binding, 2 KH and 1 Tudor domain
7.46	22.52	14.99	*PPP4R2r*	Rho GTPase activation domain
6.58	**21.28**	**13.93**	***Rheb***	**G-protein coupled receptor signaling, cell growth / division, Ras GTPase domain**
11.72	16.11	13.92	*CG18812*	N/A
5.27	20.60	12.93	*isopeptidase-T-3*	member of the ubiquitin specific protease family
5.64	19.99	12.81	*CG13489*	N/A
15.68	9.85	12.76	*CG30503*	N/A
9.85	15.46	12.65	*Tsp86D*	cell-cell adhesion, signal transduction
4.64	**19.87**	**12.25**	***slmb***	**regulator of Wnt / Frizzled signaling, component of Ubiquitin ligase complex**
6.04	18.27	12.15	*CG7912*	high affinity sulfate permease activity
13.70	10.52	12.11	*Trxr-2*	thioredoxin-disulfide reductase activity
18.00	5.97	11.99	*CG18476*	Transcription regulator activity, zinc ion binding
11.48	**12.23**	**11.86**	***Cip4***	**Rho GTPase binding, CDC42 effector, actin cytoskeleton organization**
13.66	9.95	11.81	*CG7646 /// Nca*	calmodulin / calcium ion binding, calcium-mediated signaling
10.15	12.68	11.41	*CG17370*	N/A

17.39	5.41	11.40	*CG4332*	N/A
4.97	17.00	10.98	*CG7058*	N/A
5.13	16.77	10.95	*CG18769*	N/A
6.47	15.26	10.86	*CG3860*	oxysterol / nucleic acid binding, cholesterol metabolism, lipid transport
13.23	7.86	10.55	*CG13443*	N/A
6.24	14.82	10.53	*staufen*	ds-RNA binding, required for *bicoid / oskar / prospero* mRNA localisation
11.38	9.23	10.30	*CG16807*	ubiquitin-protein ligase activity, component of ubiquitin ligase complex, nucleic acid binding
4.21	15.78	9.99	*att-ORFB*	alternative testis open reading frame B
6.37	13.59	9.98	*CG2063*	N/A
8.92	11.01	9.96	*CG14117*	nucleic acid binding, zinc ion binding
7.13	12.76	9.94	*disconnected*	transcription factor, brain development, circadian / eclosion / locomotor rythm
5.67	14.08	9.87	*CG40485*	oxidoreductase activity
6.64	12.61	9.62	*Cp190*	microtubule / nucleic acid binding, component of centrosome
8.66	10.54	9.60	*Brf (CG5419)*	transcription factor binding, component of transcription factor TFIIIB complex
12.07	**7.13**	**9.60**	***dishevelled***	**frizzled / wnt signaling, component of adherens junction**
8.51	10.13	9.32	*CG31150*	lipid transporter activity
13.81	4.59	9.20	*CG12314*	N/A
8.11	**10.28**	**9.20**	***Src42A***	**Tyr kinase, JNK signaling, forms ternary complex w/ E-Cadherin / β-Catenin**
8.57	9.79	9.18	*lectin-30A*	galactose binding
4.07	14.21	9.14	*CdsA (CG7962)*	CDP diglyceride synthetase, component of ER
4.77	13.34	9.06	*CG31915*	procollagen-lysine 5-dioxygenase activity
10.68	6.73	8.71	*CG3740*	N/A
4.39	12.89	8.64	*CG8783*	N/A
7.02	10.21	8.62	*Klp10A (CG1453)*	microtubule motor, mitotic sister chromatid segregation, component of kinesin complex
11.35	5.17	8.26	*CG6444*	N/A
9.41	6.91	8.16	*RecQ4*	ATP-dependent DNA helicase activity
8.38	7.69	8.04	*CG15645*	N/A
4.63	11.25	7.94	*TfIIE*	transcription factor TFIIE complex
5.61	9.85	7.73	*CG5807*	N/A
5.44	9.67	7.55	*phtf (CG3268)*	putative homeodomain transcriptional factor
7.16	7.56	7.36	*CG5693*	N/A
5.78	8.52	7.15	*CG8281*	N/A
5.35	8.83	7.09	*Obp44a*	Odorant-binding protein
6.16	7.77	6.97	*CG9636*	N/A
8.68	5.22	6.95	*CG5366*	transcription regulator activity
5.62	7.46	6.54	*CG7565*	chitinase activity
6.80	5.93	6.37	*CG30022*	hydrolase/lyase activity, oxygen and reactive oxygen species metabolism
4.83	7.85	6.34	*CG14442*	N/A
5.08	7.33	6.21	*CG2843*	N/A

4.33	8.05	6.19	*CG9070*	transporter activity
6.26	5.98	6.12	*CG33298*	phospholipid-translocating ATPase, cation/phospholipid transport, membrane protein
4.29	7.95	6.12	*GstE5*	glutathione transferase activity, oxygen and reactive oxygen species metabolism
5.19	7.03	6.11	*CG6138*	N/A
5.55	6.17	5.86	*CG4286*	N/A
7.29	4.37	5.83	*CG3281*	transcription factor
6.15	5.16	5.65	*CG12728*	N/A
5.60	4.35	4.97	*CG4398*	N/A
4.22	5.47	4.84	*CG7911*	nucleic acid binding
5.09	4.56	4.82	*CG8594*	Chloride transport
4.28	4.82	4.55	*RhoGAP18B*	actin filament organization, GTPase activator

Table 3.1.2 Bruno-associated mRNAs identified using Affymetrix™ microarrays.

	Enrichment over PI	Transcript
1	42.37	cAMP-dependent protein kinase 2
2	14.47	CG13848 (alpha-tocopherol transfer protein-like)
3	7.96	CG15575
4	7.58	CG7823 (Rho GDP-dissociation inhibitor 1-like)
5	7.27	CG4239
6	7.12	Calcium/calmodulin-dependent protein kinase
7	7.06	CG12930 (glutathione transferase)
8	6.55	CG1847 (chaperone)
9	6.53	CG7034 (chaperone)
10	5.99	CG5568 (luciferase-like)
11	5.72	CG8102 (NADH dehydrogenase)
12	5.60	CG13603
13	5.59	CG3831
14	5.50	CG3689
15	5.50	CG15574
16	**5.25**	**oskar**
17	5.17	CG14516 (membrane alanine aminopeptidase)
18	4.94	CG4532 (chaperone)
19	4.85	GH02974 (FBgn0028503)
20	4.78	CG3875 (RNA-binding protein)
21	4.71	CG13323
22	4.69	rhodopsin 1
23	4.67	CG8767 (protein serine/threonine kinase)
24	4.57	CG5272
25	4.48	CG2264 (cell adhesion protein)
26	4.30	CG18543
27	4.24	CG6144
28	4.15	CG5822 (ankyrin-like protein)
29	4.12	Mei-910 (CG4249)
30	4.12	CG4946
31	4.12	CG8186
32	4.12	CG8538 (signal transduction protein)
33	4.11	Porcupine
34	4.11	CG4658
35	4.07	par-6
36	4.00	MAP kinase activated Protein-Kinase-2
37	4.00	CG11851

Figure 3.1.5 Multiple sequence alignments of Bruno-associated mRNAs reveal Bruno Response Elements (BREs).

Multiple sequence alignments of the 3' UTRs of Bruno-associated mRNAs using MEME software (Bailey, 1994) identified the BRE as a consensus sequence. Sequences matching the BRE consensus in individual transcripts are boxed. The P-value represents the probability of a random sequence of equivalent length having the same match score or higher to the multilevel consensus sequence.

BRE consensus

Multilevel consensus sequence

TTGTATATTTTTGTTTGTTTTTTTGTTTTA
ACA TAT A A T A T ACGA T AC T
T G G G G

NAME	START	P-VALUE	SITES
Oskar	207	4.78e-12	TAGTCCATTA TTGTATATTATTGTGTGTTTTGTGTTCTA TGTTAGATTT
CG1847	476	3.11e-10	TTGTCCATAG TCGTATATGTATGTTTGTATTGTATTGTA TATCCCTATA
CG4532	421	2.46e-09	ATTTACCCAT ACATATATGTTCGTGTTTTTTGTGTGCTA TTTAAGTAGT
CG5568	49	1.14e-08	TGTATTTTTA TTGTATTTGTATTTGTATTTGTTGTATTT ATCGTAAGCT
CG4532	351	3.16e-08	TGTTAAACGT TTTTATATTTGTGTATGTCCTTTTTTTTA TTTTGTTTAA
porcupine	339	3.57e-08	TGATTTTTTA ATGTATATTTTTCTTTGTTGTTGGTTTTG TTTTGCTTTT
CG6144	243	8.09e-08	CATTGTGTAC ATATATATAAATGTTTGTATTACGTATTA CGGAGCAATA
CG4239	321	1.26e-07	GATTGGTAGG ATTTTTTTGTTGGTTTTTTTTTTTTTTT GGAGAACAAG
CG4532	382	1.41e-07	TTTTTTTATT TTGTTTAATTGTGTGTGTTTTAACTTTTG ATTTACCCAT
porcupine	395	3.24e-07	TGTTGGTTGG TTGTTTTCGTTTGTTTGTTTTCTCATTGA GACAAATATT
CG5822	45	3.24e-07	TCGTTACGGT TTAAATATCTTTGTTTATTGAGTCTGTTA ACACGTTTTC
CG7823	651	3.24e-07	TATTCTAACT ATATATCTCTGTGTATTTTTTGTGTACAA CATACCATAT
CG5884	1621	5.30e-07	AAAGAAAACC TTATATTTTGATGTATGTATTATTATTTT TTAATAAACC
porcupine	546	6.42e-07	CTGTGGCCTA TCGTTTGTGTTTTCATTTACTTTGTTTTT CCGCGCTTAC
CG5884	556	7.74e-07	TTTTCCTGGC ATATATATATATGTGTATTTAAATTTGTA AGATTTACGT
CG5822	133	1.02e-06	GAAATTGCAT ACGTCCTTATTTGTTTGCATTGTGTGCGA GATCGATTGT
CG4239	277	1.22e-06	GTGTAAGCCC TCGAAAATTTTAATTTGTTTTGTTTTGGT AATTTGATTG
Oskar	484	1.59e-06	ATTGCAATGC TTATAAACTGTTTTTTGTTCTATATACTT TTGTGTGGGT
Oskar	921	2.85e-06	TTATTTATTG TCTTGAATGTATGTTAATTGTATGTATTG ATGGTGATCA
CG7034	191	2.85e-06	GACCCGTTGA ACGTGTAAAATTGTATTTTGAATTTTTGA TTCTTATGTA
porcupine	629	3.35e-06	TGCAATGACA ATAAAAATATTTTTATTTACTTTGTTGAA
porcupine	310	3.35e-06	GCATACGAAT TTGTTCAAATATTTTTTATTGATTTTTTA ATGTATATTT
CG13848	222	3.93e-06	GTTGTGTTAA TCATCAATGTTATCTTTTTTTTTTTTGCTT AATAAAGTGT
CG5884	958	4.25e-06	CCATTTGTAA TTTTTAACTTTTGTTTTTTCGTCATTGTG TCCAATACTC
CG13603	198	4.59e-06	TATGTAATGT ATATATATATATATGTATTTTAATTAATTA TTCCATGTTA
porcupine	114	5.77e-06	ATCTATCTAT TCGTATCTTGTAGTCTGTGTGCTGTGTGA GTACTTAATA
CG5884	594	6.21e-06	AAGATTTACG TCTTGTTATTATTCTTGCTTGTTGTATTA GACTAGAGTG
CG5568	11	6.69e-06	TTTTGCATAT TTAATTATTGTAATGTTTATGTTGTATTT GTATTTTTAT
CG13848	192	7.20e-06	CGTTAAACCT TTTTAAAAAAGGTTATTTTCGTTGTGTTA ATCATCAATG
CG4658	178	9.60e-06	TTCGGTTTAC TTGTTTTTCTTTCTATTATCAGTGTTTAG TACTCGATTT

Chapter 2: Auto-regulation

3.2.1 Introduction

Several RNA-binding proteins bind to the mRNA transcripts that encode them. Examples include the extensively studied FMR1 and Nova1 proteins (Buckanovich and Darnell, 1997; Ashley et al., 1993). The finding that Bic-C protein associates with its own mRNA suggests that it may regulate its own expression.

3.2.2 Bic-C negatively regulates its own expression through the *Bic-C* 5'UTR

To determine whether Bic-C regulates its own expression through a post-transcriptional mechanism, I generated several *Bic-C-lacZ* transgenic fly lines that express the *β-gal* open reading frame (ORF), flanked by the *Bic-C* 5' and 3' untranslated regions (UTRs) (Fig. 3.2.1). These transgenes employed the *α-tubulin 67C* transcriptional promoter (Thio et al., 2000). Expression levels of β-gal protein from these transgenes were dramatically higher in homozygous *Bic-C* mutant ovaries than in wild-type (Fig. 3.2.2-A), suggesting that Bic-C negatively regulates its own expression. Deletion of the *Bic-C* 3' UTR did not disrupt Bic-C mediated repression, although somewhat higher expression was observed in wild-type, relative to mutant, extracts (Fig. 3.2.2-A). These results were confirmed by assessing β-gal activity in whole-mount ovary preparations, using a second series of *Bic-C-lacZ* transgenes under the control of a different promoter, *ovarian tumor* (*otu*) (Tirronen et al., 1995). I found that *otu-Bic-C-lacZ* transcripts bearing both *Bic-C* UTRs were still subject to Bic-C mediated repression (Fig. 3.2.2-B), indicating that the effect is promoter-independent. In contrast, transcripts

Figure 3.2.1 Schematic of Bic-C-lac-Z reporter constructs.

Schematic representation of the *Bic-C lac-Z* reporter constructs used to test Bic-C auto-regulation. All constructs contain the same β-galactosidase ORF, flanked by complete or partial segments of the Bic-C UTRs.

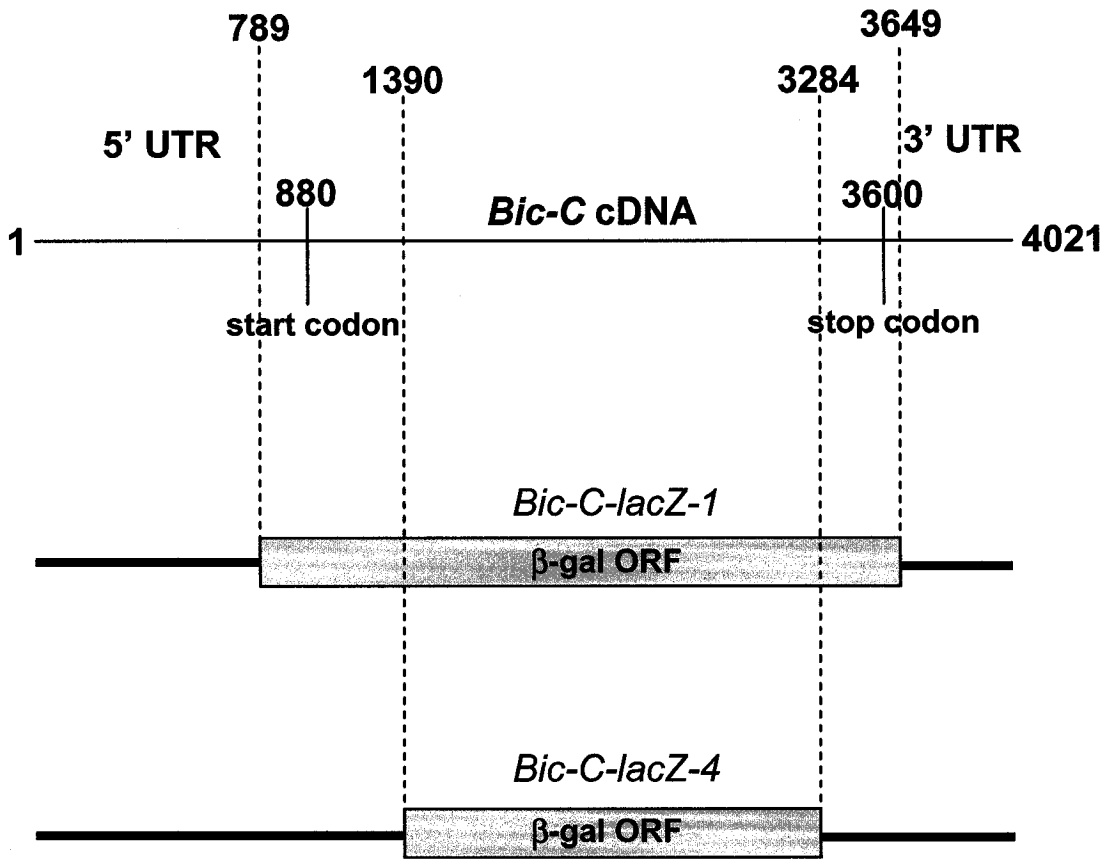
789
1390
3649
3284
5' UTR
3' UTR
880
3600
Bic-C cDNA
1
4021
start codon
stop codon
Bic-C-lacZ-1
β-gal ORF
Bic-C-lacZ-4
β-gal ORF

Figure 3.2.2 Bic-C auto-repression is mediated through *cis*-elements within its 5'UTR.

(A) Immunoblots of ovarian extracts from wild-type and homozygous *Bic-C*^{YC33} females, each bearing two copies of an *α-Tub67C-Bic-C-lacZ* reporter transgene with the complete *Bic-C* 5' and 3' UTR (left panel) or with the *Bic-C* 5' UTR alone (right panel). β-gal protein is increased in the *Bic-C* mutant extract as compared to wild-type, while eIF4A levels are equivalent.

(B-E) X-gal staining of wild-type (above dashed line) and homozygous *Bic-C*^{YC33} mutant (below dashed line) ovaries each bearing two copies of the *otu-Bic-C-lacZ* reporter transgenes illustrated.

(F) Northern blots of 10 μg total ovarian RNA from wild-type and *Bic-C*^{YC33} females show that *otu-Bic-C-lacZ* reporter transcript levels increase in *Bic-C* mutant ovaries as compared to endogenous *otu* and *RpS15A* mRNAs.

Note that the *α-Tub67C-Bic-C-lacZ* reporter transgenes (A) are based on the *Bic-C-lacZ-4* construct, while the *otu-Bic-C-lacZ* reporter transgenes (B-F) are based on the *Bic-C-lacZ-1* construct.

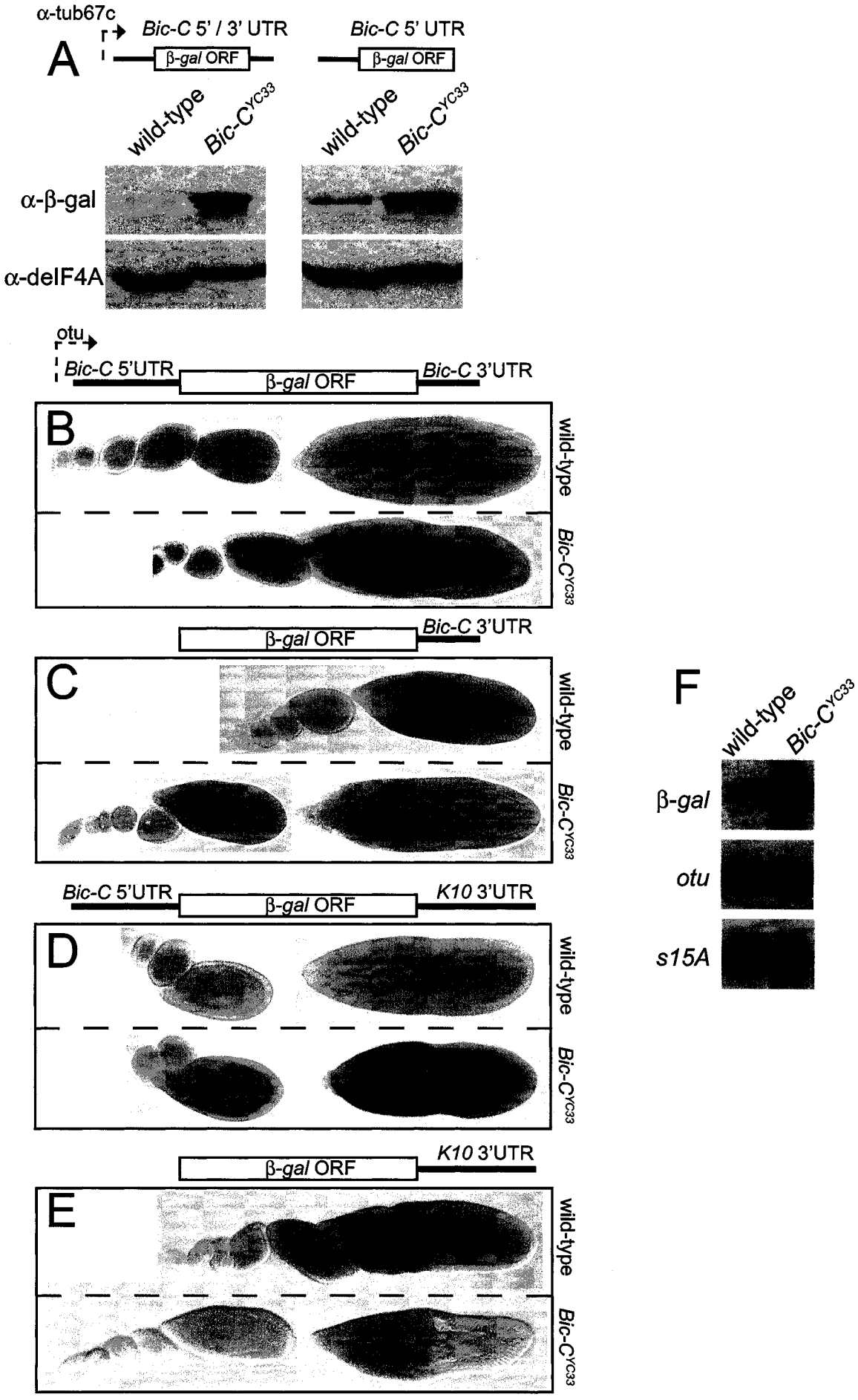
α-tub67c
A
Bic-C 5' / 3' UTR
β-gal ORF
Bic-C 5' UTR
β-gal ORF
wild-type
Bic-CYC33
wild-type
Bic-CYC33
α-β-gal
α-delF4A
otu
Bic-C 5'UTR
β-gal ORF
Bic-C 3'UTR
B
wild-type
Bic-CYC33
β-gal ORF
Bic-C 3'UTR
C
wild-type
Bic-CYC33
Bic-C 5'UTR
β-gal ORF
K10 3'UTR
D
wild-type
Bic-CYC33
β-gal ORF
K10 3'UTR
E
wild-type
Bic-CYC33
F
wild-type
Bic-CYC33
β-gal
otu
s15A

bearing the *Bic-C* 3' UTR but lacking the 5' UTR were not overexpressed in *Bic-C* mutant ovaries (Fig. 3.2.2-C). Transcripts containing the *Bic-C* 5' UTR and the *fs(1)K10* 3' UTR were still overexpressed in *Bic-C* mutant ovaries, however, deletion of the 5' UTR from this transgene abolished this effect (Fig. 3.2.2-D,E). Northern blotting indicated that *otu-Bic-C-lacZ* transcript levels are also elevated in *Bic-C* mutant ovaries (Fig. 3.2.2-C), and that the effect is promoter-independent, given that the level of endogenous *otu* mRNA does not increase in *Bic-C* mutant ovaries (Fig. 3.2.2-C). β-Gal activity from *otu-Bic-C-lacZ* transgenes was similarly elevated in a different *Bic-C* mutant ($Bic\text{-}C^{AA4}$), indicating that second-site mutations are not responsible for this overexpression effect (Fig. 3.2.3-A,B). The level of β-Gal expression from these same transgenes was also compared in wild-type and $Bic\text{-}C^{YC33}$ homozygous ovaries by Western blotting (Fig. 3.2.3-C).

I conclude that the *Bic-C* 5' UTR is both necessary and sufficient to impart Bic-C mediated repression, although the increase in β-gal protein levels in $Bic\text{-}C^{YC33}$ mutant ovaries relative to wild-type is greatest when both 5' and 3' UTRs are present. Analysis of smaller deletions within the *Bic-C* 5' UTR indicated that nucleotides 291-488 and 515-789 are dispensable for Bic-C mediated repression, while a deletion of nucleotides 196-515 abolishes auto-regulation (Fig. 3.2.4). . These results place potential auto-regulatory elements between nucleotides 196-291 and/or 488-515. Interestingly, the latter nucleotides reside within a region of the *Bic-C* 5' UTR that is highly conserved between *D. melanogaster* and *D. psuedoobscura* (Fig. 3.2.5) (Frazer et al., 2004). Transgenic flies bearing a deletion of nucleotides 1-196 were also generated but were uninformative since

Figure 3.2.3 β-Gal expression from *Bic-C-lac-Z* reporter transcripts is elevated in multiple, independently generated *Bic-C* mutants.

X-gal staining illustrates the level of β-Gal protein expression from the *otu-Bic-C-lacZ-1* transgene in wild-type (A, top) and *Bic-C*^{AA4} homozygous egg chambers (A, bottom). β-Gal expression from the *otu-Bic-C-lac-Z-4* transgene is similarly visualized in wild-type (B, top) and *Bic-C*^{AA4} homozygous egg chambers (B, bottom).

(C) The total level of β-Gal expression from the *Bic-C-lacZ-1* and *Bic-C-lacZ-4* transgenes is compared, by Western blotting, in wild-type and homozygous *Bic-C*^{YC33} ovaries. Equivalent levels of eIF4A indicate even loading.

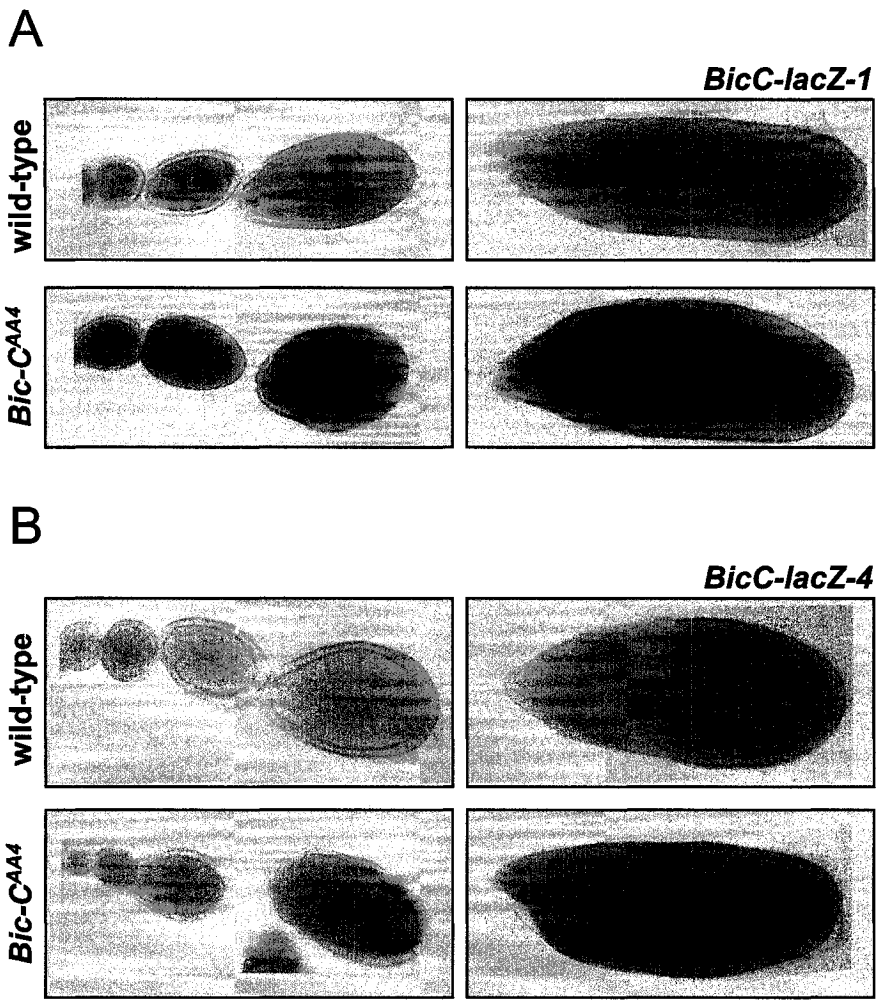
A
BicC-lacZ-1
wild-type
Bic-C^AA4
B
BicC-lacZ-4
wild-type
Bic-C^AA4
C
wild-type
BicC^YC33
wild-type
BicC^YC33
α–βGal
α-eIF4A
BicC-lacZ-1
BicC-lacZ-4

Figure 3.2.4 Deletion mapping of *cis*-acting auto-regulatory elements in the *Bic-C* 5' UTR.

A schematic of *otu-Bic-C-lacZ-1* constructs with deleted segments of the 5' UTR and accompanying X-gal stains illustrating the potential positions of *cis*-acting auto-regulatory elements.

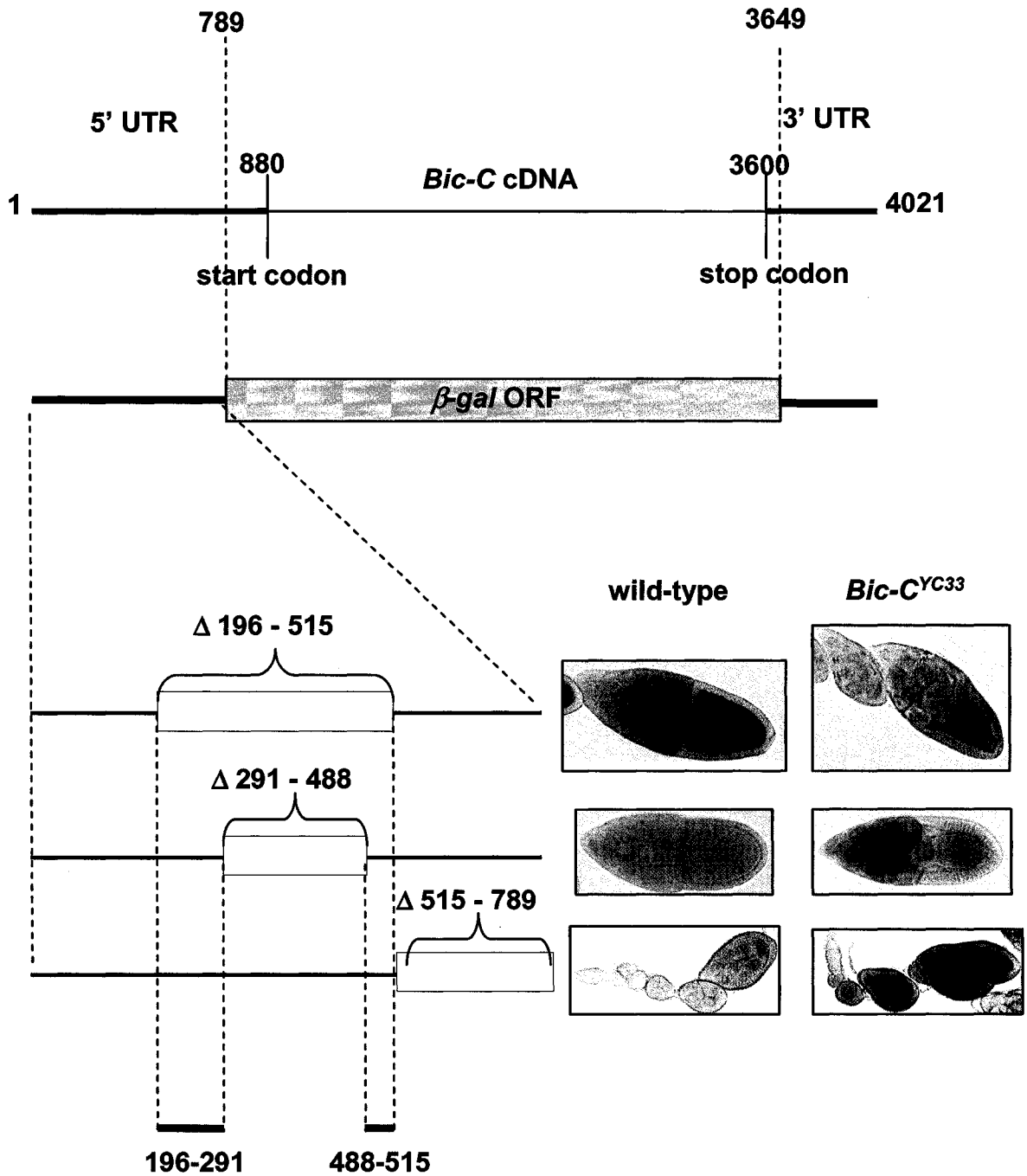

Potential Bic-C response elements

Figure 3.2.5 Sequence alignments reveal regions of the *Bic-C* 5' UTR that are highly conserved between *D. melanogaster* and *D. psuedoobscura.*

Four regions of the *Bic-C* 5'UTR that are highly conserved between different species of *Drosophila* are highlighted. The third region (nucleotides 474-570) overlaps potential *cis*-acting auto-regulatory elements.

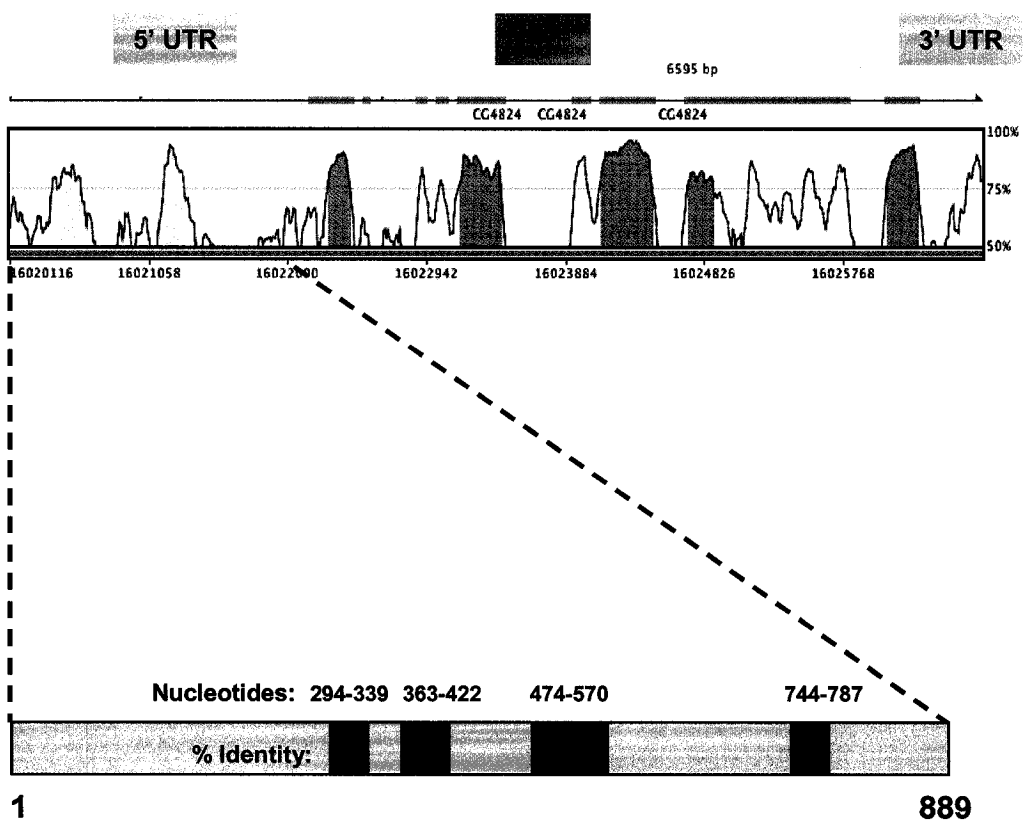
5' UTR
3' UTR
6595 bp
CG4824
CG4824
CG4824
100%
75%
50%
16020116
16021058
16022000
16022942
16023884
16024826
16025768
Nucleotides: 294-339 363-422 474-570 744-787
% Identity:
1
889

β-gal expression was below detectable thresholds in all of the lines recovered (data not shown).

Taken together, these results strongly suggest that Bic-C regulates its own expression through a negative feedback loop by specifically destabilizing its own transcript via *cis*-acting elements within its 5' UTR.

Chapter 3: Bic-C overexpression

3.3.1 Introduction

Reduced maternal *Bic-C* activity produces patterning defects, indicating that *Bic-C* is highly dosage-sensitive. This is exemplified by the dominant embryonic patterning defects that result from decreasing the dose of maternal Bic-C with chromosomal deletions (Mahone et al., 1995). An auto-regulatory mechanism in which "free" Bic-C suppresses the production of additional Bic-C could ensure that the correct stoichiometry is maintained between Bic-C and its mRNA targets and/or other interacting proteins. The evolution of such a mechanism implies that over-production of Bic-C would have negative consequences on the developmental program.

3.3.2 Overexpression of Bic-C antagonizes pole plasm assembly, posterior patterning and pole cell specification.

To examine the developmental consequences of Bic-C overexpression, I produced transgenic flies carrying *UASP-Bic-C* transgenes which contained the full *Bic-C* ORF but lacked the 5' UTR and contained the *fs(1)K10* 3' UTR instead of the *Bic-C* 3' UTR (Fig. 3.3.1). Efficient germline expression was achieved using a *nosGal4::VP16*

Figure 3.3.1 Schematic of *UASP-Bic-C* expression construct.

To eliminate the *Bic-C* UTRs, the *Bic-C* ORF was first subcloned into pBluescript using flanking *Eco*RI sites. The surrounding *Kpn*I and *Not*I sites in the pBluescript poly-linker were then used for directional cloning of the *Bic-C* ORF into UASP.

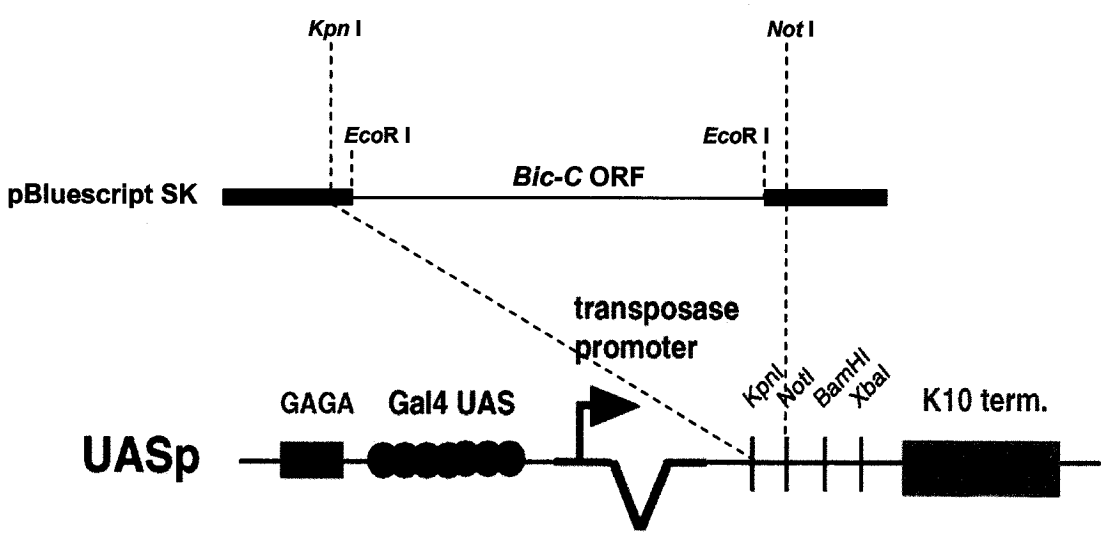

Modified from Rorth, 1998.

driver (Van Doren et al., 1998) (Fig. 3.3.2). The consequences of Bic-C overexpression were severe. The hatching frequency of eggs produced by *Bic-C* overexpressing females was approximately 2-8%, and 50% of the eggs that were laid did not initiate nuclear divisions. Most of the remaining embryos produced by *Bic-C* overexpressing mothers (referred to as *Bic-C* O/E embryos) exhibited fusion and/or loss of posterior segments, as revealed in cuticle preparations (Fig. 3.3.3) and by *in situ* hybridization for *ftz* mRNA (Fig. 3.3.4, A-C). Since posterior patterning is linked to pole cell formation, 3-6 hr embryos were stained for Vasa (Vas) (Lasko and Ashburner, 1990), to determine if pole cell specification is affected by maternal *Bic-C* overexpression. I found that 67% of the *Bic-C* O/E embryos that survived to gastrulation lacked pole cells, and the remainder contained an average of only 10, unlike wild-type controls that contained an average of 30 (Fig. 3.3.4, D-F). Since posterior accumulation of *osk* mRNA and protein are prerequisites for both pole cell formation and posterior somatic patterning, the distribution of *osk* was analyzed by *in situ* hybridization in 0-2 hr embryos. In contrast to wild-type (Fig. 3.3.4-G), >90% of *Bic-C* O/E embryos did not detectably localize *osk* (Fig. 3.3.4-H), while the remainder displayed an extremely weak posterior accumulation (Fig. 3.3.4-I). In contrast, anterior localization of *bcd* mRNA was only slightly weaker in 0-2 hr *Bic-C* O/E embryos (Fig. 3.3.4-K) than in wild-type controls (Fig. 3.3.4-J).

Figure 3.3.2 Germline overexpression of Bic-C.

Confocal immunofluorescence illustrates Bic-C (red) expression in wild-type stages 5 and 7 (A) and stage 10 (B) egg chambers. Egg chambers overexpressing Bic-C display increased Bic-C in the nurse cells during early and mid-oogenesis (C). At stage 10, Bic-C overexpression increases the amount of Bic-C (D), however, its distribution is similar to that of the endogenous protein. DNA is visualized by DAPI staining (blue).

UASP-Bic-C^{7}/ nosGal4::VP16

Figure 3.3.3 The progeny of Bic-C overexpressing females display patterning defects.

Cuticle preparations of a wild-type egg (A), as well as eggs (B, C) and larval progeny (D, E) of Bic-C overexpressing females, reveal loss or fusion of posterior body segments upon Bic-C overexpression in the maternal germline.

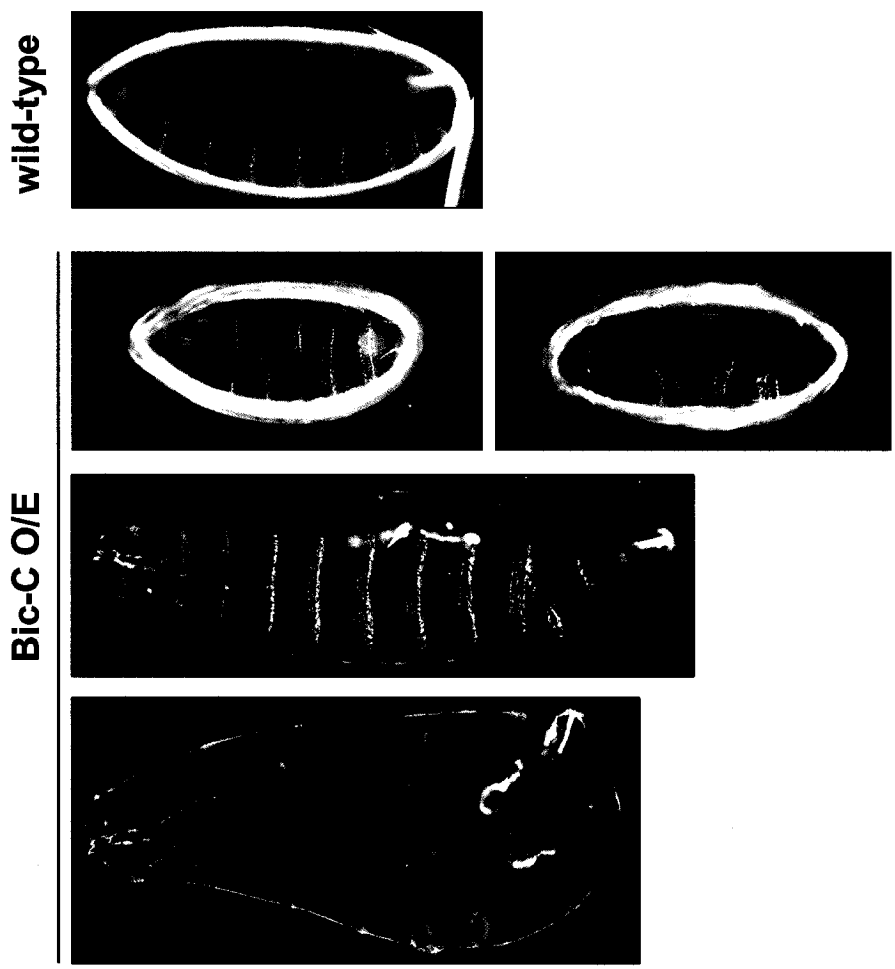

UASP-Bic-C^{7}/ nosGal4::VP16

Figure 3.3.4 Overexpression of Bic-C antagonizes posterior patterning and pole cell specification.

(A-C) *In situ* hybridization with an anti-sense *ftz* probe illustrates defects in posterior patterning in the progeny of Bic-C overexpressing females. (D-F) Immunostaining of 3-6 hr embryos with α-Vas demonstrates a complete loss or severe reduction in pole-cell number in the progeny of Bic-C overexpressing females. (G-I) *In situ* hybridizations indicate that posterior accumulation of *osk* mRNA is reduced or undetectable in 0-2 hr embryos produced by Bic-C overexpressing females. (J, K) Bic-C overexpression does not substantially affect the anterior accumulation of *bcd* mRNA in 0-2 hr embryos.

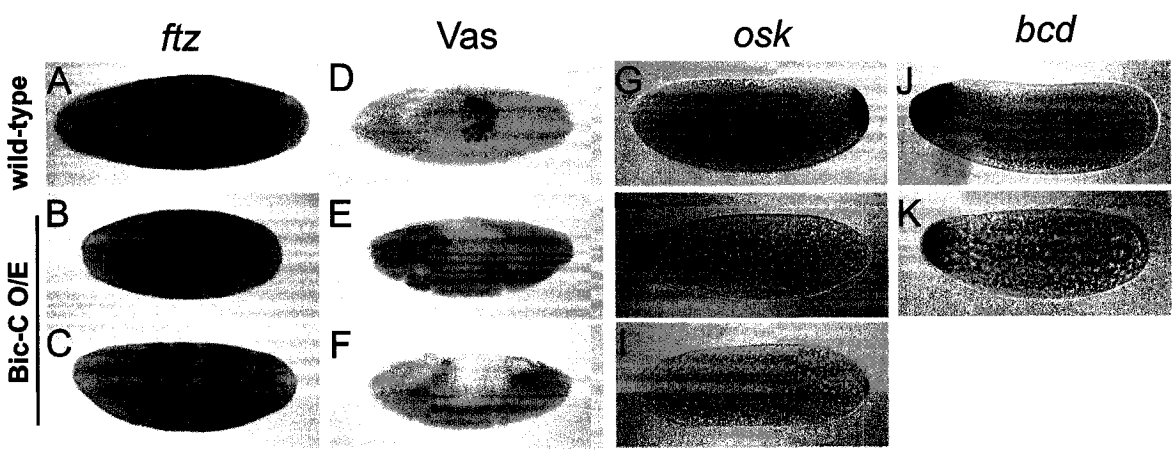
ftz
Vas
osk
bcd
wild-type
Bic-C O/E
A
B
C
D
E
F
G
J
K
L

3.3.3 Bic-C overexpression alters oocyte polarity and initiates premature cytoplasmic streaming

Abdominal patterning defects and reduction or loss of pole cells are both indicative of a failure to assemble or maintain pole plasm at the posterior of the oocyte or early embryo. To determine if Bic-C overexpression disrupts initiation of pole plasm assembly, I analyzed the distribution of *osk* mRNA in ovaries. In wild-type oocytes, *osk* mRNA begins accumulating at the posterior cortex during stage 8 (Fig. 3.3.5-A) where it remains anchored through stage 10 (Fig. 3.3.5-B) and the remainder of oogenesis. I found that *Bic-C* overexpression disrupts posterior accumulation of *osk* from stage 8 onward (Fig. 3.3.5-C), as well as posterior localization of the pole plasm components Vas and Aubergine that accumulate downstream of Osk (data not shown). To determine if this phenotype reflects a specific defect in *osk* localization or an underlying defect in oocyte polarity, the distribution of a fragment of kinesin heavy chain fused to β-gal was analyzed (Khc:β-gal; Clark et al., 1994). Kinesin heavy chain is a plus-end directed motor protein that normally accumulates, in a microtubule dependent manner, at the posterior of the oocyte during stages 9-10 (Fig. 3.3.5-D). Posterior accumulation of Khc:β-gal was not detectable in >90% of stage 9-10 oocytes overexpressing Bic-C (Fig. 3.3.5-E), indicating that microtubule polarity is disrupted upon Bic-C overexpression. To confirm this observation, the distribution of Tyrosinylated Tubulin (Tyr-Tub) was examined using the monoclonal YL1/2 antibody. Unlike wild-type stage 9-10 egg chambers, which display a clear anterior to posterior gradient of Tyr-Tub within the oocyte (with the lowest concentration at the posterior) (Fig. 3.3.5-F), Bic-C

Figure 3.3.5 Bic-C overexpression disrupts posterior accumulation of *osk* mRNA during oogenesis, alters oocyte polarity and initiates premature cytoplasmic streaming.

Posterior localization of *osk* mRNA is visualized by whole mount *in situ* hybridizations in wild-type (A) stage 8 and (B) stage 10 egg chambers. (C) Posterior localization of *osk* mRNA is undetectable in equivalently-staged egg chambers from Bic-C overexpressing females. (D) In wild-type stage 10 oocytes the plus-end directed motor kinesin heavy chain:β-gal (green) is localized to the posterior cortex where Osk protein (red) is translated. (E) In Bic-C overexpressing egg chambers, posterior accumulation of both kinesin heavy chain:β-gal and Osk are both undetectable. Bic-C-overexpressing oocytes display an abnormal concentration of Tyr-Tub uniformly around the cortex (G), unlike wild-type stage 9-10 egg chambers, which display a clear anterior to posterior gradient of Tyr-Tub (F). Auto-fluorescing yolk granules were visualized at 4-sec intervals for a total of 1 min and the images were superimposed to illustrate yolk movement. Yolk particles are relatively static in a wild-type stage 9 oocyte (H) but are far more dynamic in a stage 7 Bic-C overexpressing oocyte (I).

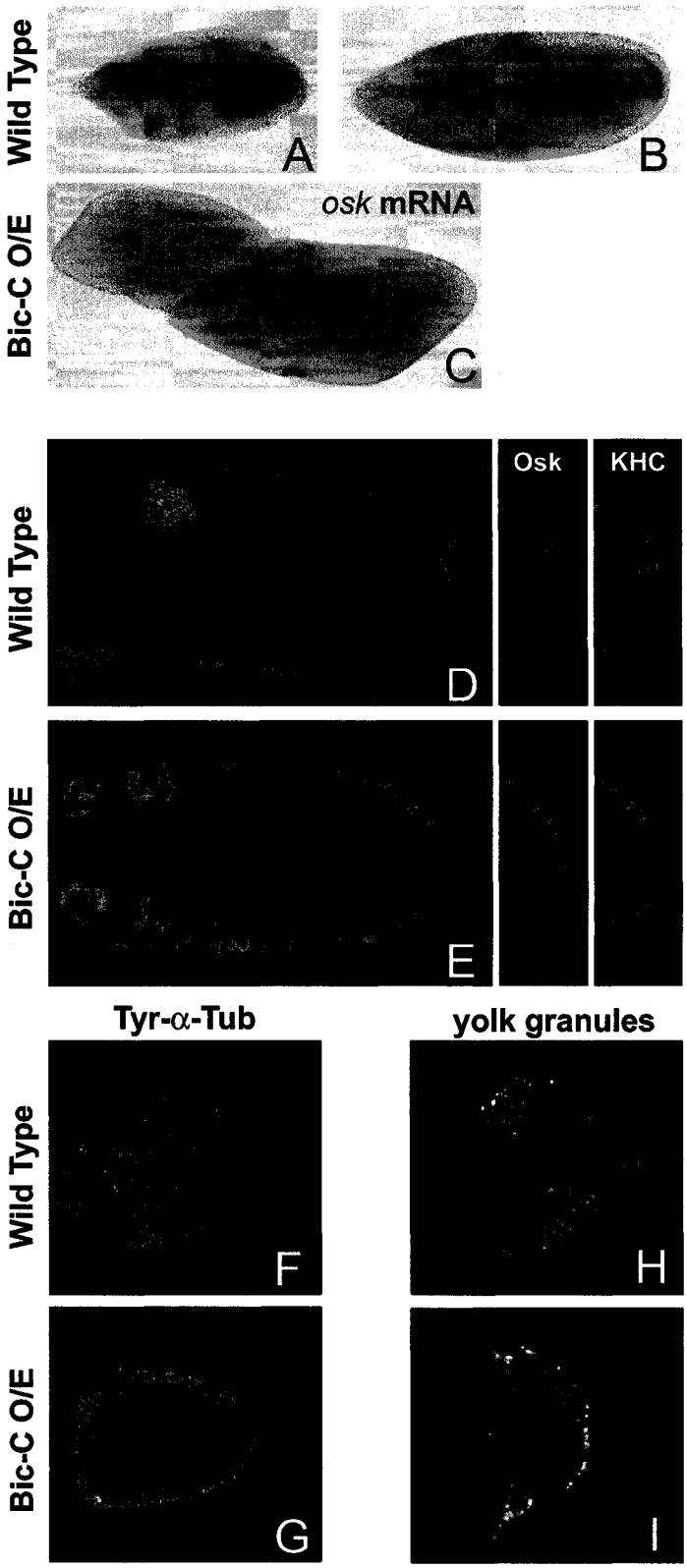
Wild Type
A
B
Bic-C O/E
osk mRNA
C
Wild Type
Osk
KHC
D
Bic-C O/E
E
Tyr-α-Tub
yolk granules
Wild Type
F
H
Bic-C O/E
G
I

overexpressing oocytes concentrate Tyr-Tub uniformly around the cortex at these stages (Fig. 3.3.5-G).

A rapid phase of cytoplasmic streaming is normally initiated at stage 10b within the oocyte, and Osk provides a cortical anchor to resist displacement of posterior determinants (Vanzo and Ephrussi, 2002). In mutants that initiate this phase prematurely, *osk* is displaced from the posterior before getting translated, leading to defective pole plasm assembly (Theurkauf, 1994b; Manseau et al., 1996; Martin et al., 2003). These mutants also exhibit redistribution of α-tubulin around the oocyte cortex at stage 9, as seen in Bic-C overexpressing oocytes.

To determine if Bic-C overexpression disrupts posterior patterning through an effect on cytoplasmic streaming, time-lapsed confocal images of auto-fluorescent yolk granules were compared in wild-type and Bic-C overexpressing oocytes. A series of 15 images taken at 4-second intervals were superimposed to generate a single image. In a wild-type stage 9 egg chamber the stationary yolk granules appear as dots (Fig. 3.3.5-H), while in a stage 7 oocyte overexpressing Bic-C, the yolk granules appear as curved lines due to the rapid circular movement of the cytoplasm (Fig. 3.3.5-I).

3.3.4 Bic-C overexpression attenuates EGFR activation and dorsal appendage formation

In addition to disrupting posterior patterning, mutations that induce premature cytoplasmic streaming disrupt *grk* mRNA localization and dorsal/ventral patterning, resulting in dorsal appendage defects (Manseau and Schupbach, 1989; Neuman-Silberberg and Schupbach, 1993). Consistent with these results, eggs produced by

females overexpressing *Bic-C* also exhibited defects in dorsal appendage morphology. Approximately 60% of such eggs completely lacked dorsal appendages, while the remaining eggs either had fused dorsal appendages (~25%) or two dorsal appendages that were often abnormally short and/or thin (~15%) (Fig. 3.3.6). Reduction of endogenous Bic-C (in a *Bic-C*^{YC33}/+ genetic background) suppressed the dorsal appendage defects caused by Bic-C overexpression, increasing the fraction of eggs with two dorsal appendages to 34%. This indicates that endogenous Bic-C contributes to the molecular events that produce these defects (Fig. 3.3.7).

Dorsal appendage formation requires activation of the follicle-cell bound EGFR by the TGF-α homologue Gurken (Grk), which is synthesized at the dorsal-anterior corner of the oocyte and locally secreted (Peri and Roth, 2000). The genes *mirror* (*mirr*) and *kekkon (kek*) are transcribed in the follicle cells in response to EGFR activation. *Mirr* encodes a transcription factor that is required for specification of the dorsal appendage producing cells (Jordan et al., 2000), whereas *kek* encodes a transmembrane protein that binds to and down-regulates the activity of EGFR. Since the dorsal appendage defects observed upon *Bic-C* overexpression are consistent with either a defect in the production or deployment of Grk, I analyzed Grk distribution within the oocyte and the expression of *mirr* and *kek* within the overlying follicle cells using the established *lacZ* reporter lines *l(3)6D1* (Zhao et al., 2000) 15A6 (Ghiglione et al., 1999) respectively.

In Bic-C overexpressing egg chambers, Grk distribution appeared normal until stage 7 (not shown), however, dorsal anterior accumulation of Grk beginning at stage 8-9 was greatly reduced and often undetectable (Fig. 3.3.8-A,B). Accordingly, *mirr* was also dramatically reduced and often undetectable in the overlying follicle cells.

Figure 3.3.6 Dorsal appendage formation is disrupted by Bic-C overexpression.

Unlike wild-type eggs with two dorsal appendages (top), eggs laid by Bic-C overexpressing females often lack or have fused dorsal appendages (bottom).

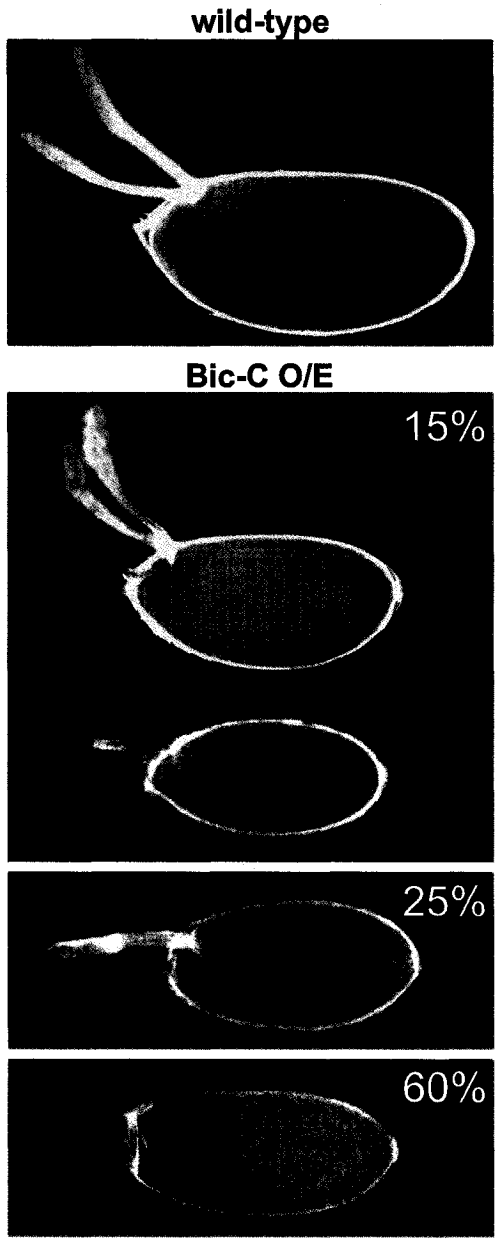
wild-type
Bic-C O/E
15%
25%
60%

Figure 3.3.7 Reduction of endogenous Bic-C suppresses Bic-C overexpression defects.

Maternal genotypes are listed below the graph. The total number of eggs counted for each genotype is listed below the X-axis. The Y-axis represents the percentage of eggs with the specified number of dorsal appendages. Numbers below the X-axis (red) represent the percentage of eggs that have hatched 36 hours after deposition.

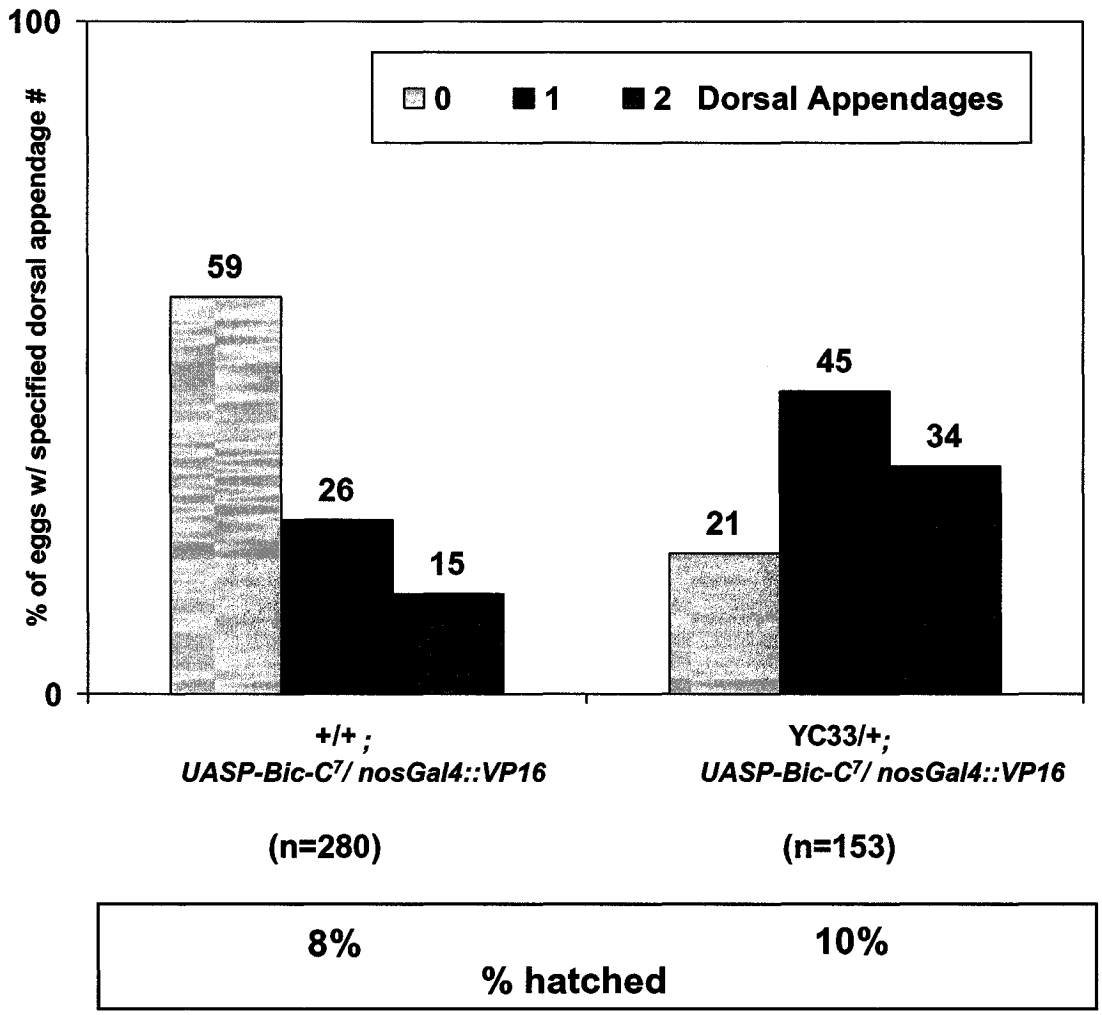
100
0
% of eggs w/ specified dorsal appendage #
0
1
2 Dorsal Appendages
59
26
15
21
45
34
+/+ ;
UASP-Bic-C7/ nosGal4::VP16
YC33/+;
UASP-Bic-C7/ nosGal4::VP16
(n=280)
(n=153)
8%
10%
% hatched

Figure 3.3.8 Bic-C overexpression disrupts anterior-dorsal accumulation of Grk and attenuates EGFR activation.

In wild-type egg chambers (A), *mirr* (green) is expressed in the dorsal/anterior follicle cells in response to EGFR activation by Grk (red). (B) Bic-C overexpression strongly reduces dorsal/anterior accumulation of Grk within the oocyte, resulting in reduced *mirr* expression. (C) Grk overexpression causes EGFR activation and *mirr* expression in an expanded domain of follicle cells. (D) Overexpression of both Bic-C and Grk prevents anterior Grk accumulation and consequent *mirr* expression. (E) Western blots of ovarian extracts demonstrate that co-overexpression of Bic-C and Grk does not result in *mirr* activation despite Grk levels that are substantially higher than in control ovaries. α-Tubulin was used as a loading control.

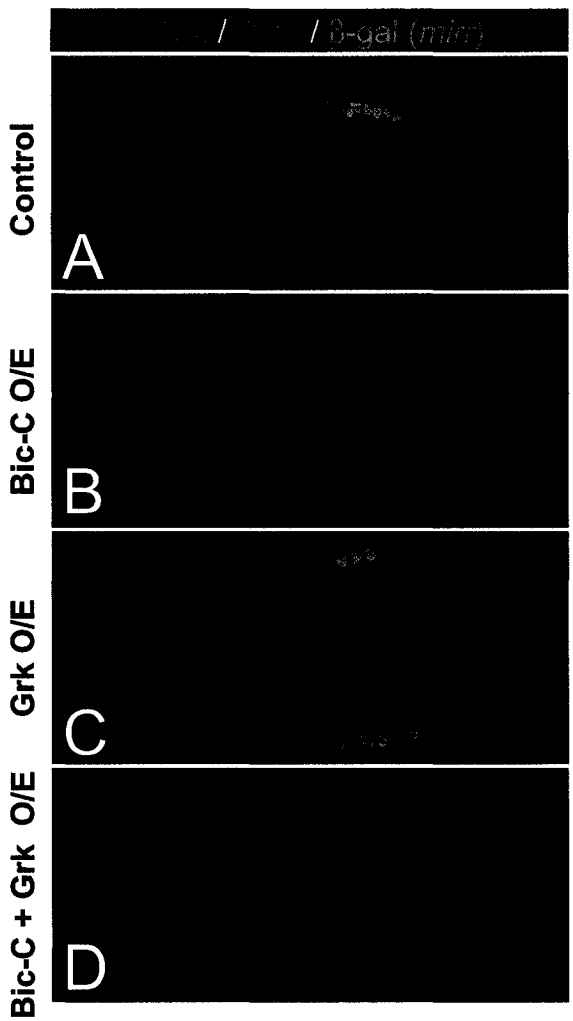
/ β-gal (mirr)
Control
A
Bic-C O/E
B
Grk O/E
C
Bic-C + Grk O/E
D

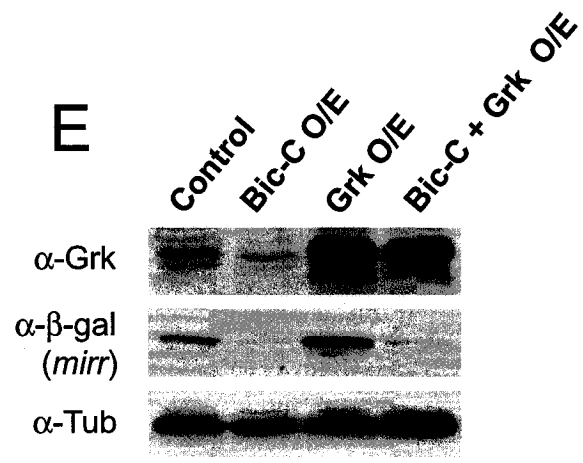
E
Control
Bic-C O/E
Grk O/E
Bic-C + Grk O/E
α-Grk
α-β-gal
(mirr)
α-Tub

I overexpressed both *grk* and *Bic-C* using the GAL4/UASP system (Rorth, 1998), and examined the resulting effects on *mirr* activation. As the *UASP-grk* transgene that was used only contains the *grk* ORF, the normal transcriptional and translational mechanisms controlling Grk expression were circumvented (Ghiglione et al., 2002). If excess Bic-C attenuates EGFR activation by suppressing Grk synthesis, then overexpression of both Grk and Bic-C should activate *mirr* expression. On the other hand, should Bic-C affect the distribution of Grk protein, due to premature cytoplasmic streaming, then overexpression of both Grk and Bic-C would likely resemble Bic-C overexpression alone and *mirr* should remain repressed. My observations support the latter alternative. Immunostaining revealed that while *grk* overexpression alone produced a visible enrichment of Grk around the anterior oocyte cortex and an expanded domain of *mirr* expression (Fig. 3.3.8-D), overexpression of both *Bic-C* and *grk* led to an overall increase in Grk without enriching it specifically at the anterior cortex. Thus minimal activation of *mirr* was observed (Fig. 3.3.8-E). Western blotting of whole ovaries confirmed these results, revealing that despite Grk levels that were markedly higher than in wild-type control ovaries, β-Gal (representative of *mirr*) was dramatically reduced in ovaries co-overexpressing *Bic-C* and *grk* (Fig. 3.3.8-F). These results were consistent with the dorsal appendage morphology of eggs laid by these females. *grk* over-expression alone resulted in an anterior ring of ectopic dorsal appendage material (Fig. 3.3.9-A), while females co-overexpressing *Bic-C* and *grk* produced eggs with no dorsal appendages (Fig. 3.3.9-B), fused dorsal appendages (Fig. 3.3.9-C) or with two shortened, laterally placed dorsal appendages (Fig. 3.3.9-D).

Figure 3.3.9 Bic-C overexpression suppresses the dorsalizing effect of Grk overexpression on dorsal appendage formation.

Grk overexpression results in a ring of ectopic dorsal appendage material around the anterior of the egg (A). Co-overexpression of Bic-C and Grk result in eggs that lack dorsal appendages (B), have a single, fused dorsal appendage (C) or have two, abnormally small dorsal appendages, displaced laterally (D).

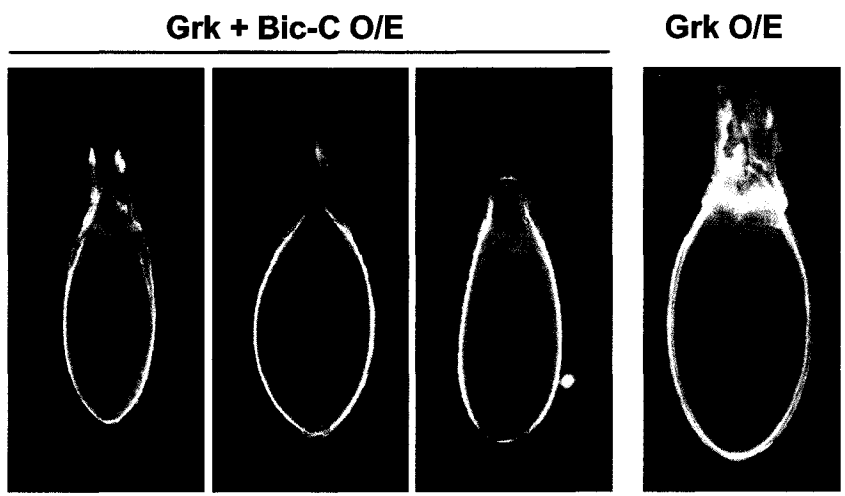
Grk + Bic-C O/E
Grk O/E

Since Dpp has also been implicated in transcriptional activation of *mirr* (Twombly et al., 1996; Atkey et al., 2006), it is also possible that Bic-C overexpression suppresses *mirr* expression through attenuation of the Dpp signal. If this is the case, then reducing the dosage of *dpp* in the context of Bic-C overexpression should increase the frequency of dorsal appendage defects. This possibility was explored; however, the opposite result was obtained, in that reduction of *dpp* actually suppressed the effects of Bic-C over-expression (Fig. 3.3.10). Therefore, the reduction of *mirr* expression observed in Bic-C overexpressing egg chambers is likely due to reduced EGFR activation by Grk and not an inability to transmit or receive the Dpp signal.

Surprisingly, Bic-C overexpression caused the domain of *kek* expression to expand laterally and towards the posterior in stage 9/10 egg chambers (Fig. 3.3.11). To determine if this effect was due to an expanded domain of Grk expression or caused by some unknown mechanism, independent of EGFR activation by Grk, Bic-C was over-expressed in a homozygous grk^{HK} mutant background. Relative to wild-type controls, *kek* expression displayed a similar reduction in the grk^{HK} egg chambers with or without Bic-C overexpression (Fig. 3.3.12). Therefore, the expansion of *kek* expression, induced by Bic-C overexpression, is dependent on EGFR activation by Grk and although not readily detectable by immunofluoresence, Grk must also be expanded along the oocyte cortex.

Since Kek attenuates EGFR activity and overexpression of Kek has been shown to suppress dorsal appendage formation (Ghiglione et al., 2003), overexpression of Bic-C in a *kek* null background was used to determine the extent that Kek expansion may

Figure 3.3.10 Reduction of Dpp suppresses Bic-C overexpression defects.
Maternal genotypes are listed below the graph and the total number of eggs (n) counted for each genotype is listed below the X-axis. The Y-axis represents the percentage of eggs with the specified number of dorsal appendages. The percentages of eggs that have hatched 36 hours after deposition are listed in red below the X-axis.

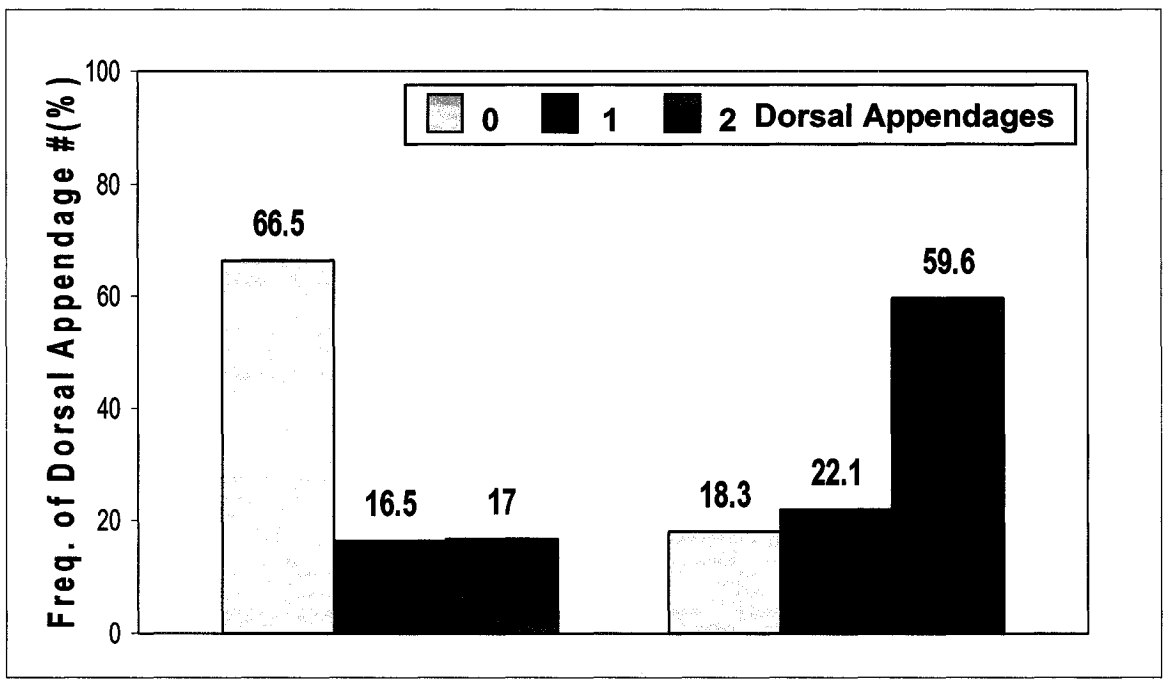

+/+;
UASP-BicC^{7} / nosGal4::VP16

(n=218)

Dpp^{hr56} /+;
UASP-BicC^{7} / nosGal4VP16

(n=235)

4.2%	**25.7%**
(n=462)	(n=435)
% hatched	

Figure 3.3.11 Bic-C overexpression results in an expanded domain of *kekkon* expression.

X-gal staining of control (top) and Bic-C overexpressing (bottom) egg chambers illustrates the domain of *kekkon* expression (represented by β-Gal) in the follicle cells.

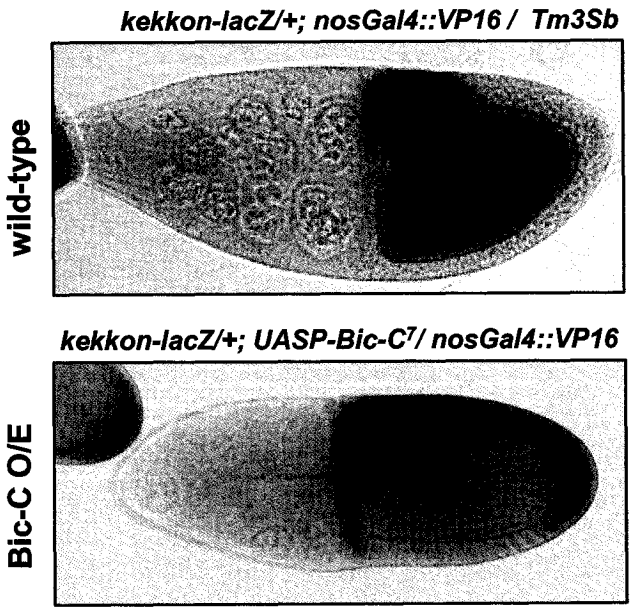
kekkon-lacZ/+; nosGal4::VP16 / Tm3Sb
wild-type
kekkon-lacZ/+; UASP-Bic-C7/ nosGal4::VP16
Bic-C O/E

Figure 3.3.12 The expanded domain of *kekkon* expression in Bic-C overexpressing egg chambers is dependent upon EGFR activation by Grk.

X-gal staining illustrates the domain of *kekkon* expression in wild-type controls (top panels), homozygous grk^{HK} (middle panels) and Bic-C overexpressing, grk^{HK} homozygous egg chambers (bottom panels).

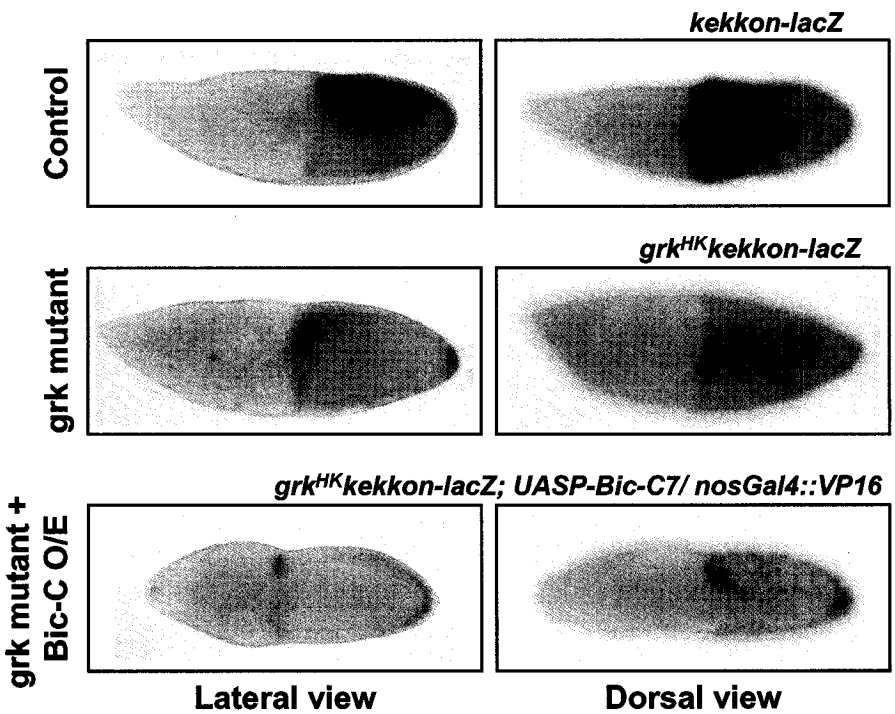
kekkon-lacZ
Control
grk^HK kekkon-lacZ
grk mutant
grk^HK kekkon-lacZ; UASP-Bic-C7/ nosGal4::VP16
grk mutant + Bic-C O/E
Lateral view
Dorsal view

contribute to the observed dorsal appendage defects. This was done using overlapping deficiencies that converge on the *kek* locus. Loss of Kek produced a clear suppression of the phenotype, however 10% of the eggs still lacked dorsal appendages and 17% had only one (Fig. 3.3.13). Therefore, the presence of Kek enhances these defects through attenuation of EGFR activation, however it is not the underlying cause.

Taken together, these results strongly suggest that Bic-C overexpression causes diffusion of Grk rather than a reduction in the amount of Grk produced. As a result, the dispersed signal is weakened to an intensity sufficient to activate *kek* transcription in an expanded domain of follicle cells but insufficient to activate *mir* transcription.

3.3.5 Bic-C expression disrupts eye morphology without altering EGFR activation

Bic-C expression is normally restricted to the germline and early embryogenesis, however the UASP/Gal4 system permits selective expression in a variety of tissues including the eye (Brand and Perrimon, 1993). Using the GMR-Gal4 driver line (Freeman, 1996), Bic-C was expressed in the eye where it appeared to disrupt ommatidial organization, generating a rough-eye phenotype (Fig. 3.3.14, A-D). This phenotype was specifically caused by Bic-C expression as the eyes of flies bearing either the Gal-4 driver or UASP-Bic-C transgenes appeared normal. Modifications of several signaling pathways, including those downstream of EGFR and Frizzled/Dishevelled signaling, have been shown to induce similar rough-eye phenotypes (Penton et al., 2002; Voas and Rebay, 2004). To determine if altered EGFR activity might underlie this phenotype, I examined the expression of *kek* using the 15A6 reporter line which is also expressed in

Figure 3.3.13 Disruption of dorsal appendage formation is suppressed but not rescued by loss of *kekkon.*

Maternal genotypes and the total number of eggs counted for each genotype are listed below the X-axis. The Y-axis represents the percentage of eggs with the specified number of dorsal appendages. The percentage of eggs that have hatched 36 hours after deposition is listed below the graph. Note that all of the genotypes listed are in a Bic-C overexpression background (*UASP-Bic-C7/ nosGal4::VP16).*

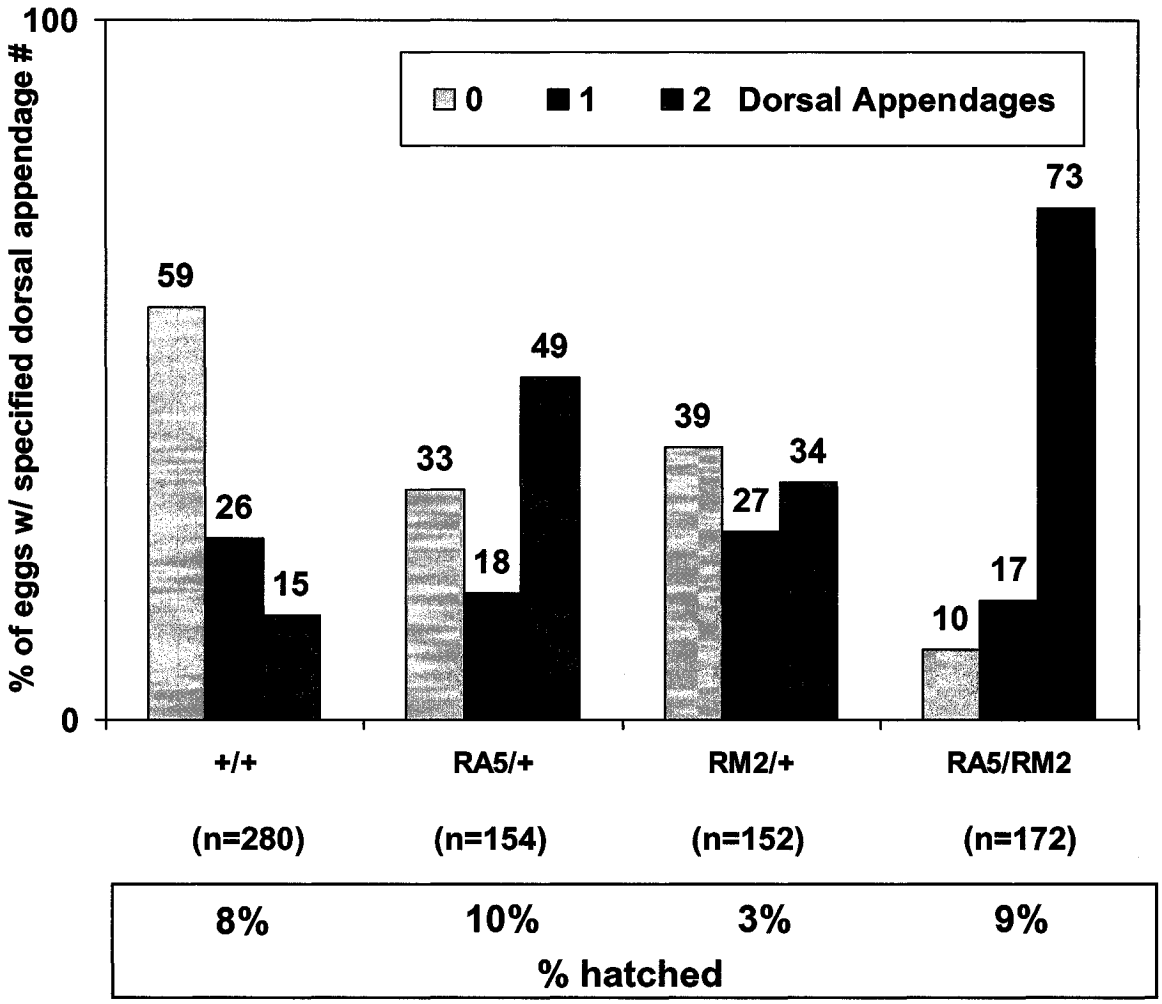
100
0
% of eggs w/ specified dorsal appendage #
0
1
2 Dorsal Appendages
59
26
15
33
18
49
39
27
34
10
17
73
+/+
RA5/+
RM2/+
RA5/RM2
(n=280)
(n=154)
(n=152)
(n=172)
8%
10%
3%
9%
% hatched

Figure 3.3.14 Bic-C expression in the eye induces a rough-eye phenotype without altering EGFR activation.

In *UASP-Bic-C/+* (A) and *GMR-Gal4/+* (B) flies, eye morphology is normal, however, when Bic-C expression is driven in the eyes of flies bearing both transgenes, they appear rough and the regular distribution of the ommatidia are disrupted as seen from overhead (C) and the side (D). (F) *kekkon* expression (represented by β-Gal, green) is similar in control and Bic-C overexpressing eye imaginal discs.

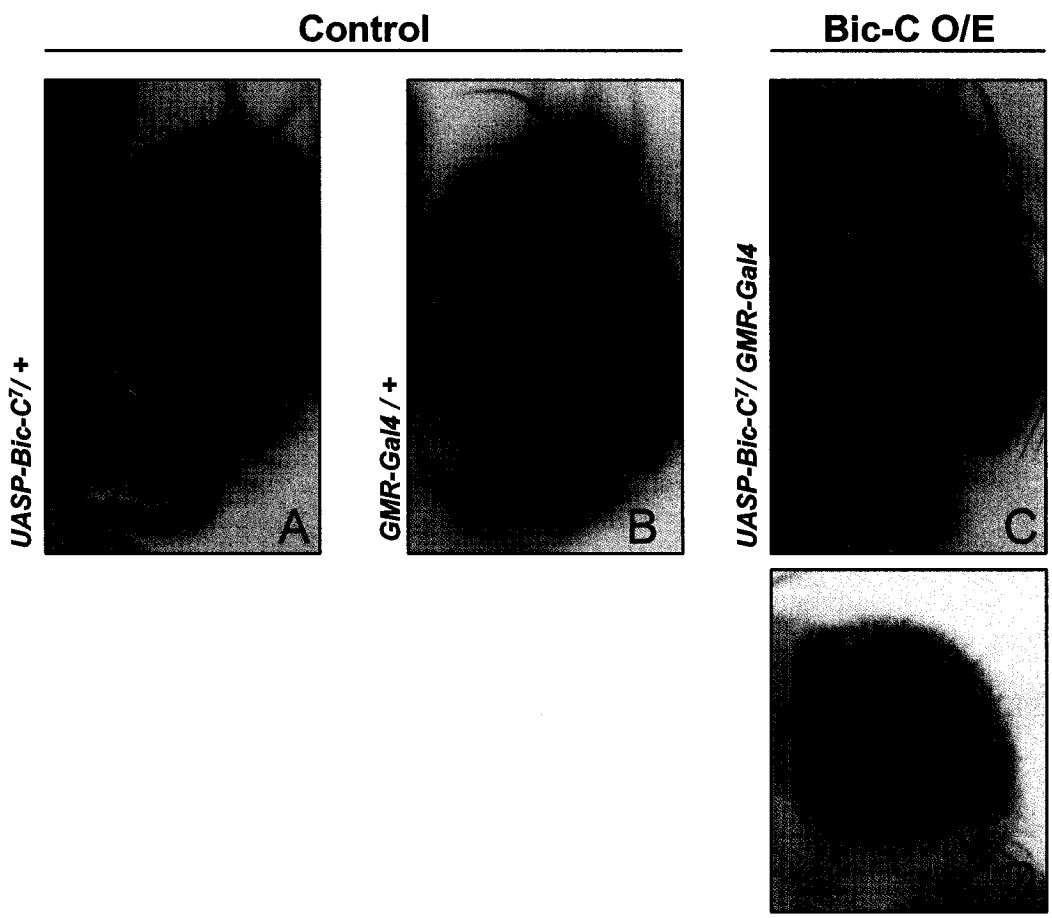
Control
Bic-C O/E
UASP-Bic-C7/ +
GMR-Gal4 / +
UASP-Bic-C7/ GMR-Gal4
A
B
C
D

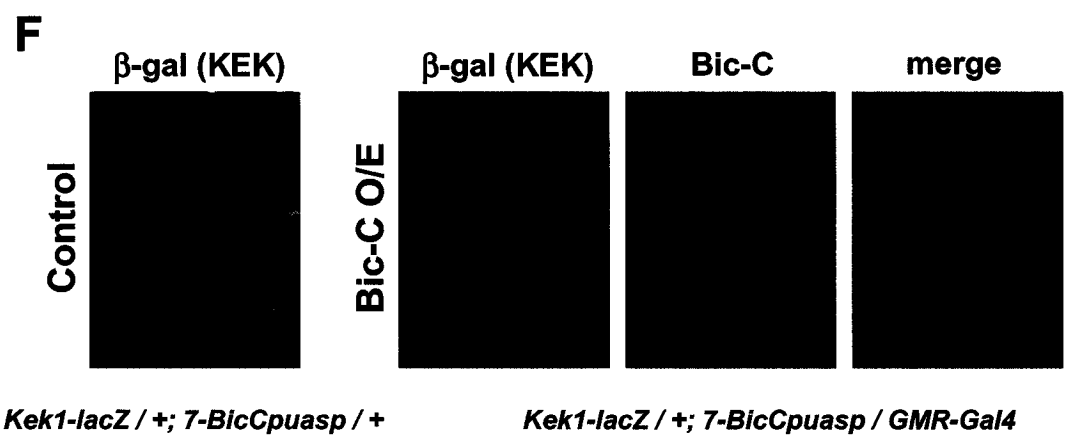
F
β-gal (KEK)
β-gal (KEK)
Bic-C
merge
Control
Bic-C O/E
Kek1-lacZ / +; 7-BicCpuasp / +
Kek1-lacZ / +; 7-BicCpuasp / GMR-Gal4

eye imaginal discs (Ghiglione et al., 1999). I found that β-Gal expression, representative of *kek*, was not substantially altered by Bic-C expression (Fig. 3.3.14-F). Therefore, alteration of EGFR activation does not appear to be the cause of the rough-eye phenotype induced by Bic-C expression.

3.3.6 RNA binding activity is required for the Bic-C overexpression phenotypes

To determine the relative importance of RNA binding in producing the *Bic-C* overexpression phenotypes during oogenesis, I expressed, in the same manner as for wild-type Bic-C, a mutant form of the protein (Bic-C^{G296R}) with reduced RNA binding activity (Saffman et al., 1998). Despite elevated levels of expression (Fig. 3.3.15-C, D), Bic-C^{G296R} failed to disrupt posterior accumulation of Osk (Fig. 3.3.15-C) or to produce any dorsal appendage defects (data not shown). This suggests that the induction of premature cytoplasmic streaming, which underlies both of these defects, is mediated through one or more mRNA targets that are bound by Bic-C and become mis-regulated upon its overexpression.

3.3.7 Bic-C overexpression phenotypes are modified by mutations affecting *orb* and mRNA polyadenylation

Previous studies have established that Bic-C and Orb physically interact in co-immunoprecipitation experiments and that *orb* mutations can dominantly suppress *Bic-C* mutations (Castagnetti and Ephrussi, 2003), suggesting that Bic-C and Orb may act antagonistically within a common complex. Consistent with this interpretation, the

Figure 3.3.15 RNA binding activity is required for the Bic-C overexpression phenotypes.

(A-C) Confocal microscope images of (A) an early stage 10 egg chamber from a wild-type female, showing posterior accumulation of Osk (green) and endogenous Bic-C expression (red). DNA is visualized by DAPI staining (blue). (B) A similarly-staged egg chamber from a Bic-C overexpressing female, in which posterior accumulation of Osk is not detectable. (C) A similarly-staged egg chamber from a female overexpressing Bic-C^{G296R}, shows normal posterior accumulation of Osk. (D) The level of endogenous Bic-C protein expression in OreR ovaries (lane 1) is similar to UASP-Bic-C expression levels in a homozygous *Bic-C^{YC33}* protein-null background (lane 3), while UASP-Bic-C^{G296R} levels are visibly higher (lane 4). Lane 2 contains an equivalent amount of ovarian extract from homozygous *Bic-C^{YC33}* females.

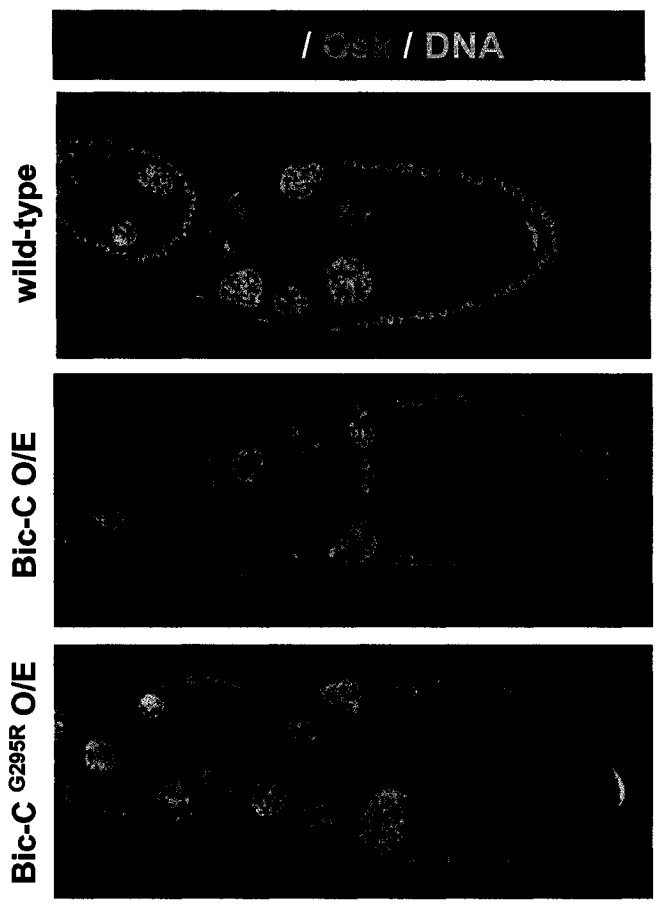
/ Gsk / DNA
wild-type
Bic-C O/E
Bic-C G295R O/E

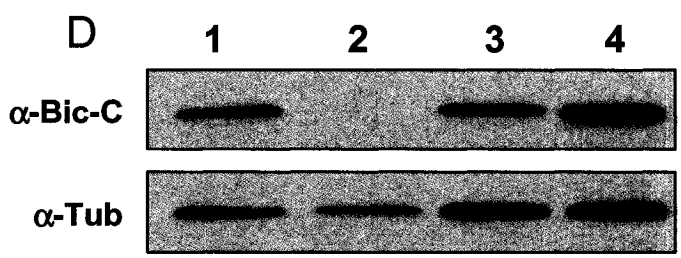
D
1
2
3
4
α-Bic-C
α-Tub

defects caused by *Bic-C* overexpression are strikingly similar to those previously described for hypomorphic *orb* mutants (Lantz et al., 1994; Martin et al., 2003).

To determine if Bic-C overexpression produces *orb*-like phenotypes by antagonizing *orb* function or through an *orb*-independent mechanism, I investigated whether reducing *orb* activity in the context of *Bic-C* overexpression would enhance the *Bic-C* overexpression phenotype. A weaker *Bic-C* overexpression line, derived from an independent insertion of the *UASP-Bic-C* transgene, was employed for these experiments to facilitate the detection of potential genetic enhancements. In an orb^{F343}/+ genetic background, *Bic-C* overexpressing females were virtually sterile and produced almost no eggs with two dorsal appendages (1.2%). Similar but slightly less extreme results were obtained from the hypomorphic orb^{mel} allele (Table 3.3.1). Neither *orb* allele displayed any dominant phenotypes in the absence of *Bic-C* overexpression.

Since Orb acts to promote polyadenylation of specific transcripts, I asked if a mutation in *hiiragi* (*hrg*, which encodes poly(A) polymerase; (Murata et al., 2001) would also act as a dominant enhancer of the *Bic-C* overexpression phenotypes. In fact, *Bic-C* overexpression phenotypes were dramatically enhanced in a hrg^{PAP45}/+ genetic background (Juge et al., 2002; Table 3.3.1). Given that reductions in *orb* or *hrg* activity enhanced the *Bic-C* overexpression phenotype, it seemed plausible that reducing the level of CCR4, the major deadenylase in *Drosophila* oocytes (Morris et al., 2005), might produce the opposite effect. Indeed the dorsal appendage defects induced by *Bic-C* overexpression were almost completely rescued in a $ccr4^{KG00877}$/+ genetic background (Temme et al., 2004), and survival to hatching also increased dramatically (Table 3.3.1).

Table 3.3.1 Bic-C overexpression phenotypes are modified by mutations affecting *orb* and mRNA polyadenylation.

Bic-C overexpression phenotypes are dominantly enhanced by *orb* and *poly(A) polymerase* (*hiiragi*) mutants and dominantly suppressed by a mutation in the deadenylase CCR4 (*twin*). n designates the total number of eggs scored for each genotype.

Maternal Genotype	Hatching Frequency		% with Specified Dorsal Appendage Number			
	%	n	0	1	2	n
orb^{F343}/+ ; nosGal4::VP16/+	96.9	803	0	0	100	803
orb^{mel}/+ ; nosGal4::VP16/+	98.4	696	0	0	100	696
hrg^{pap45}/+ ; nosGal4::VP16/+	93.4	253	0	0	100	253
+/+ ; nosGal4::VP16/ ccr4^{KG00877}	86.2	319	0	0	100	319
UASP-Bic-C/+ ; nosGal4::VP16/+	36.3	2194	20.9	15.9	63.2	1652
UASP-Bic-C/ orb^{F343} ; nosGal4::VP16/+	1.2	692	70.8	28.0	1.2	692
UASP-Bic-C/ orb^{mel} ; nosGal4::VP16/+	21.4	822	26.7	42.7	30.6	559
UASP-Bic-C/ hrg^{pap45} ; nosGal4::VP16/+	7.4	586	55.3	15.3	29.4	542
UASP-Bic-C/+ ; nosGal4::VP16/ ccr4^{KG00877}	78.0	1371	0.7	1.1	98.2	699

Given the apparent need for CCR4 in mediating the Bic-C over-expression phenotypes, I decided to test the same allele of *ccr4/twin* for a dominant interaction with the *Bic-C*^{YC33} mutant allele (Fig. 3.3.16). Consistent with the genetic interactions observed in the overexpression background, the mutant alleles acted synergistically to enhance dominant maternal-effect lethality (Fig. 3.3.16).

Since NOT3 was identified in a yeast-two hydrid screen as a putative Bic-C-binding protein (Paliouras, M., Ph.D. Thesis, 2005) and it is a component of the CCR4 deadenylase complex (Temme et al., 2004), a fly line containing a homozygous lethal P-element insertion in the *not3* 5' UTR (l(2)NC136^{KG10496}); (Myster et al., 2004) was also tested for genetic interactions in a Bic-C overexpression background (Fig. 3.3.17). For this experiment the stronger Bic-C overexpression line was used. This *not3* insertion dominantly suppressed the negative effects of Bic-C overexpression (Fig. 3.3.17).

3.3.8 Bic-C overexpression produces a low frequency of oocyte positioning and specification defects

In addition to premature cytoplasmic streaming, Bic-C overexpression produced a variety of defects, at a low frequency (<5%) in younger egg chambers. These included egg chambers in which the oocyte had failed to migrate to the posterior and egg chambers containing two oocytes (Fig. 3.3.18). Similar defects in oocyte specification and positioning have been reported in *orb* mutants (Lantz et al., 1994).

Figure 3.3.16 Reduction of CCR4 reduces the fertility of *Bic-C*^{YC33} heterozygous females.

Maternal genotypes and the total number of eggs counted for each genotype are listed below the graph. The Y-axis represents the percentage of eggs that have hatched 36 hours after deposition.

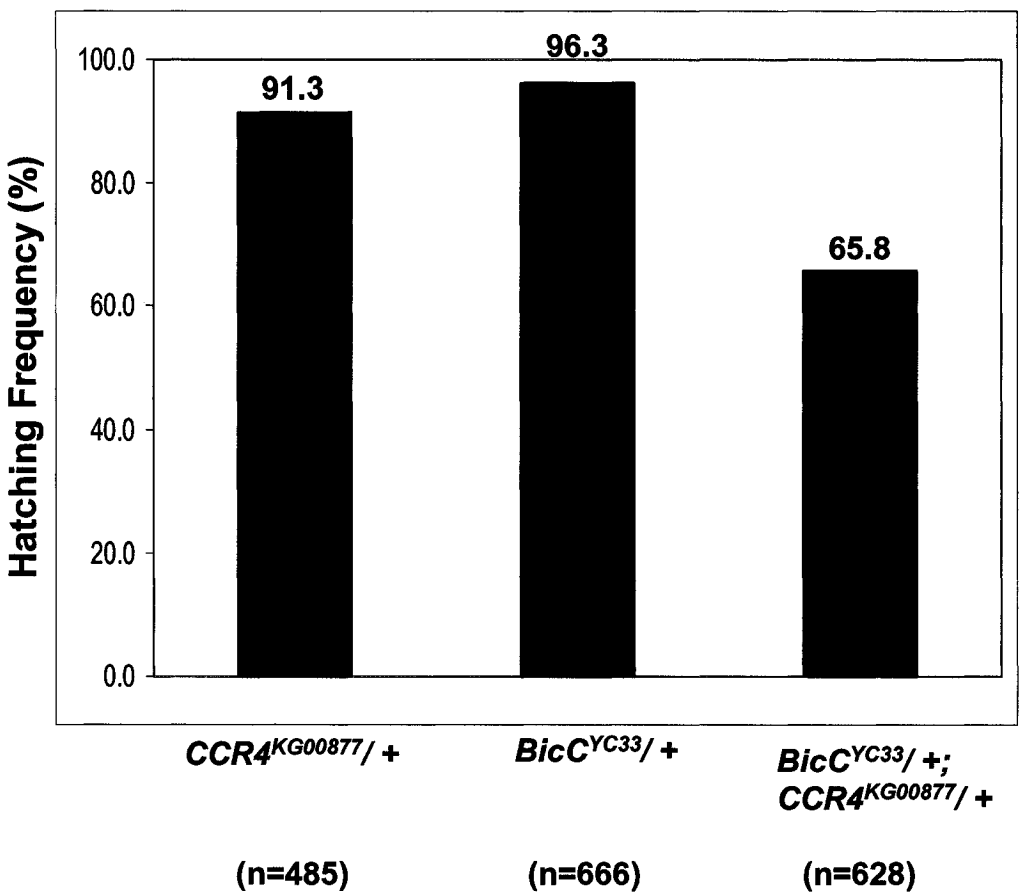
Hatching Frequency (%)
100.0
80.0
60.0
40.0
20.0
0.0
91.3
96.3
65.8
CCR4KG00877/ +
BicCYC33/ +
BicCYC33/ +;
CCR4KG00877/ +
(n=485)
(n=666)
(n=628)

Figure 3.3.17 Reduction of NOT3 suppresses the Bic-C induced dorsal appendage defects and maternal-effect lethality.

Maternal genotypes and the total number of eggs counted for each genotype are listed below the X-axis. The Y-axis represents the percentage of eggs with the specified number of dorsal appendages. The percentage of eggs that have hatched 36 hours after deposition is listed below the graph.

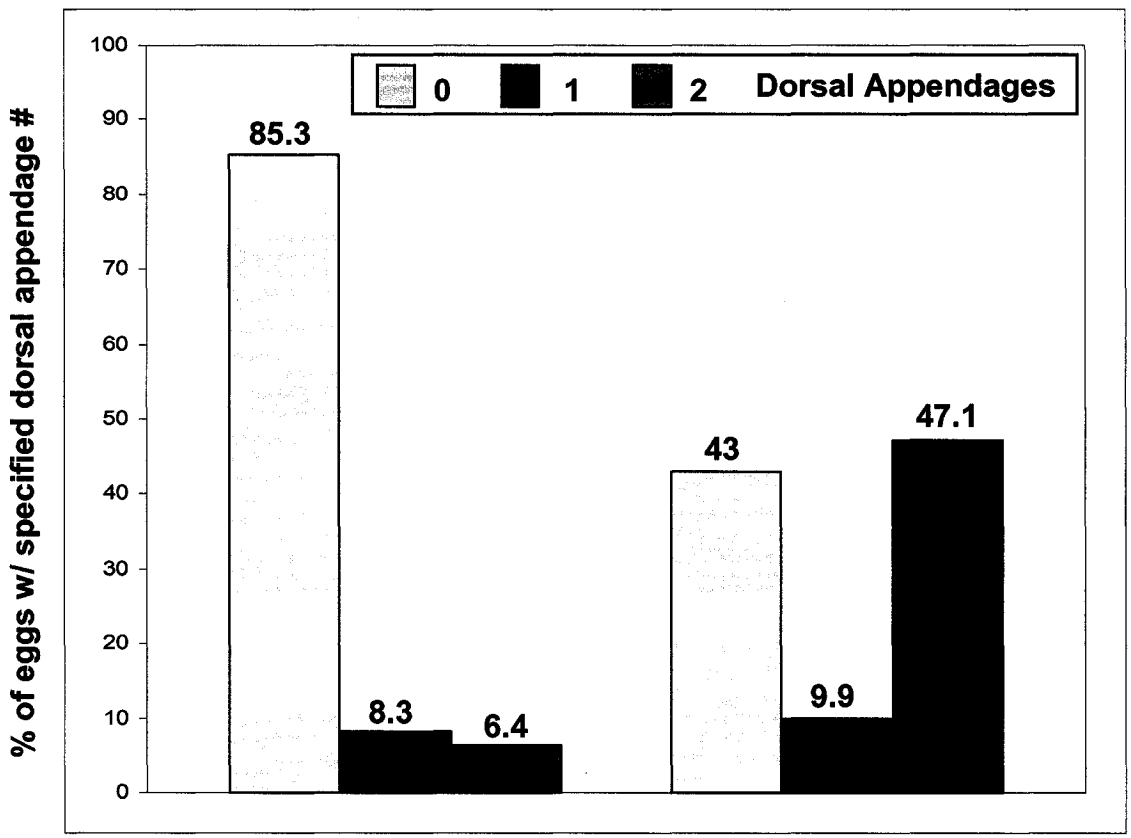

(n=451) (n=425)

2%	26%
(n=684)	(n=659)

% hatched

Figure 3.3.18 Bic-C overexpression produces defects in oocyte positioning and specification.

Orb protein (green) marks the position of the oocyte in wild-type (A) and Bic-C overexpressing egg chambers (B, C). Actin is visualized by rhodamine-phalloidin (red).

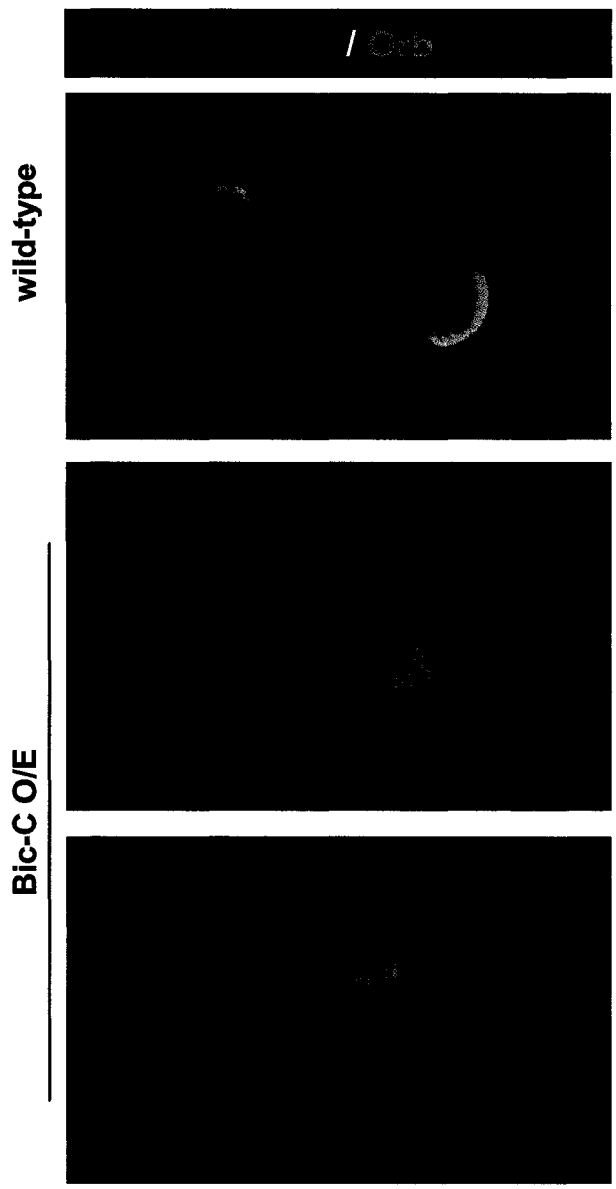

UASP-Bic-C^{7}/ nosGal4::VP16

When Orb levels were reduced in the context of Bic-C overexpression, both the frequency and severity of these early defects appeared to increase, however, these effects were not quantified (Fig. 3.3.19). Since the amount of Orb protein is not significantly reduced by Bic-C overexpression at these stages, the observed phenotypes may be due to a direct repression of Orb-target mRNAs.

3.3.9 Bic-C overexpression induces *orb*-like phenotypes before a reduction of Orb protein is detectable

Since Bic-C and Orb proteins associate *in vivo*, function antagonistically in genetic assays, and the RNA binding activity of Bic-C is essential for its function, a logical hypothesis would be that Bic-C acts on Orb target mRNAs to suppress Orb-mediated increases in polyadenylation. However, given that Orb expression is auto-regulated through a positive feedback loop involving polyadenylation (Tan et al., 2001), the Bic-C overexpression phenotypes could also result from repressing Orb expression. To determine if Orb expression is affected by Bic-C overexpression, Orb levels were analyzed by Western blotting. When whole ovaries are compared, a slight decrease in over-all Orb expression is apparent upon Bic-C overexpression (Fig. 3.3.20-A). However, when ovaries are separated by filtration (to isolate separate stages) prior to Western blotting, it is evident that Bic-C overexpression does not produce a decrease in Orb levels before stage 9 (Fig. 3.3.20-B).

To assess whether the absence of posterior Osk coincides with a reduction in Orb levels, Orb and Osk were visualized simultaneously by whole-mount immunofluorescence. Despite obvious defects in posterior Osk accumulation beginning

Figure 3.3.19 Bic-C-induced disruption of egg chamber morphology is enhanced by reduction of Orb.

Orb protein (green) marks the position of the oocyte in heterozygous $orbF^{343}$ (A), Bic-C overexpressing (B) and a heterozygous $orbF^{343}$ egg chamber overexpressing Bic-C (C). Actin and DNA are visualized by rhodamine-phalloidin (red) and DAPI (blue) staining, respectively.

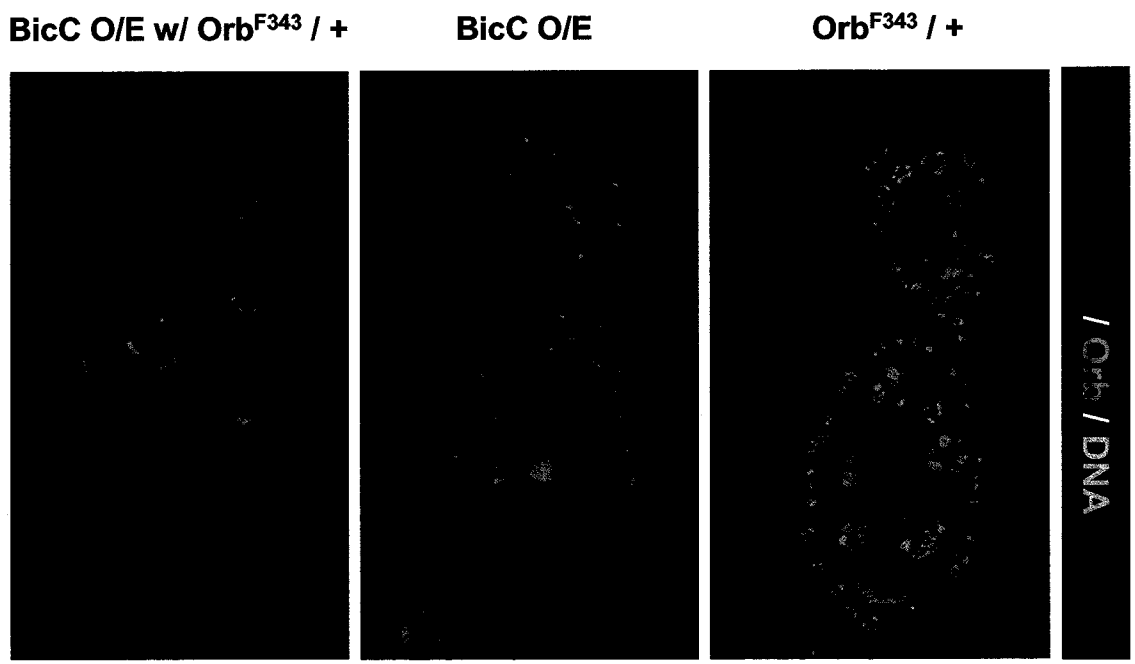
BicC O/E w/ Orb^{F343} / +
BicC O/E
Orb^{F343} / +
/ Orb / DNA

Figure 3.3.20 Bic-C overexpression does not reduce Orb expression prior to the onset of rapid cytoplasmic streaming.

(A) Western blotting of ovarian proteins with α-Orb reveals a slight decrease in Orb expression, relative to the α-tubulin loading control, upon Bic-C overexpression. (B) Egg chambers were separated by passage through a 100 μM filter prior to analysis. Western blotting with α-Orb indicates that Orb levels do not fall below wild type levels until late in oogenesis (stages 9-14). Equivalent levels of a-tubulin indicate even loading.

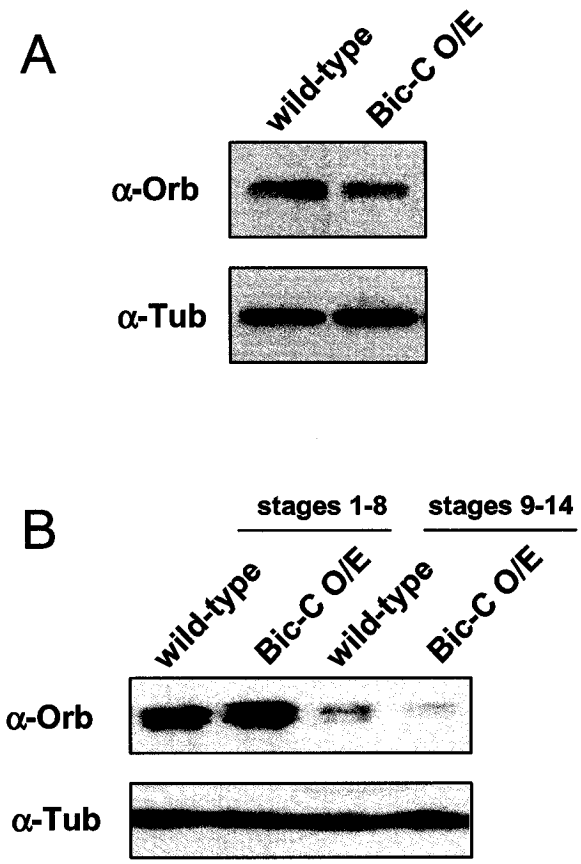
A
wild-type
Bic-C O/E
α-Orb
α-Tub
B
stages 1-8
stages 9-14
wild-type
Bic-C O/E
wild-type
Bic-C O/E
α-Orb
α-Tub

at stage 8, Orb levels were similar to wild-type controls at that stage (Fig. 3.3.21-A, B). Consistent with the Western analysis, a marked reduction of Orb levels is visible in older Bic-C overexpressing egg chambers relative to wild-type controls, however, this may be an indirect consequence of premature cytoplasmic streaming, as a similar reduction of Orb expression was observed in $capu^{EE}$ ovaries (Fig. 3.3.21, C-E).

It was also evident that stage 8-9 oocytes produced by Bic-C overexpressing females were substantially larger than wild-type oocytes (compare Fig. 3.3.21-B with A), although the egg chamber as a whole was not. The size differential between Bic-C overexpressing oocytes and wild-type oocytes is no longer obvious at stage 10 (compare Fig. 3.3.21-D with C). To illustrate this effect more clearly I immunofluorescently labeled wild-type, Bic-C overexpressing and $Bic\text{-}C^{YC33}$ homozygous mutant ovaries with α-Armadillo, which marks the border cells (Fig. 3.3.22). The relative position of the border cells, along the anterior/posterior axis, serves as a precise temporal marker during mid-oogenesis. They begin migrating from the extreme anterior of the egg chamber during stage 8 and come to rest at the anterior surface of the oocyte during the transition between stages 9 and 10. In a wild-type stage 8 egg chamber, the oocyte occupies approximately one third of the total volume of the egg chamber (Fig. 3.3.22-A), whereas in a Bic-C overexpressing egg chamber (Fig. 3.3.22-B), the oocyte occupies about half of the total egg chamber volume. Interestingly, the reciprocal effect is observed in *Bic-C* mutants, where cytoplasmic transfer into the oocyte is often delayed relative to wild-type controls (Fig. 3.3.22-C). Also note that the posterior migration of the follicle cells overlying the egg chamber is premature in the Bic-C overexpressing egg chamber and delayed in the *Bic-C* mutant.

Figure 3.3.21 Bic-C overexpression disrupts pole plasm assembly prior to any reduction of Orb expression.

Confocal immunofluorescence illustrates Orb (green) and Osk (red) expression in wild-type (A) and Bic-C overexpressing (B) stage 8 egg chambers. Note the substantially larger oocyte in the Bic-C overexpressing egg chamber, which was staged by the position of the border cells (white arrows). By stage 10, Orb levels decrease in wild-type egg chambers (C), however this reduction is more dramatic upon Bic-C overexpression (D) and in $capu^{EE}$ homozygotes (E).

/ DNA / Orb
Osk
A
B
C
D
E
Stage 8
Stage 10
wild-type
Bic-C O/E
wild-type
Bic-C O/E
capu^EE

Figure 3.3.22 Bic-C promotes cytoplasmic transfer from the nurse cells to the oocyte

Confocal immunofluorescence of ovaries labelled with α-armadillo (green) illustrates the posteriorly-migrating border cells (marked by white arrows) in wild-type (A), Bic-C overexpressing (B) and homozygous *Bic-C*^{YC33} mutant (C) egg chambers. Actin and DNA are visualized by rhodamine-phalloidin (red) and DAPI (blue) staining respectively.

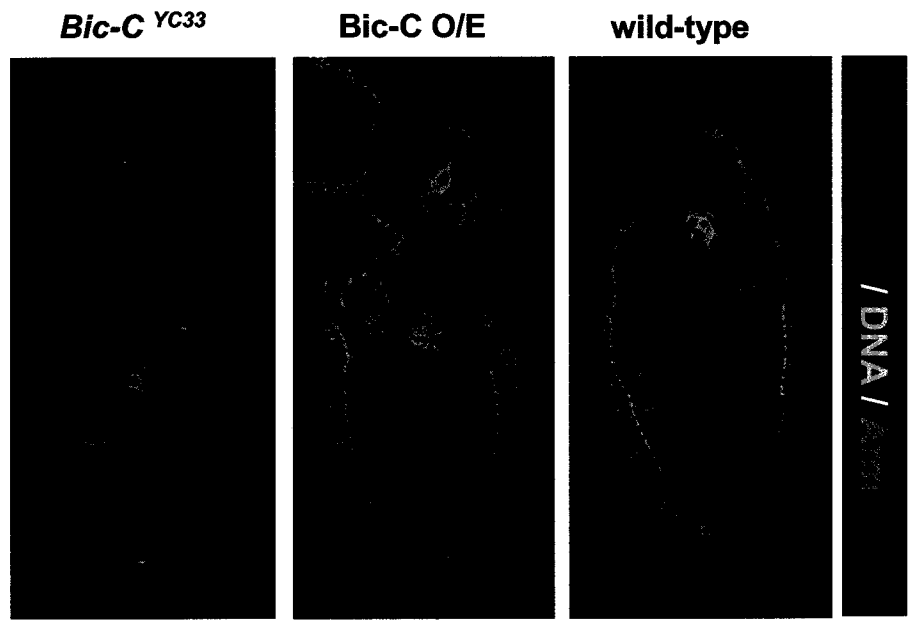
Bic-C YC33
Bic-C O/E
wild-type
/ DNA / ATP1

3.3.10 Bic-C physically associates with Orb and components of the deadenylase machinery

To determine if Bic-C forms a complex with any components of the deadenylase machinery, Bic-C was immunoprecipitated from OreR ovarian extracts and from ovarian extracts containing an HA-tagged CCR4 (CCR4-HA). Western blotting of co-precipitating proteins revealed that, in addition to Orb, both CCR4-HA and NOT3 form an RNase resistant complex with Bic-C (Fig. 3.3.23). To control for non-specific enrichment, these samples were also probed with α-Vasa. Unlike CCR4-HA, NOT3 and Orb, Vasa was not enriched in the Bic-C immune complex, demonstrating the specificity of these interactions (Fig. 3.3.23).

The interaction between CCR4-HA and Bic-C was confirmed by the reciprocal experiment, in which CCR4-HA was immunoprecipitated from ovarian extracts with α-HA (Fig. 3.3.24). Pop2-HA, another component of the deadenylase complex, was also immunoprecipitated, while OreR ovarian extract was used to control for direct binding to the α-HA resin (Fig. 3.3.24). Western blotting demonstrates that Bic-C, while detectable at low levels in the negative control, is specifically and substantially enriched in the CCR4-HA and Pop2-HA immune complexes.

Figure 3.3.23 Bic-C forms an RNase-resistant complex with CCR4, NOT3 and Orb.

Bic-C immune complexes were isolated from ovarian extracts in the absence or presence of RNase A, while pre-immune sera served as a negative control. Immunoblotting of co-precipitating proteins indicate that CCR4-HA, NOT3 and Orb are specifically enriched in the Bic-C immune complex (independently of intact RNA), while Vasa is not.

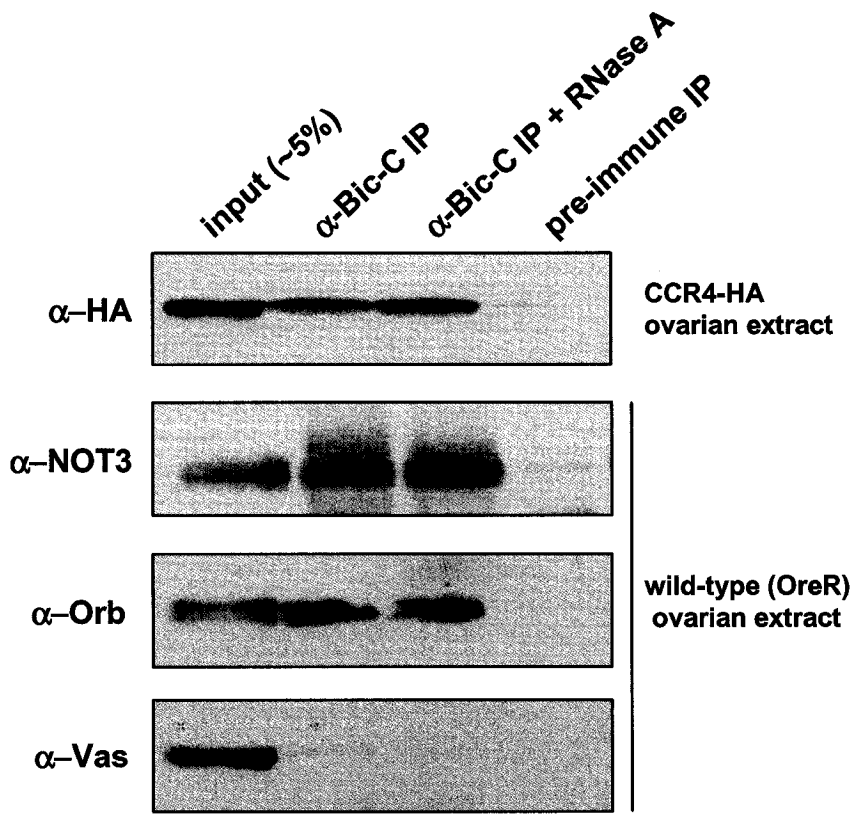
input (~5%)
α-Bic-C IP
α-Bic-C IP + RNase A
pre-immune IP
α–HA
α–NOT3
α–Orb
α–Vas
CCR4-HA
ovarian extract
wild-type (OreR)
ovarian extract

Figure 3.3.24 Bic-C is enriched in CCR4-HA and Pop2-HA immune complexes.

Western blotting demonstrates that Bic-C is enriched in CCR4-HA and Pop2-HA ovarian immunoprecipitates relative to an OreR control. Immunoprecipitations were performed with an α-HA antibody.

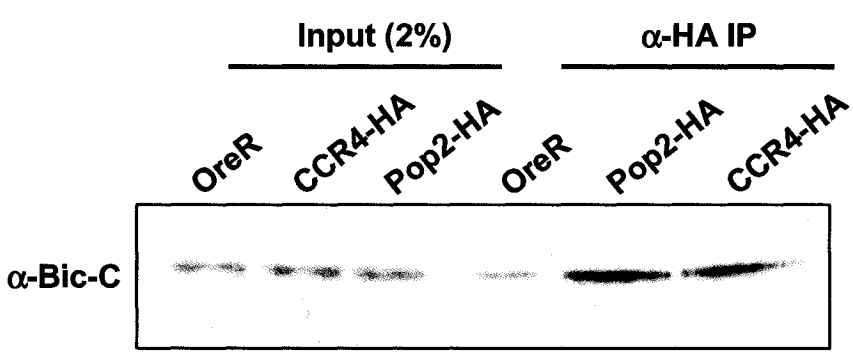
Input (2%)
α-HA IP
OreR
CCR4-HA
Pop2-HA
OreR
Pop2-HA
CCR4-HA
α-Bic-C

Chapter 4: Bic-C may promote exocytosis through an association with the Trailer Hitch complex

3.4.1 Introduction

Exocytosis is essential for the maintenance of cellular membranes and inter-cellular communication. Two critical examples during *Drosophila* oogenesis are the secretion of Grk and the Vitellogenin receptor, Yolkless. When these molecules are not properly secreted from the oocyte, eggs become ventralized due to a failure to activate EGFR and are flaccid due to a failure in yolk uptake (Murthy et al., 2003). Recently, an ER associated RNP complex containing Trailer Hitch (Tral), Me31B, YPS, PABP and Cup among other proteins, has been implicated in the proper maintenance of COPII exit sites from the ER and for efficient exocytosis during oogenesis (Wilhelm et al., 2005). Similar to mutants of the exocyst component sec5, *tral* mutants are defective in both Grk and Yolkless secretion (Murthy et al., 2003; Wilhelm et al., 2005). Interestingly, flaccid stage 14 egg chambers with reduced or missing dorsal appendages are produced by some of the weaker *Bic-C* alleles, suggesting a possible defect in exocytosis (Mahone, 1994). Furthermore, the putative protein interaction between Bic-C and Me31B, detected in a yeast two-hybrid screen (Paliouras, M., Ph.D Thesis 2005), suggests a possible association with the Trailer Hitch complex.

3.4.2 Homozygous Bic-C phenotypes may reflect a defect in exocytosis

Visualization of the actin cytoskeleton with rhodamine-conjugated phalloidin reveals several morphological defects in *Bic-C* mutant ovaries that may reflect defects in exocytosis. In wild-type ovaries, F-actin is closely associated with cell membranes and is

not detectable on the oocyte cytoplasm (Fig. 3.4.1-A,B), whereas *Bic-C* mutant oocytes accumulate actin-coated structures (resembling vesicles) beginning at stage 6/7 (Fig. 3.4.1-C). These actin-coated structures increase in size and number and accumulate primarily near the oocyte nucleus at the anterior cortex (Fig. 3.4.1-C,E). In some cases the oocyte cortex appears highly disorganized (Fig. 3.4.1-C) or to separate from the overlying follicle cells (Fig. 3.4.1-D). Also, the oocyte nucleus is sometimes mispositioned, having dissociated from the anterior / dorsal cortex (Fig. 3.4.1-D). A similar defect has been reported in *sec5* mutants and is believed to result from an inability to target an unidentified nuclear tethering factor to the plasma membrane (Murthy et al., 2003). Hypomorphic germline clones of *sec5* also result in stage 10 egg chambers where the nurse cells appear to protrude into the oocyte (Murthy et al., 2003). Interestingly, this is one of the characteristic terminal phenotypes of homozygous *Bic-C* mutants (Fig. 3.4.2; (Schupbach and Wieschaus, 1991).

3.4.3 Grk secretion is disrupted in Bic-C mutants

To determine whether Bic-C is required for Grk secretion, the distribution of Grk protein was visualized by immunofluorescence. In wild-type oocytes, Grk protein begins accumulating at the anterior/dorsal cortex, in close association with the nucleus, at stage 7 (Fig. 3.4.3-A), where it remains through late stage 9 (Fig. 3.4.3-B). At comparable stages in *Bic-C*^{YC33} ovaries, Grk is abnormally concentrated in clumps around the entire surface of the oocyte nucleus and appears diffusely in the oocyte cytoplasm (Fig. 3.4.3-C, D).

Figure 3.4.1 Bic-C mutants display defects in actin morphology.

Phalloidin staining illustrates the normal distribution of F-actin in wild-type stage 6 and 9 (A) and stage 10 (B) egg chambers. In Bic-C deficient egg chambers, actin-coated aggregates accumulate near the anterior of the oocyte as early as stage 6 (C) and appear to increase in size and number through stage 9 (C), until egg chambers degenerate at stage 10 (D). DNA is visualized by DAPI staining (blue).

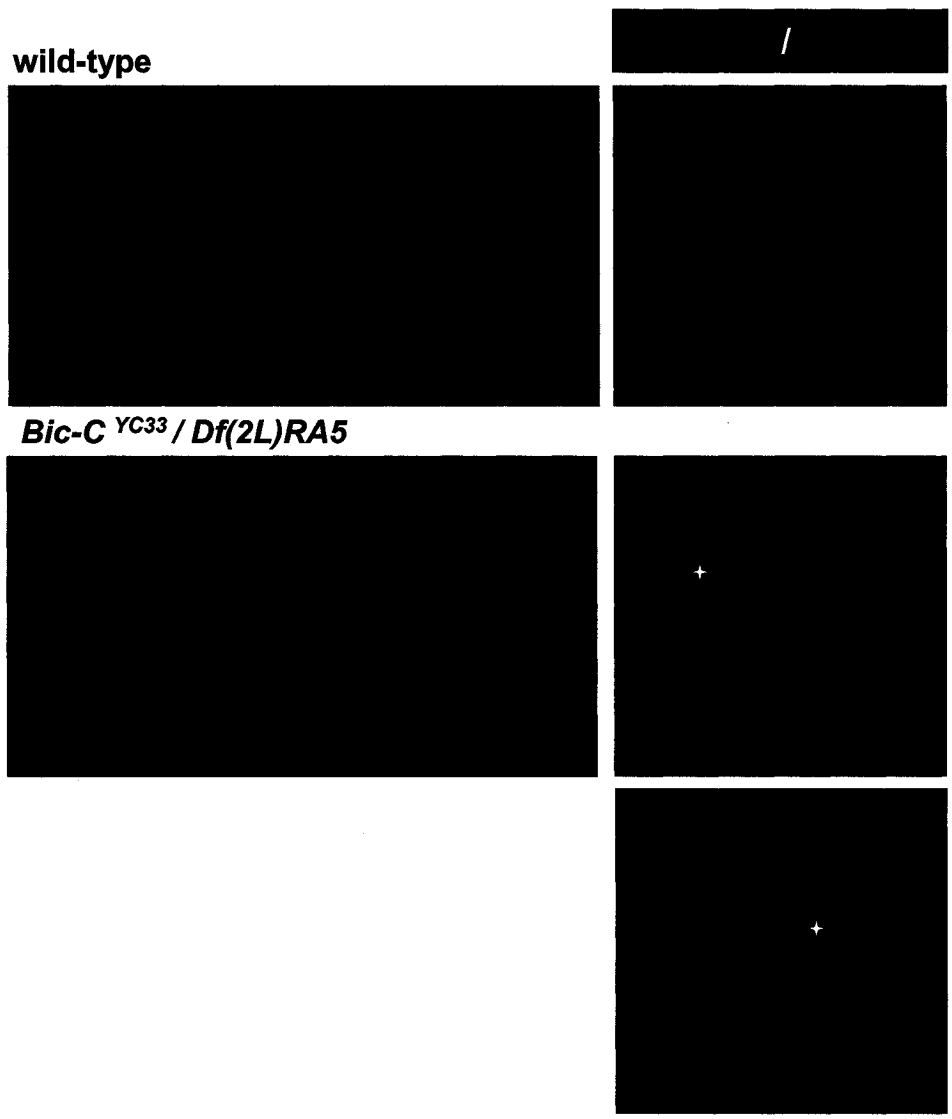
wild-type
/
Bic-C YC33 / Df(2L)RA5

Figure 3.4.2 Nurse cells protrude into the oocyte space in Bic-C mutants.

In wild-type egg chambers (A), a subset of follicle cells migrate centripetally between the nurse cells and the oocyte at stage 10. In homozygous *Bic-C* mutants, centripetal migration of the follicle cells does not occur and the nurse cells invade the space normally occupied by the oocyte (B). α-Armadillo staining (green) was used to highlight the border cells and follicle cell membranes, while Actin (red) and DNA (blue) were visualized by rhodamine-phalloidin and DAPI staining respectively.

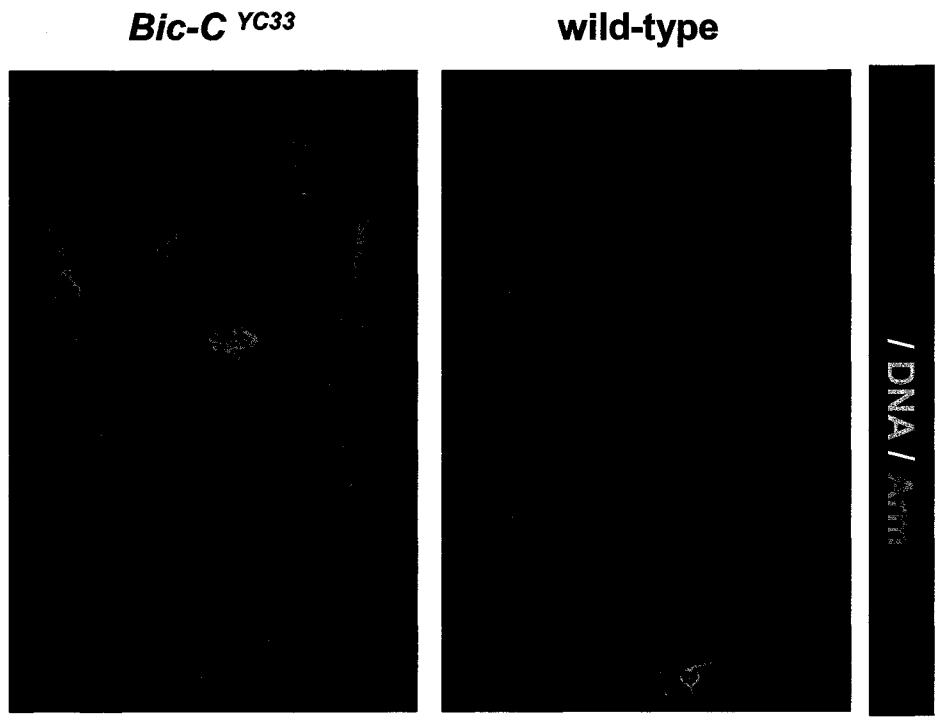
Bic-C YC33
wild-type
/ DNA / Actin

Figure 3.4.3 Grk accumulates in aggregates in Bic-C mutants.

Confocal immunofluorescence with α-Grk antibodies shows that in wild-type stage 7 (A) and late stage 9 (B) oocytes, Grk protein (green) is tightly localized between the nucleus and the anterior/dorsal cortex. In comparably staged homozygous *Bic-C*^{YC33} mutant ovaries (C and D), Grk accumulates in large aggregates that are concentrated around the entire nuclear surface. DNA is visualized by DAPI staining (blue). Note that A-C consist of single confocal sections, while D is composed of multiple sections (along the Z-axis) that have been compressed into a single image.

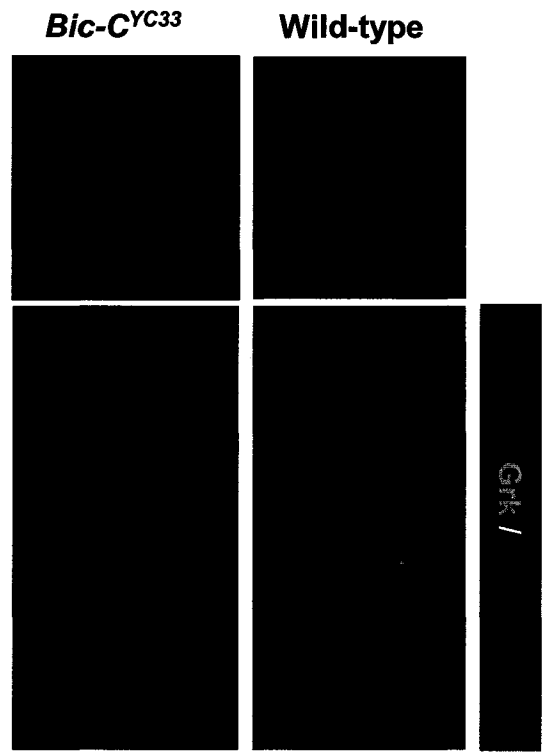
Bic-C^YC33
Wild-type
GLK

grk mRNA localization is a highly regulated process and is a prerequisite for local secretion of Grk protein to the anterior/dorsal follicle cells (Herpers and Rabouille, 2004). To ascertain whether a defect in *grk* mRNA localization might underlie the abnormal protein distribution observed in *Bic-C* mutants, *grk* mRNA and protein were visualized simultaneously by *in situ* hybridization and immunofluorescence (Fig. 3.4.4). In both wild-type (Fig. 3.4.4-A,B) and *Bic-C* mutant egg chambers (Fig. 3.4.4-C,D), *grk* mRNA is closely associated with the oocyte nucleus. In wild-type oocytes, this localization closely mirrors the distribution of Grk protein, whereas in Bic-C deficient oocytes, Grk protein appears to diffuse away from the site of transcript accumulation. These results imply that *grk* mRNA localization is unaffected by the loss of Bic-C and aberrant Grk protein accumulation likely results from a subsequent defect in Grk processing or sorting through the ER/Golgi complex.

The level of EGFR activation in the anterior/dorsal follicle cells was compared in *Bic-C*^{YC33} heterozygotes and *Bic-C* null ovaries using the *mirror lacZ* reporter line *l(3)6D1* (Zhao et al., 2000), to determine if any functional Grk is secreted in the absence of Bic-C. Immunofluorescent labeling demonstrates that in *Bic-C* heterozygotes (*Bic-C*^{YC33}/+) Grk and *mirr* expression are both normal (Fig. 3.4.5-A). However, in *Bic-C* null ovaries (*Bic-C*^{YC33}/ *Df(2L)RA5*), *Mirror* expression is not activated (Fig. 3.4.5-B,C). Therefore, the abnormal distribution of Grk observed in *Bic-C* mutants likely reflects a defect in Grk secretion which prevents delivery of the protein to the follicle cells and activation of the EGFR.

Figure 3.4.4 *grk* mRNA is properly localized in *Bic-C* mutants.

Immunofluorescence and fluorescent mRNA *in situs* reveal the distribution of Grk protein (green) and *grk* mRNA (red) in wild-type (A and B) and Bic-C deficient (C and D) ovaries. DNA is visualized by DAPI staining (blue).


wild-type
/ Grk /
Bic-C^YC33 / Df(2L) RA5

Figure 3.4.5 Bic-C is essential for GRK secretion and EGFR activation but not for Grk cleavage.

(A-B) Confocal immunofluorescence illustrates Grk (red) and β-Gal (representative of Mirr, green) expression in wild-type (A) and Bic-C deficient ovaries (B and C). Arrows mark the position of the border cells, indicating that the egg chambers are equivalently staged. DNA is visualized by DAPI staining (blue). (D) Soluble and insoluble fractions were separated from ovaries expressing myc-tagged Grk in a wild-type (lane 1) or a *Bic-C*^{YC33} mutant background (lane 2). Proteins were resolved by SDS-PAGE and Grk-$(Myc)_6$ was visualized by Western blotting with an α-myc antibody.

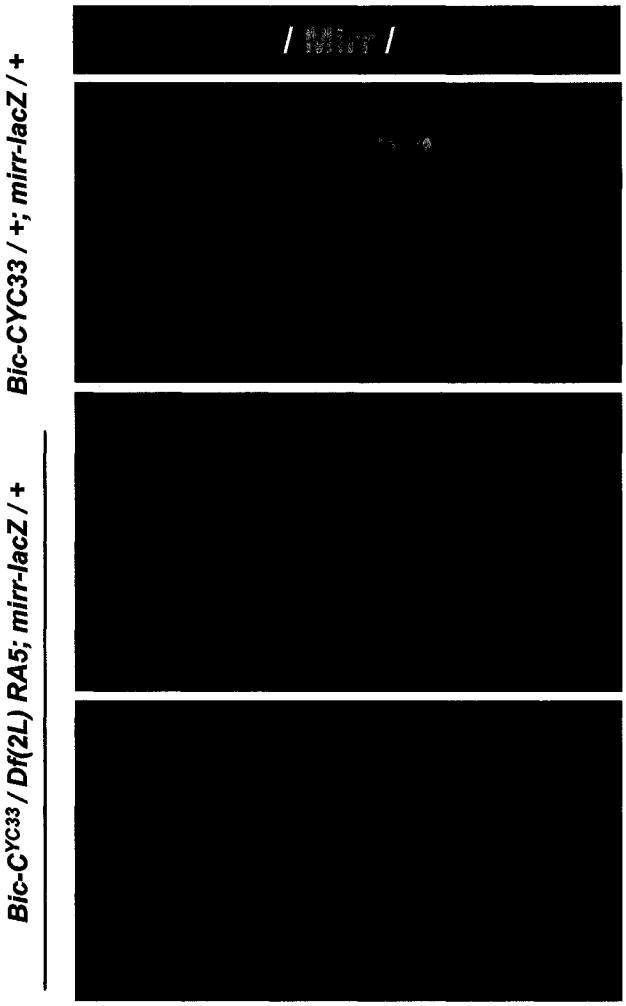
Bic-CYC33 / +; mirr-lacZ / +
Bic-CYC33 / Df(2L) RA5; mirr-lacZ / +

D

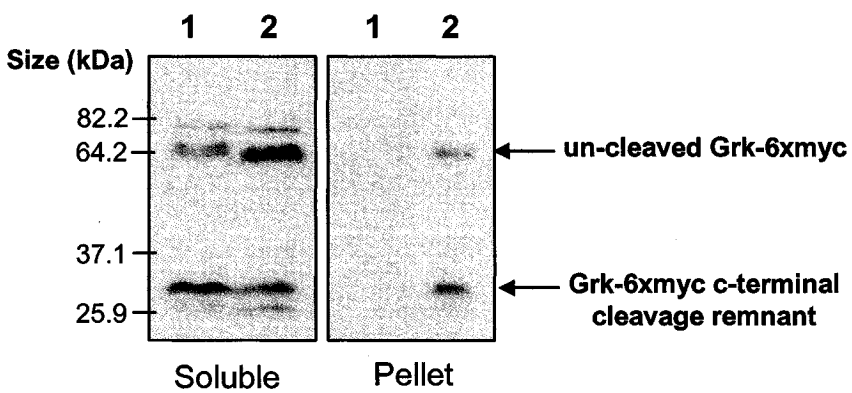
1
2
1
2
Size (kDa)
82.2
64.2
37.1
25.9
un-cleaved Grk-6xmyc
Grk-6xmyc c-terminal cleavage remnant
Soluble
Pellet

An essential step in Grk secretion is cleavage in the ER by the combined activities of *Star* and *Brother of rhomboid* (a.k.a. *rhomboid-2*) (Ghiglione et al., 2002; Bokel et al., 2005). To determine if this processing step is impaired by loss of Bic-C, a version of Grk bearing six copies of the myc epitope at its C-terminus was expressed in wild-type and *Bic-C*^{YC33} ovaries using the Gal4/ UASp system (Ghiglione et al., 2002). Uncleaved Grk (Fig. 3.4.5-D, top arrow) and the C-terminal cleavage remnant (Fig. 3.4.5-D, bottom arrow) were both detectable by western blotting with α-myc, in extracts from wild-type and *Bic-C*^{YC33} ovaries, indicating that Bic-C is not essential for Grk cleavage. However, the ratio of uncleaved Grk to the cleaved C-terminal remnant appears to be higher in the absence of Bic-C, suggesting that the efficiency of this process may be slightly reduced in *Bic-C* mutants. A substantial fraction of the Grk-$(Myc)_6$ was detected in the insoluble fraction from *Bic-C*^{YC33} ovaries but not from wild-type controls (Fig. 3.4.5-D), despite the fact that both extracts were prepared in parallel under identical conditions. This suggests that in *Bic-C* mutants, Grk solubility is reduced through vesicular sequestration or the formation of protein aggregates.

3.4.4 Bic-C associates with Me31B-eGFP *in vivo*

Ovaries expressing Me31B-eGFP (Nakamura et al., 2001) were fixed and stained with α-Bic-C to discern whether Bic-C and Me31B co-localize *in vivo*. Me31B-eGFP accumulates in discrete cytoplasmic foci (Fig. 3.4.6-C), while Bic-C distribution is granular but more diffuse than that of Me31B (Fig. 3.4.6-A). However, both proteins clearly co-localize in punctate structures within the oocyte cytoplasm of a stage 5 egg chamber (Fig. 3.4.6-E). During stage 7, both proteins are enriched in the same regions of

Figure 3.4.6 Bic-C and Me31B co-localize during oogenesis.

Immunofluorescently labeled Bic-C (A, B), shown in red and ME31B-eGFP (C, D), shown in green, co-localize in the oocyte during mid-oogenesis (E, F).

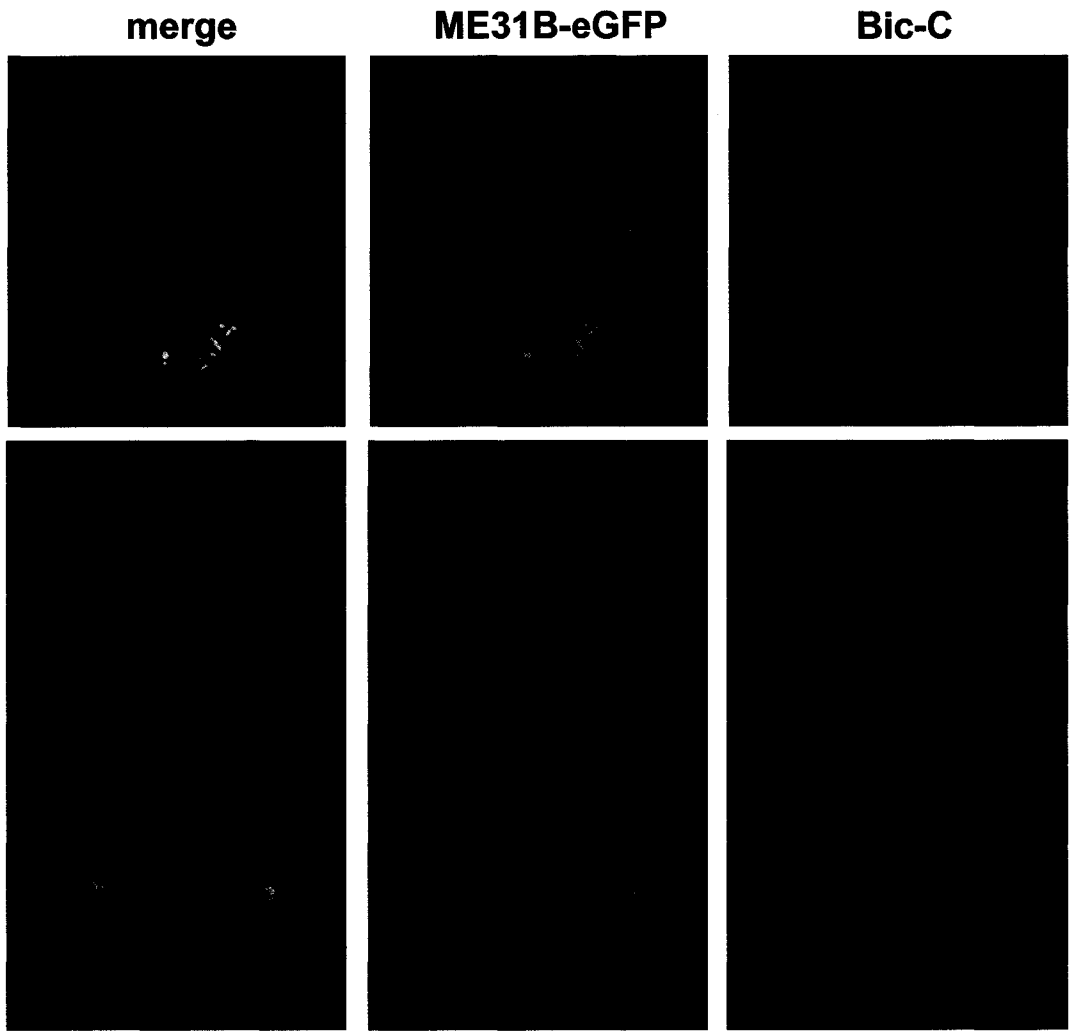
merge
ME31B-eGFP
Bic-C

the anterior/lateral cortices (Fig. 3.4.6-B,D,F). Interestingly, the reported distribution of oocyte-localized Trailer Hitch is remarkably similar at both of these stages of oogenesis (Wilhelm et al., 2005), where it has also been shown to co-localize with Me31B-eGFP in cytoplasmic granules (Boag et al., 2005).

Co-localization of Bic-C and Me31B suggests that these proteins may interact *in vivo*. To test this possibility, Bic-C was immunoprecipitated from ovarian extracts containing Me31B-eGFP. Western blotting of co-precipitating proteins revealed that Me31B-eGFP associates with Bic-C in an RNA-dependent complex (Fig. 3.4.7-A). The requirement for RNA stabilization or bridging of this interaction is somewhat unexpected given that these proteins interact in the yeast two-hybrid system, which usually reflects direct binding. It is possible however, that these proteins also require RNA to interact in yeast. Alternatively, this interaction may be direct but unstable in the absence of RNA. Interestingly, the association between Me31B and Trailer Hitch is also RNA-dependent, suggesting that RNA is a central component of this complex (Boag et al., 2005).

To determine if Bic-C associates with other components of the Trailer Hitch RNP complex, Bic-C immunoprecipitates from OreR ovarian extracts were analyzed by western blotting with antibodies specific to PABP and Trailer Hitch. PABP was specifically enriched in the Bic-C immune complex (Fig. 3.4.7-B). The α-Trailer Hitch serum recognized several protein species, all of which migrated very close to the predicted size of Trailer Hitch. The top band was specifically co-precipitated with Bic-C in an RNA-dependent manner, while the lower bands were detected in all samples (Fig. 3.4.7-C). It is currently unclear if these results reflect an interaction between Bic-C and a specific isoform of Trailer Hitch or if some form of post-translational modification,

Figure 3.4.7 Bic-C associates with components of the Trailer Hitch complex including Me31B.

Bic-C immune complexes were isolated from ovaries expressing Me31B-eGFP (A) or OreR ovarian extracts (B and C), while pre-immune sera served as a negative control. Co-precipitating proteins were detected by Western blotting with α-GFP (A), α-PABP (B) or α-Tral (C). The arrow (C) marks the band believed to be Trailer Hitch, which migrates slightly higher than an unidentified cross-reacting protein.

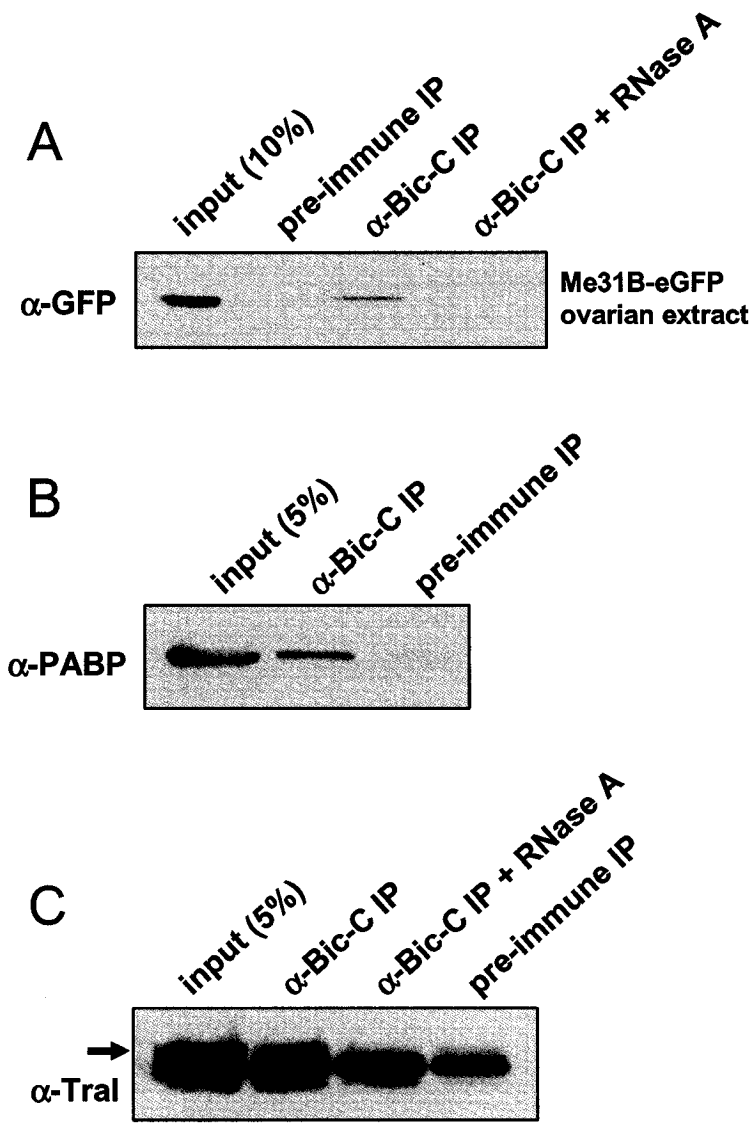
A
input (10%)
pre-immune IP
α-Bic-C IP
α-Bic-C IP + RNase A
α-GFP
Me31B-eGFP
ovarian extract
B
input (5%)
α-Bic-C IP
pre-immune IP
α-PABP
C
input (5%)
α-Bic-C IP
α-Bic-C IP + RNase A
pre-immune IP
α-Tral

altering the electrophoretic mobility of Trailer Hitch, is required for complex formation with Bic-C. Alternatively, it is possible that the α-Trailer Hitch serum exhibits cross-reactivity to an unrelated co-migrating protein.

Chapter 5: Bic-C phosphorylation

3.5.1 Introduction

Phosphorylation is an important mechanism for relaying signals and modulating protein function in response to external cues. Several RNA binding proteins are regulated through phosphorylation. For example, tyrosine phosphorylation of hnRNP K by c-Src disrupts its RNA binding activity and leads to de-repression of target transcripts (Ostareck-Lederer et al., 2002). Similarly, phosphorylation of the chicken Zipcode Binding Protein 1 (ZBP-1) by c-Src causes ZBP-1 to release *β-actin* mRNA, allowing localized translation of β-actin at actin-rich protrusions in primary fibroblasts and neurons (Huttelmaier et al., 2005).

The SAM domain of Bic-C contains a highly conserved tyrosine residue (Tyr822) that appears to mediate SH2 domain binding when phosphorylated in some members of the EPH receptor tyrosine kinase family of proteins (Stein et al., 1996; Shultz et al., 1997). To investigate whether Bic-C may be similarly regulated, Tyr822 was mutated and an analysis of Bic-C phosphorylation was performed.

3.5.2 Bic-C is phosphorylated *in vivo*

To assess the phosphorylation state of Bic-C *in vivo*, OreR ovaries were cultured in phosphate-free media containing ^{32}P-labeled ortho-phosphate prior to homogenization and immunoprecipitation with α-Bic-C. The incorporation of radiolabeled phosphate

permitted detection of Bic-C by auto-radiography, indicating that Bic-C is a phospho-protein (Fig. 3.5.1). To gauge the importance of Tyr822 in Bic-C phosphorylation, the same assay was performed on flies expressing a mutant form of Bic-C (Bic-C^{Y822F}) where Tyr822 was converted to a phenylalanine. This was done in a mutant background where endogenous Bic-C was truncated due to a premature stop codon (*Bic-C^{IIF34}/Df(2L)RA5*) and thus would not co-migrate with the full-length protein during resolution by SDS-PAGE. Although both forms of Bic-C (wild-type and Y822F) were present in equal quantities, as determined by Western blotting (Fig. 3.5.1), the level of ^{32}P incorporation in the Y822F mutant protein was several-fold lower than that of the endogenous wild-type protein (Fig. 3.5.1).

3.5.3 Tyrosine 822 is essential for Bic-C function

To assess the importance of Tyr822 in Bic-C function, the *Bic-C^{Y822F}* transgene and an equivalent transgene expressing a wild-type version of Bic-C were introduced into a homozygous *Bic-C^{YC33}* mutant background. Fertility was restored to mutant females bearing the wild-type transgene but not to females bearing the Bic-C^{Y822F} transgene (Fig. 3.5.2-A), whose ovaries resembled those of homozygous *Bic-C^{YC33}* females. To verify that both transgenes produced comparable amounts of Bic-C protein, a comparison to endogenous Bic-C expression was performed by immunoblotting. For this experiment, transgenic Bic-C expression was assessed in a homozygous mutant background (*Bic-C^{AA4}*) that produces very little Bic-C protein (Fig. 3.5.2-B, lane 2). I found that Bic-C^{Y822F} expression (lane 3) was somewhat lower than the transgenic wild-type Bic-C expression (lane 4) but similar to endogenous Bic-C expression (lane 1).

Figure 3.5.1 Bic-C is a phosphoprotein and a Y822F mutation in the SAM domain substantially reduces phosphorylation *in vivo.*

Auto-radiography of Bic-C immunoprecipitates from ^{32}P-ortho-phosphate labeled ovaries illustrates the level of ^{32}P incorporation in endogenous Bic-C and Bic-C^{Y822F}. Western blotting of the same membrane demonstrates that equivalent amounts of both proteins are present.

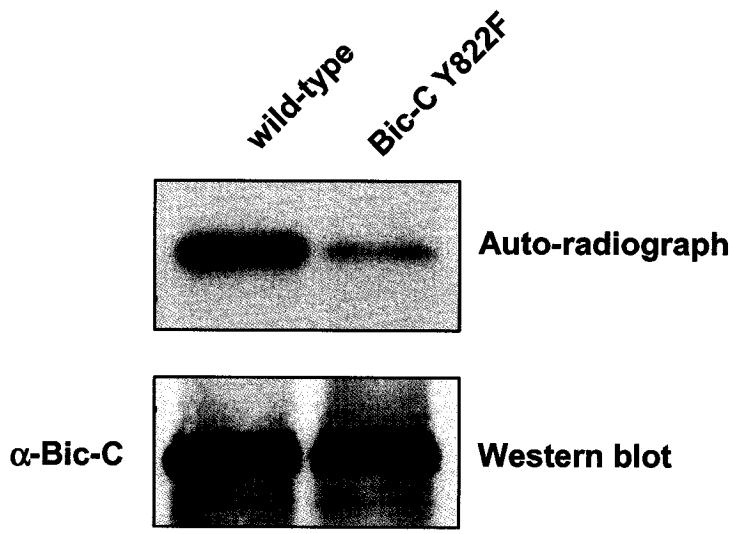
wild-type
Bic-C Y822F
Auto-radiograph
α-Bic-C
Western blot

Figure 3.5.2 The Y822F mutation disrupts Bic-C function.

(A) Two copies of the transgene expressing wild-type Bic-C restore fertility to *Bic-C*^{YC33} homozygous females, while two copies of the *Bic-C*^{Y822F} transgene do not. (B) Western blotting illustrates the level of transgene-derived Bic-C^{Y822F} and Bic-C^{WT} (wild-type) expression in a Bic-C^{AA4} homozygous background. eIF4A was used as a loading control. Approximately 25 μg of total protein was loaded per lane.

A

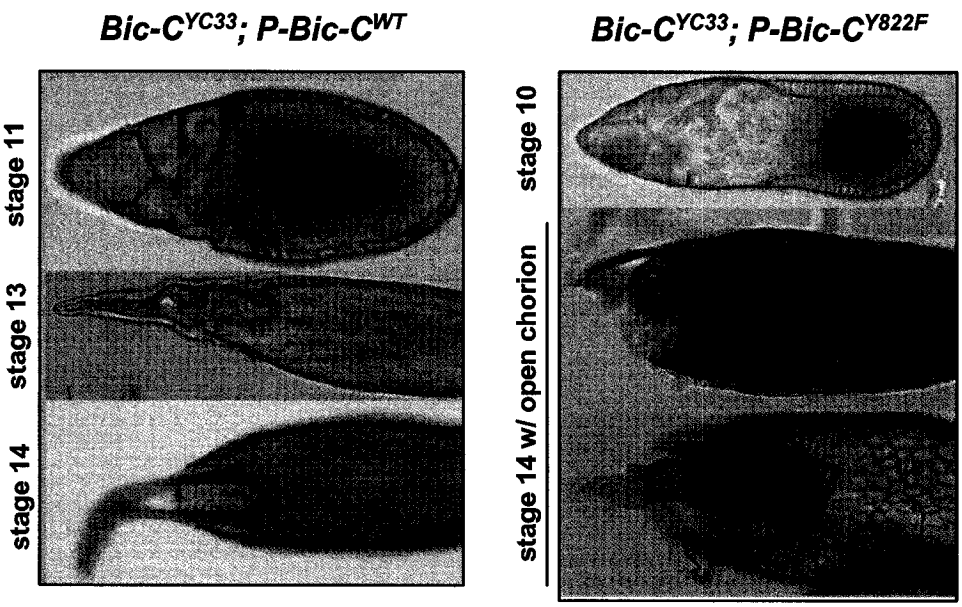
Bic-C^YC33; P-Bic-C^WT
Bic-C^YC33; P-Bic-C^Y822F
stage 11
stage 13
stage 14
stage 10
stage 14 w/ open chorion

B

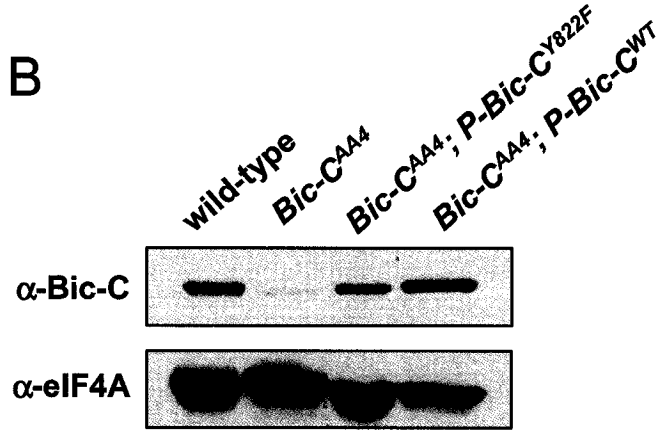
wild-type
Bic-C^AA4
Bic-C^AA4; P-Bic-C^Y822F
Bic-C^AA4; P-Bic-C^WT
α-Bic-C
α-eIF4A

Therefore, the inability of Bic-C^{Y822F} to restore Bic-C function likely results from a direct requirement for Tyr822 rather than inadequate levels of expression, although the latter possibility has not been definitively excluded.

3.5.4 Bic-C is phosphorylated on one or more serines

To determine the nature of the amino acid(s) incorporating the ^{32}P label, Bic-C was recovered and its peptide bonds were hydrolyzed to reduce the protein to its constituent amino acids. These amino acids were then subjected to phosphoamino acid analysis through resolution by thin layer chromatography. The ^{32}P label migrated exclusively with the serine standard indicating that Bic-contains one or more phospho-serines (Fig. 3.5.3-A). The NetPhos (v2.0) phosphorylation prediction software (Blom et al., 1999) was used to analyze the Bic-C amino acid sequence (Fig. 3.5.3-B). Bic-C contains 99 serine residues, many of which are in a sequence context that is favorable for phosphorylation.

Figure 3.5.3 Bic-C phosphorylation occurs on one or more serine residues.

(A) After ^{32}P-ortho-phosphate labeling and immuno-precipitation, Bic-C was hydrolyzed into its constituent amino acids for phosphoamino acid analysis on thin layer chromatography. Co-migration of the ^{32}P isotope with the serine standard indicates that phosphorylation occurs on one or more serine residue(s). (B) NetPhos 2.0 software predicts multiple phospho-serines in Bic-C.

A

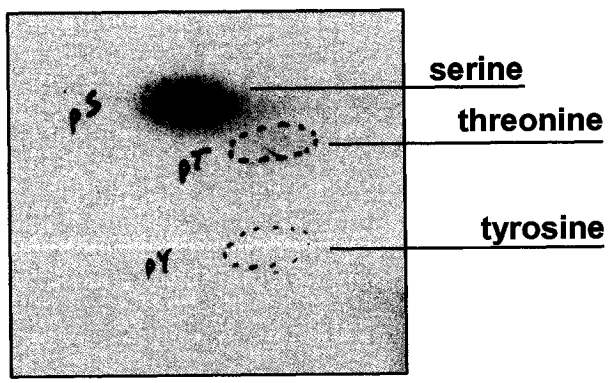

Phosphoamino acid analysis

B

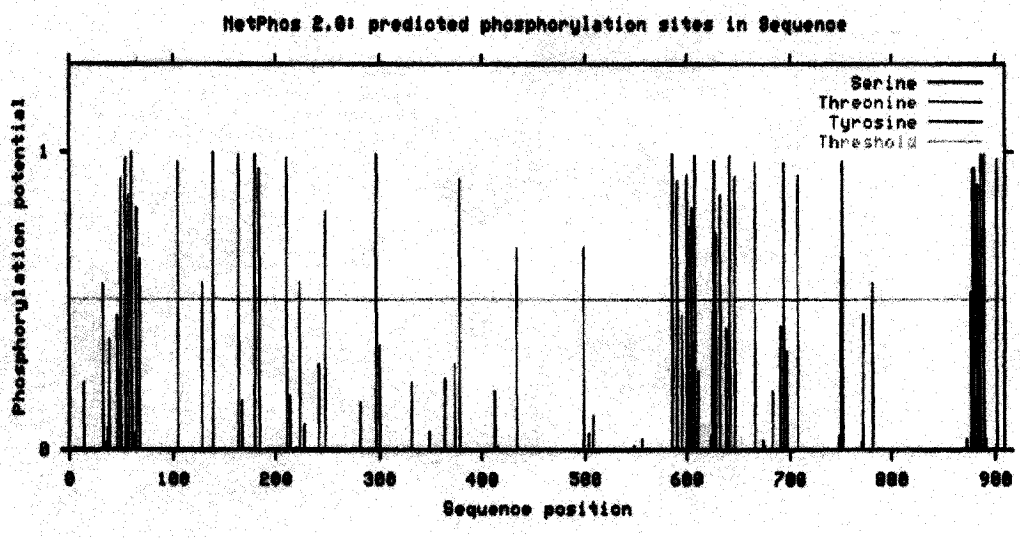

Section 4: Discussion and Conclusions

4.1 Bic-C mRNPs and emerging views of mRNP infrastructure

In our traditional image of eukaryotic gene expression, transcriptional control has occupied center stage while mechanisms controlling translation were widely regarded to play a supporting role. It is generally accepted that transcription factors can coordinate the expression of functionally related genes. However, the technical advances that have ushered in the modern genomic era have revealed surprising discrepancies between the transcriptome and the proteome (Gygi et al., 1999; Ideker et al., 2001), implying a greater degree of post-transcriptional regulation than anticipated. Accordingly, a growing body of evidence suggests that coordinated expression of functionally related genes can be regulated post-transcriptionally (Hieronymus et al., 2004). Much of this evidence has been acquired through a strategy termed ribonomic profiling, whereby an RNA-binding protein of interest is used as a molecular "handle" to isolate mRNP complexes. Associated mRNAs are then identified en masse, typically using microarray technology. This approach does have some caveats as it cannot distinguish which region of an RNA mediates binding or whether an RNA/protein interaction is direct or indirect. However, this approach provides the first means by which to perform a comprehensive survey of mRNP infrastructure and, as demonstrated for Nanos-mediated regulation of *hunchback*, biologically relevant interactions are not always direct (Sonoda and Wharton, 1999).

Several ribonomic-based studies have identified multiple mRNAs, encoding functionally related proteins, within the same mRNP complex (Keene and Lager, 2005). In some cases these functional relationships reflect participation in a common pathway or

process (Hieronymus and Silver, 2003; Ule et al., 2003; Gerber et al., 2006), while others reflect incorporation into a common macromolecular machine, such as the ribosome (Intine et al., 2003). Thus, eukaryotic mRNPs may represent a post-transcriptional equivalent of bacterial operons, coordinating spatial and temporal production of functionally related proteins (Keene and Tenenbaum, 2002). Unlike operons, however, mRNPs are dynamic structures and multiple combinations of *cis*-acting elements can generate substantial combinatorial power by directing transcripts into a multitude of differentially-regulated mRNPs. Various aspects of mRNA metabolism, such as pre-mRNA splicing (Ule et al., 2003), nuclear export (Hieronymus and Silver, 2003), stability (Gao et al., 1994; Tenenbaum et al., 2000) and translation (Gerber et al., 2004; Gerber et al., 2006) can be coordinated in this fashion.

Interestingly, ribonomic profiling of Bic-C-containing mRNPs has provided additional evidence for the "mRNP operon" model, as 7 of the 53 most highly enriched transcripts in the Bic-C immune complex encode proteins that are either directly involved in the *frizzled/dishevelled* signaling pathway (Par-1, Dishevelled, Slimb, Diego) or are downstream effectors of the pathway (Cip4, Src42A, Rheb). Frizzled (Fz) is a seven-pass transmembrane receptor for the Wnt family of signaling molecules that regulate various aspects of development, including morphogenic cell movements, cell polarization, cell adhesion, actin dynamics and transcriptional programs that ultimately guide cell-fate decisions (Strutt, 2003). Downstream of Fz, Dishevelled (Dsh) acts at the branch point between the canonical pathway, which controls β-catenin levels, and the Planar Cell Polarity (PCP) pathway that regulates actin dynamics. In *Drosophila*, the PCP pathway is critical for orienting wing hairs and for R3/R4 cell specification and ommatidial

rotation in the eye, whereas, the canonical pathway is essential for maintaining segment polarity during embryogenesis (Strutt, 2003). A number of factors, including Par-1 and Diego (Dgo) act on Dsh to determine which branch of the pathway will be active in a given cell or tissue. In *Drosophila*, Par-1 has been shown to promote the canonical Fz/Dsh signaling, while inhibiting the PCP pathway, presumably through phosphorylation of Dsh (Sun et al., 2001). In *Xenopus*, and probably other organisms, regulation by Par-1 is more complex; specific isoforms of Par-1 have opposing effects on the branch point decision (Ossipova et al., 2005). The ankyrin-repeat protein Diego interacts with multiple components of the PCP pathway, including the atypical cadherin Flamingo, the PCP antagonist Prickle and Dsh. Diego performs at least two PCP-related functions, as it promotes initiation of this pathway by preventing Prickle from binding to Dsh (Jenny et al., 2005) and it is required for polarized apical localization of Flamingo (Das et al., 2004).

The canonical Fz/Dsh pathway is regulated in part by Slimb, a substrate-specific adapter for the SCF E3-ubiquitin ligase complex that specifically targets β-catenin and several other proteins, for ubiquitin-mediated degradation (Jiang and Struhl, 1998; Bocca et al., 2001). In *Drosophila* oogenesis, Slimb is required for several processes, including cytoplasmic transfer from the nurse cells to the oocyte and down-regulation of Dpp activity in the follicle cells (Muzzopappa and Wappner, 2005).

CIP4 (Cdc42-interacting protein 4) is an effector protein of the Rho-GTPase Cdc42, which regulates actin polymerization and cytoskeletal reorganization (Bishop and Hall, 2000). A splice variant of CIP4 that produces a truncated version of the protein has been linked to renal cell carcinoma in humans (Tsuji et al., 2006). Truncation of CIP4

causes an increase in β-catenin phosphorylation and induces β-catenin mistrafficking from cell membranes to cytoplasmic aggresomes, disrupting cell-cell adhesion (Tsuji et al., 2006). Mammalian CIP4 binds to the Dishevelled-Associated Activator of Morphogenesis (DAAM1), which is required for Rho activation by the Wnt/Fz/Dsh PCP pathway during the convergent extension movements of vertebrate gastrulation (Aspenstrom et al., 2006; Habas et al., 2001).

Analysis of *DAAM* mutants in *Drosophila* suggest that DAAM does not play an essential role in the PCP pathway in flies, possibly due to some functional redundancy. However, it is required to organize a specialized array of actin cables that are structurally important for tracheal system development (Matusek et al., 2006). Genetic experiments indicate that the non-receptor tyrosine kinase Src42A acts in parallel or downstream of DAAM in this process (Matusek et al., 2006). Interestingly, Src42A binds to Armadillo (Arm; the *Drosophila* homologue of β-catenin) and co-localizes with Arm/β-catenin and E-cadherin at adherens junctions, which are essential for cell-cell adhesion (Takahashi et al., 2005). Src42A is required for Arm/β-catenin phosphorylation, which weakens adherens junctions, leading to reduced cell-cell adhesion and increased invasiveness (Takahashi et al., 2005).

Rheb (Ras homologue enriched in brain) is a member of the Ras superfamily of proteins that bind and hydrolyze GTP. Mutations in either *Tsc1* or *Tsc2* (Tuberous sclerosis 1/2) result in over-activation of GTP-bound Rheb, which is believed to cause tuberous sclerosis complex, a genetic disease causing mental retardation, seizures and the formation of benign tumors in various parts of the body (Aspuria and Tamanoi, 2004). Evidence gathered in *Drosophila* indicates that Rheb acts downstream of Tsc1 (Tuberous

sclerosis 1) and Tsc2 in the TOR (Target Of Rapamycin) signaling pathway to promote cell growth (Stocker et al., 2003). Interestingly, Wnt/Fz signaling can regulate Tsc2 phosphorylation through inhibition of glycogen synthase kinase 3 (GSK3), which in turn activates Rheb and the mammalian TOR pathway (Inoki and Guan, 2006).

Thus, several of the putative mRNA targets of Bic-C are functionally related to the canonical and PCP Fz/Dsh signaling pathways. Many of the other mRNAs found to be enriched in the Bic-C immune complex encode uncharacterized proteins, raising the intriguing possibility that some of these proteins may also be regulated by or function in Fz/Dsh signaling. It is interesting that several of the putative Bic-C target mRNAs connected to Fz/Dsh signaling regulate actin dynamics, as the actin cytoskeleton plays a pivotal role regulating cytoplasmic streaming during oogenesis. Although this pathway has not been linked to cytoplasmic streaming, overexpression of Bic-C could produce phenotypes that reflect a simultaneous repression of several functionally related transcripts and thus reveal regulatory relationships that would not be easily uncovered by conventional mutagenesis screens that target individual genes.

Both the canonical and PCP Wnt/Fz/Dsh signaling pathways are essential in vertebrates for proper kidney formation. The canonical pathway is required initially for the induction of metanephric mesenchyme and for cell proliferation in branching morphogenesis (Simons and Walz, 2006). It is believed that urine flow bends primary cilia on the surface of tubular epithelial cells in the developing kidney, triggering a signal cascade that initiates the production of inversin (Simons et al., 2005). Inversin, a vertebrate protein that is related to *Drosophila* Diego, specifically targets cytoplasmic Dishevelled for ubiquitin-mediated degradation but not Dishevelled associated with the

plasma membrane, thereby triggering a switch from the canonical to the PCP pathway (Simons et al., 2005). The exact role of the PCP pathway in kidney development is not yet known, however, it may be required for maintaining tubular geometry later in development (Simons and Walz, 2006). Interestingly, constitutive activation of the canonical Fz/Dsh pathway in mice causes a form of polycystic kidney disease that is strikingly similar to that caused by mutations in the mouse homologue of Bic-C (Saadi-Kheddouci et al., 2001; Cogswell et al., 2003). It is therefore tempting to speculate that Bic-C may perform an evolutionarily conserved role as a post-transcriptional regulator of the Fz/Dsh signaling in both flies and mammals.

4.2 Auto-regulation

In addition to the discovery of functional clustering within mRNPs, ribonomic profiling has also provided additional evidence for widespread auto-regulation by mRNA-binding proteins (Hieronymus and Silver, 2003; Waggoner and Liebhaber, 2003). However, even without high-throughput methods, several mRNA-binding proteins have been demonstrated to bind specifically to their own transcripts. Examples include Nova-1, FMR1P, PABP, TTP and Bcl-2 (Dredge et al., 2005; Schaeffer et al., 2001; de Melo Neto, 1995; Brooks et al., 2004; Bevilacqua et al., 2003a). In several cases these interactions have been shown to be biologically significant. For instance, Nova-1 regulates alternative splicing of its pre-mRNA (Dredge et al., 2005) and PABP can repress its own translation via adenine-rich sequences in its 5' UTR (Bag, 2001), while TTP and Bcl-2 target their own transcripts for degradation through an interaction with

AU-rich elements (AREs) located in their 3' UTRs (Brooks et al., 2004; Bevilacqua et al., 2003a).

In this study, I have discovered that Bic-C protein and *Bic-C* mRNA are associated in the same ovarian mRNPs. Using reporter transcripts, I have also provided evidence that this interaction is biologically relevant, acting to destabilize the *Bic-C* transcript. Although sequences in the 5' UTR of *Bic-C* are both necessary and sufficient to impart Bic-C-mediated repression, auto-repression appears to be greatest when both the 5' and 3' UTRs are present (see Figure 3.2.2) indicating a certain degree of functional synergy between these two regions. Interestingly, the *Bic-C* 3' UTR harbors 5 copies of the AU-rich element (AUUUA) that has been associated with the rapid turnover of many short-lived mRNAs (Bevilacqua et al., 2003b) and that are involved in mediating TTP and Bcl-2 auto-repression (Brooks et al., 2004; Bevilacqua et al., 2003a).

Surprisingly, when the Bic-C 5'UTR was removed from reporter transcripts, a reciprocal effect on protein expression was observed rather than an equalization of β-Gal levels. β-Gal expression in *Bic-C* mutants dropped below the level observed in wild-type ovaries. This may reflect a general decrease in translational efficiency and/or protein or RNA stability in *Bic-C* mutants, although decreases as such have not been reported in the Bic-C literature. Alternatively, the *Bic-C* and *K10* 3' UTRs might inhibit translation and a certain threshold of Bic-C may be required to overcome these inhibitory effects.

The fact that post-transcriptional auto-regulatory mechanisms exist is no longer in question, although, the exact purpose of such mechanisms and how they may have evolved is less obvious. Auto-repression, as observed for *Bic-C*, may provide a means of rapidly adjusting the level of an RNA-binding protein to match the number of mRNA

targets that it regulates. Such a mechanism could establish equilibrium between silenced and translated mRNAs, particularly if the RNA-binding protein in question acts in an additive fashion when regulating mRNA targets.

4.3 Overexpression of Bic-C reveals a novel function in regulating cytoplasmic movements

Given the existence of an auto-repressive mechanism, a logical assumption is that excess Bic-C will have harmful consequences. I tested this and found it to be true. Overexpression of Bic-C in the female germline induced microtubule rearrangements and premature cytoplasmic streaming which in turn produced defects in pole plasm assembly, posterior patterning and dorsal appendage formation. I used the Gal4-UASP system rather than the endogenous *Bic-C* promoter to perform these experiments since females constitutively overexpressing an unregulated *Bic-C* transcript would not produce viable progeny. Although this system does not recapitulate the normal transcriptional regulation of *Bic-C*, the amount of Bic-C protein produced from this system was comparable to endogenous levels (see Figure 3.3.15-D). Therefore, the total amount of Bic-C expression needed to initiate premature cytoplasmic streaming, derived from a combination of endogenous and transgenic sources, should not exceed twice the amount of endogenous Bic-C protein. Since I observed a much greater increase in β-Gal reporter protein expression in *Bic-C* deficient ovaries relative to wild-type, I believe that abrogation of Bic-C auto-regulation *in vivo* would generate sufficient levels of Bic-C to disrupt axial patterning.

Germline expression of the UASP-*Bic-C* transgene restored fertility to *Bic-C*^{YC33} homozygous females (data not shown), albeit at a low frequency due to the persistence of overexpression phenotypes. This demonstrates that the Bic-C protein produced from these transgenes is fully functional. Furthermore, I observed a decrease in the frequency and severity of dorsal appendage defects induced by Bic-C overexpression through a concomitant reduction of endogenous *Bic-C* dosage. I am thus confident that the phenotypes observed upon Bic-C overexpression result from an increase in normal *Bic-C* function.

By analyzing the effects of Bic-C overexpression I have discovered a novel function of *Bic-C* in regulating the onset of rapid cytoplasmic streaming. This function could not be uncovered through an analysis of strong *Bic-C* mutant alleles, since oogenesis arrests in homozygous *Bic-C* females before rapid cytoplasmic streaming is normally initiated. Bic-C overexpression also resulted in a transient increase in oocyte size from stages 8-9 relative to wild-type controls (Fig. 3.3.22), which is reciprocal to what occurs in *Bic-C* mutant egg chambers where stage 8-9 oocytes are often abnormally small (Mahone et al., 1995). These observations provide strong evidence that *Bic-C* promotes cytoplasmic transfer from the nurse cells to the oocyte during stages 8-9. Rapid streaming is believed to be required for mixing the oocyte cytoplasm with incoming cytoplasm from the nurse cells, thus temporal coordination of these two events is essential. Several gene products have been implicated in controlling cytoplasmic streaming but mutations affecting these genes have not been reported to result in premature cytoplasmic transfer into the oocyte. Therefore, Bic-C overexpression is the first context in which cytoplasmic transfer from nurse cells to the oocyte, and

cytoplasmic streaming within the oocyte, both occur prematurely, suggesting that *Bic-C* function may be responsible for coordinating these events. The endogenous *Bic-C* expression pattern is consistent with such a role, as there is a dramatic increase in *Bic-C* mRNA and protein levels in the nurse cells beginning at stage 10, just prior to bulk cytoplasmic transfer and rapid streaming (Mahone et al., 1995; Saffman et al., 1998). Multiple lines of evidence indicate that the nonmuscle myosin II heavy chain, encoded by *zipper*, provides the mechanical force that drives rapid transfer of the nurse cell cytoplasm into the oocyte, through an actin-based contraction mechanism (Wheatley et al., 1995; Edwards and Kiehart, 1996). This activity requires the nonmuscle myosin II regulatory light chain, encoded by *spaghetti squash* (*sqh*) (Edwards and Kiehart, 1996), which is activated by phosphorylation (Jordan and Karess, 1997). Sqh is also required to drive centripetal follicle cell migration over the anterior surface of the oocyte at stage 10, a process that is defective in *Bic-C* mutants (Edwards and Kiehart, 1996). Interestingly, the Fz/Dsh pathway has been shown to regulate Sqh phosphorylation through the *Drosophila* Rho-associated kinase (Drok) and this phosphorylation event is critical for the establishment of planar cell polarity in both the wing and the eye (Winter et al., 2001). These intriguing connections make it tempting to speculate that Bic-C may regulate both cytoplasmic movements and centripetal follicle cell migration by influencing the expression of Fz/Dsh pathway components. However, Sqh is also required for border cell migration (Edwards and Kiehart, 1996), which is unaffected in *Bic-C* mutants, thus any mechanism by which Bic-C might influence Sqh activity is likely to be complex.

Overexpression of Bic-C^{G296R} did not affect cytoplasmic transfer or cytoplasmic streaming, suggesting that Bic-C acts through RNA substrates in both contexts. *orb* is among the genes that, when mutated, produce the premature cytoplasmic streaming phenotype and *orb* encodes a CPEB-like protein that is believed to promote polyadenylation of specific transcripts including *osk* (Chang et al., 1999). Since reduction of Orb can suppress dominant *Bic-C* mutant phenotypes and Bic-C and Orb have been shown to interact in ovarian extracts by co-immunoprecipitation (Castagnetti and Ephrussi, 2003), it seemed likely that premature cytoplasmic streaming induced by Bic-C overexpression might occur through post-transcriptional suppression of Orb or Orb target mRNAs. Consistent with this hypothesis, I observed a remarkable increase in the severity of the Bic-C overexpression phenotype in a heterozygous *orb* mutant background. Because Bic-C overexpression disrupts posterior recruitment of pole plasm components prior to any detectable effects on Orb levels or distribution, I conclude that Bic-C activity must directly regulate the expression of Orb target mRNAs, rather than operate solely through an effect on *orb* mRNA itself. Antagonistic effects have already been described for Bic-C and Orb on *osk* mRNA (Saffman et al., 1998; Castagnetti and Ephrussi, 2003). However, *orb* mutant oocytes differ from Bic-C overexpression oocytes in that they do not display an increase in oocyte volume during stages 8-10, implying that activation of cytoplasmic transfer by Bic-C is independent of Orb and of Orb target mRNAs.

Mutations affecting poly(A) polymerase and the deadenylase CCR4 enhance or suppress the Bic-C overexpression phenotypes respectively. This evidence supports a model in which Bic-C acts to destabilize and/or silence mRNA substrates through

shortening of their poly(A) tails (Fig 4.3.1). This could occur by preventing recruitment of poly(A) polymerase by Orb, however, this would require target transcripts to be in a constant state flux between elongated and shortened poly(A) tails to explain the requirement of wild-type CCR4 levels for producing the Bic-C overexpression phenotypes. Alternatively, Bic-C could recruit the deadenylase machinery to target transcripts, and actively promote deadenylation, or Bic-C could deliver target transcripts to another complex, such as P-bodies, where deadenylation and translational silencing or degradation would follow. A visual representation of some of the various Bic-C-interacting proteins illustrates their physical and functional relationships (Fig. 4.3.2).

4.4 Bic-C, exocytosis and the Trailer Hitch complex

Given the similarities between the *Bic-C* mutant phenotypes and those described in *sec5* and *trailer hitch* mutants, it seems likely that Bic-C regulates some aspect of Grk exocytosis. It may perform this function through an association with Me31B and PABP, as a component of the Trailer Hitch complex. If this is the case, Bic-C's role in exocytosis is probably not limited to Grk secretion. Accordingly, the pleiotropic nature of the *Bic-C* phenotypes is more consistent with a general defect in protein secretion. However, the direct evidence demonstrating an interaction between Bic-C and Trailer Hitch is currently ambiguous; therefore a clear association between Bic-C and this complex has not yet been proven.

A general defect in protein secretion from the oocyte would result in a communication breakdown with the overlying follicle cells because signaling molecules, such as Grk, would not reach their target receptors on the follicle cells, and receptors

Figure 4.3.1 The mechanism of Bic-C-mediated induction of rapid cytoplasmic streaming

Bic-C represses a subset of Orb mRNA targets by deadenylation, leading to reduced mRNA stability and/or translation. When expression of these factors falls below a critical threshold, rapid cytoplasmic streaming is initiated, displacing Grk from the anterior/dorsal cortex and preventing posterior accumulation of Osk.

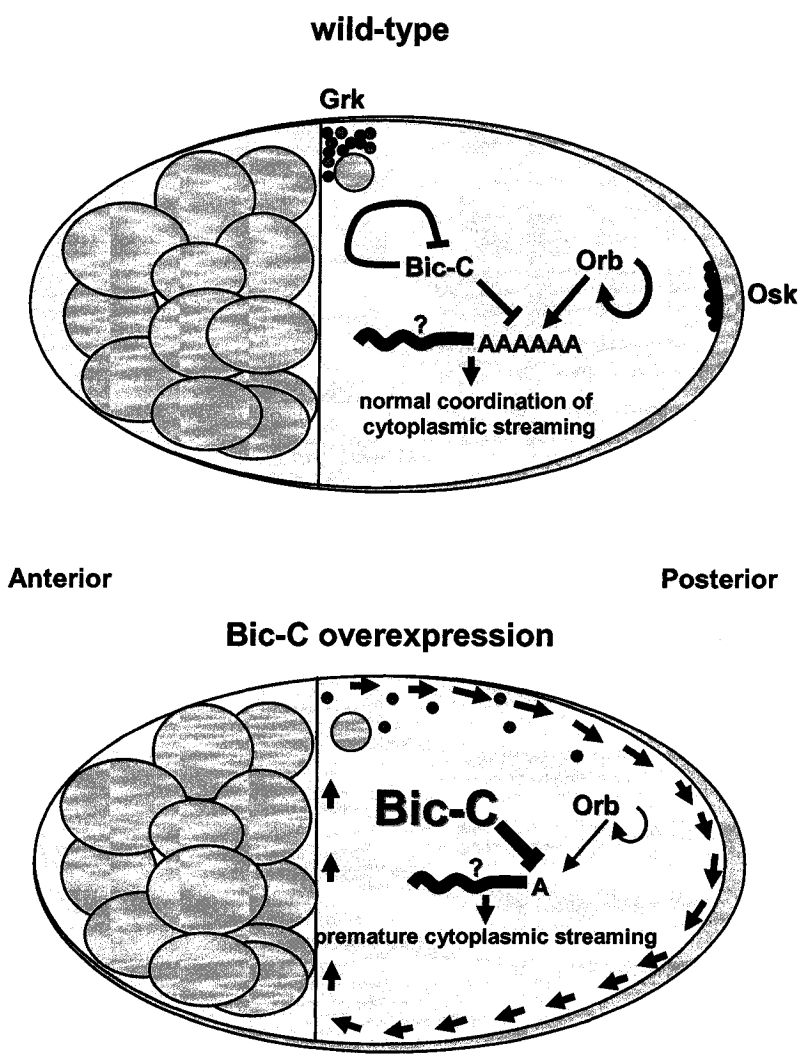
wild-type
Grk
Bic-C
Orb
Osk
?
AAAAAA
normal coordination of
cytoplasmic streaming
Anterior
Posterior
Bic-C overexpression
Bic-C
Orb
?
A
premature cytoplasmic streaming

Figure 4.3.2 Schematic of Bic-C protein interactions: bridging the gap between P-bodies and deadenylation

A schematic representation of protein interactions in *D. melanogaster* and other organisms illustrates that Bic-C is physically linked to multiple components of P bodies, which regulate deadenylation and mRNA degradation.

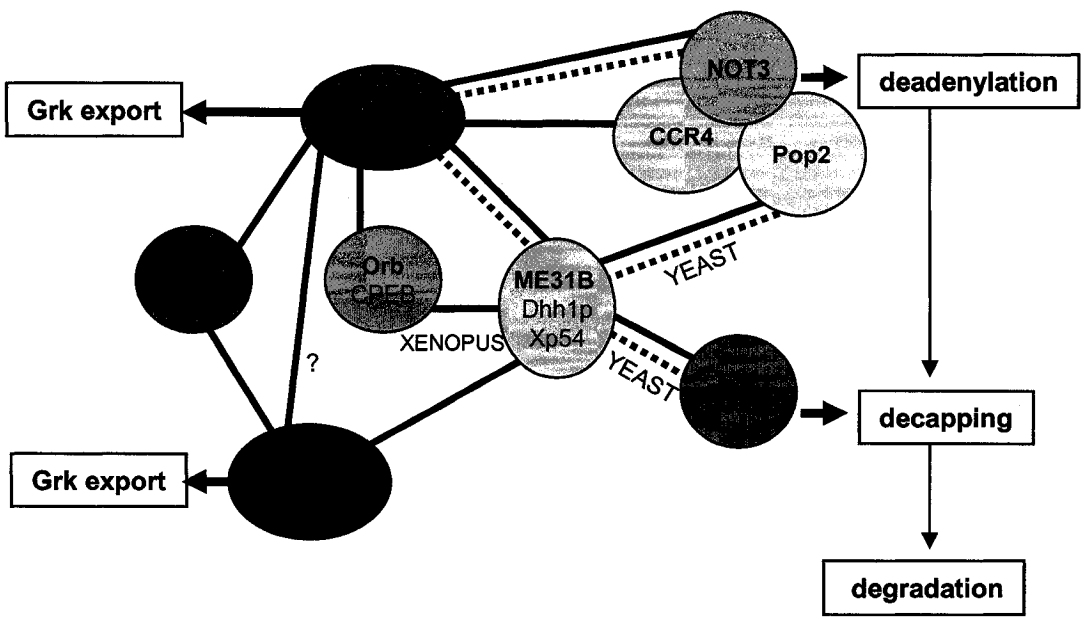
Grk export
NOT3
deadenylation
CCR4
Pop2
Orb
CPEB
ME31B
Dhh1p
Xp54
XENOPUS
YEAST
YEAST
?
Grk export
decapping
degradation
Co-IP
Two-hybrid

would not reach the surface of the oocyte to convey signals back into the germline. Thus, a general requirement for Bic-C in protein secretion may explain the defective centripetal follicle cell migration observed in *Bic-C* mutants, as Saxophone, the receptor for Dpp, is required in the germline for these migratory events to occur (Twombly et al., 1996).

Abnormal Grk accumulation is readily detectable as early as stage 6/7 in *Bic-C* mutants, providing the first evidence that Bic-C has a function, other than auto-regulation, prior to stage 8 when it is required to suppress Osk translation (Saffman et al., 1998). However, *Bic-C* is not essential for Grk signaling to the posterior follicle cells at stage 6, since nuclear migration to the anterior of the oocyte, which depends on this event, still occurs in most *Bic-C* mutant egg chambers. Interestingly, mutant alleles of *grk* and *cornichon*, which encodes an integral membrane protein required for Grk trafficking through the ER (Bokel et al., 2005), are both strong dominant enhancers of maternal-effect lethality when in *trans* to heterozygous *Bic-C* mutants (Rother, 1998). This suggests that Bic-C levels become a critical factor in Grk deployment when the amount of functional Grk is reduced, implying that the efficiency of exocytosis is sensitive to Bic-C levels. Therefore, any disruption of exocytosis caused by the loss of Bic-C probably reflects a genuine requirement for Bic-C in this process rather than an indirect consequence of some unknown developmental block.

4.5 Bic-C phosphorylation

In vivo labeling experiments indicate that Bic-C is a phosphoprotein and that detectable phosphorylation only occurs on one or more serine residues. Why then should the Y822F mutation decrease the level of phosphorylation? There are several

possibilities, the first being that Tyr822 is in fact phosphorylated and this event is a prerequisite for phosphorylation at other sites. This form of sequential phosphorylation has been documented (Gingras et al., 2001). If this is the case, phosphorylation of Tyr822 may be a transitory event and thus difficult to detect. Another possibility is that Tyr822 is not phosphorylated but is specifically required to recruit a kinase that phosphorylates Bic-C on other residues. It is also possible that replacement of this residue results in structural changes to the protein, possibly due to aberrant folding, that indirectly disrupt function and/or phosphorylation. Finally, Bic-C phosphorylation may be temporally regulated, occurring primarily after stage 10. In this case, Tyr822 may be critical for some aspect of Bic-C function which is unrelated to phosphorylation but since the Y822F mutant cannot restore fertility in the *Bic-C*^{YC33} mutant background, oogenesis remains blocked at stage 10 and high levels of phosphorylation are not achieved.

A growing number of examples demonstrate the importance of phosphorylation as a means of regulating RNA-binding proteins. As previously mentioned, phosphorylation causes some proteins, such as ZBP-1 and hnRNP-K, to release their RNA substrates, providing a means of spatial and temporal regulation respectively (Huttelmaier et al., 2005; Ostareck-Lederer et al., 2002). Alternatively, phosphorylation can alter the complement of proteins an RNA-binding protein recruits to a specific RNA, as in the case of *Xenopus* CPEB (Mendez et al., 2000b). Regardless of the specific mechanism employed to silence maternal mRNAs, the process must be reversible. Therefore, mechanisms must exist to "free" silenced mRNAs from repression at specific times in development. Phosphorylation of Bic-C may serve such a purpose in oogenesis by promoting release of bound RNAs or exchange of the deadenylase machinery for

translational activators. At this point, it is not known if phosphorylation is essential for Bic-C function, however, further mapping and mutagenesis experiments should clarify this issue.

4.6 Future directions

My hope is that this work has enhanced our understanding of *Bic-C* function in a meaningful way that can be utilized by my successors to continue the ongoing process of discovery. To those successors, I would propose that a crucial step towards unravelling the intricacies of *Bic-C* function will be identifying the full complement of proteins that Bic-C associates with *in vivo*. To facilitate this task, I have produced *UASP-TAP-Bic-C* transgenic fly lines that can be used to express a tagged version of Bic-C for Tandem Affinity Purification (TAP) of Bic-C-containing mRNP complexes in ovaries or embryos (Fig. 4.6.1; Puig et al., 2001). Germline expression of this transgene can restore fertility to homozygous $Bic\text{-}C^{YC33}$ females, indicating that TAP-Bic-C is fully functional and is therefore a suitable biochemical "handle" for isolating biologically relevant complexes. Preliminary small-scale experiments indicate that large-scale recovery of such complexes should be feasible (Fig 4.6.2).

Another important task will be confirming the microarray-based characterization of Bic-C-associated mRNAs through alternate methods and determining which of these associations reflect biologically relevant interactions *in vivo*. This should facilitate the identification of *bona fide* Bic-C binding sites in targeted transcripts, through multiple sequence alignments and ultimately *in vitro* binding assays. As Bic-C appears to be a

Figure 4.6.1 Germline expression of *UASP-TAP-Bic-C* restores fertility to homozygous Bic-C^{YC33} females.

(A) Schematic representation of the *UASP-TAP-Bic-C* construct design.

(B) Confocal immunofluoresence of ovaries stained with α-Bic-C (green) illustrate the distribution of endogenous Bic-C (top) in a stage 10 OreR egg chamber and TAP-Bic-C in a homozygous *Bic-C^{YC33}* mutant. Centripetal follicle cell migration (marked by the white arrow) is rescued by TAP-Bic-C expression and these females lay eggs that produce viable offspring. Actin and DNA are visualized by rhodamine-phalloidin (red) and DAPI (blue) staining respectively.

A

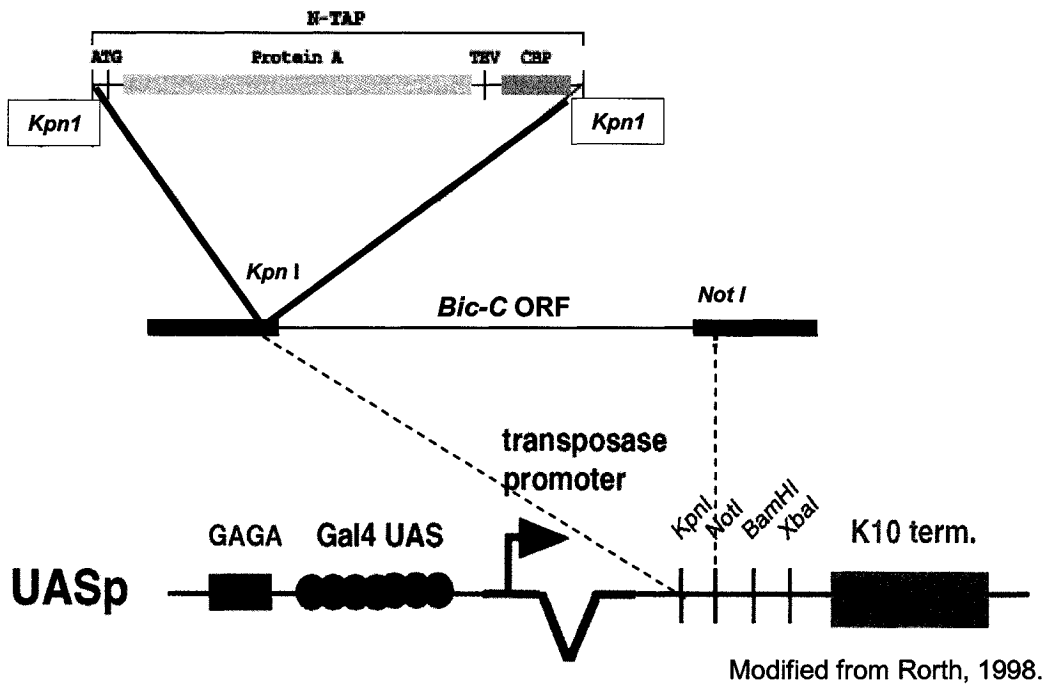

Modified from Rorth, 1998.

B

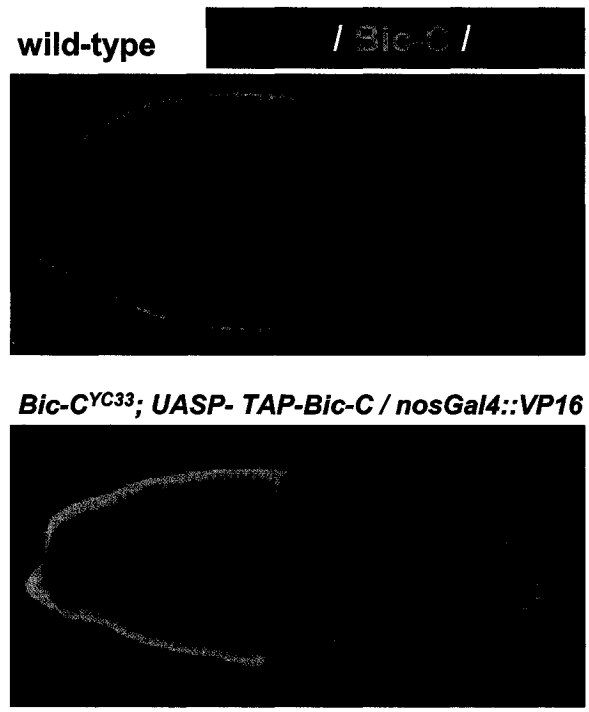

Figure 4.6.2 Small-scale purification of TAP-Bic-C from ovarian lysates.

Protein samples were collected at various stages during the TAP-Bic-C protein purification procedure and resolved by SDS-PAGE (10%) to visualize TAP-Bic-C by Western blotting with α-Bic-C. Protein purification was performed using the conventional method, by binding to IgG beads first, followed by Tev cleavage and then binding to calmodulin (A) or in the reverse order, without cleavage by the Tev protease (B). With both methods, Bic-C is detected in the final samples (A-lanes 7-9, B-lane 9).

(A) Lanes: 1 – input; 2 – IgG supernatant after 3 hrs; 3 – IgG supernatant after 16 hrs; 4 – bound to IgG after Tev cleavage; 5 – supernatant after TEV cleavage; 6 – supernatant after calmodulin binding; 7 – bound to calmodulin; 8 – calmodulin EGTA eluate (fraction 1); 9 – calmodulin EGTA eluate (fraction 2).

(B) Lanes: 1 – input; 2 – pooled calmodulin eluates; 3 – calmodulin eluate fraction 1; 4 – calmodulin eluate fraction 2; 5 - calmodulin eluate fraction 3; 6 - calmodulin eluate fraction 4; 7 – bound to calmodulin after EGTA elution; 8 – supernatant after IgG binding; 9 – bound to IgG.

A

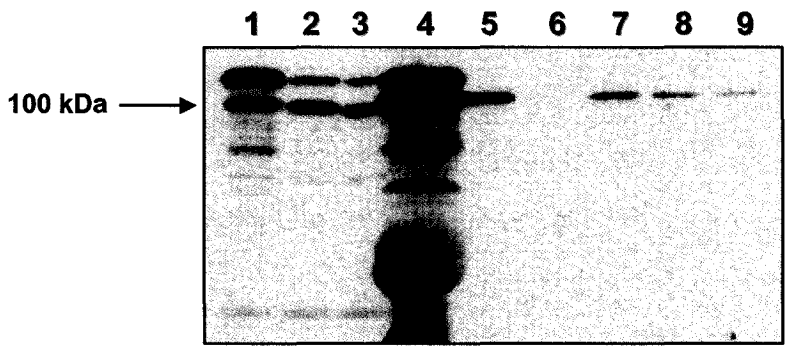

B

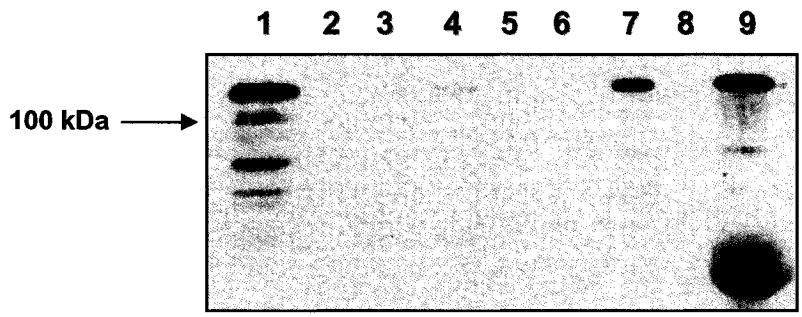

negative regulator of RNA stability and probably translation, high-throughput methods, such as microarray-based comparisons of mRNA abundance and of polysome-association, may be used to identify which putative target transcripts are affected by reductions or increases in Bic-C protein levels. Reciprocal effects on mRNA stability and translatability in these two contexts would provide strong evidence of specific Bic-C-mediated regulation. Bic-C overexpression has provided a useful platform for testing functional relationships through genetic interactions. Such genetic interaction assays may be extended to identify biologically relevant target transcripts, as the relative quantities of these transcripts and Bic-C are likely to be critical for normal development.

Due to the defect in centripetal follicle cell migration in *Bic-C* mutants, Bic-C has long been suspected to influence inter-cellular communication between the germline and the soma. This suspicion is supported by observations that germline-specific expression of *UASP-Bic-C* or *UASP-TAP-Bic-C,* using the nosGal4::VP16 driver, can rescue the centripetal follicle cell migration defect. Furthermore, posterior migration of the follicle cells, which precedes centripetal migration, appears to be accelerated upon germline overexpression of Bic-C and retarded in *Bic-C* mutants (Fig. 3.3.22). The discovery that Bic-C is required for Grk secretion suggests a possible role for Bic-C in exocytosis, which provides a clear link to inter-cellular communication. Visualization of various secreted proteins in *Bic-C* mutants should provide some insight into how general this defect is. Also, analysis of COPII exit sites and the trans-Golgi network in *Bic-C* mutants, using available molecular markers, should help to identify the point at which Bic-C may be required in this process. A future challenge will be identifying the exact

role of Bic-C in exocytosis and determining how this function may relate to putative mRNA targets, control of cytoplasmic streaming and anterior/posterior patterning.

Section 5: Original Contributions to Knowledge

1- The KH domains of Bic-C were demonstrated to bind RNA directly and endogenous Bic-C was found to co-purify with ovarian mRNPs.

2- Endogenous Bic-C was demonstrated to preferentially associate with a specific subset of ovarian mRNAs, including its own transcript and a biologically coherent set of transcripts encoding functionally-related components of the Wnt/Frizzled/Dishevelled signaling pathway.

3- The stability of a reporter transcript bearing portions of the *Bic-C* 5' and 3' UTRs was shown to increase in the absence of Bic-C and *cis*-acting auto-repressive elements were mapped to the *Bic-C* 5' UTR.

4- Bic-C was overexpressed for the first time and found to induce premature cytoplasmic streaming, cytoplasmic transfer and follicle cell movements.

5- Genetic modifiers of the Bic-C overexpression phenotype provided *in vivo* evidence that the mechanism of Bic-C function involves deadenylation of target transcripts.

6- Biochemical evidence demonstrating that Bic-C specifically associates NOT3, CCR4 and Pop2 was provided.

7- An association with the maternal mRNA silencing factor Me31B was confirmed by co-immunoprecipitation and *in vivo* co-localization of Me31B-eGFP and Bic-C.

8- Secretion of Gurken protein was found to be defective in the absence of Bic-C.

9- *In vivo* phosphorylation of Bic-C on one or more serine residues was demonstrated.

References

Adinolfi, S., Bagni, C., Castiglione Morelli, M. A., Fraternali, F., Musco, G., and Pastore, A. (1999). Novel RNA-binding motif: the KH module. Biopolymers *51*, 153-164.

Ambros, V. (2004). The functions of animal microRNAs. Nature *431*, 350-355.

Anderson, P., and Kedersha, N. (2006). RNA granules. J Cell Biol *172*, 803-808.

Ashley, C. T., Jr., Wilkinson, K. D., Reines, D., and Warren, S. T. (1993). FMR1 protein: conserved RNP family domains and selective RNA binding. Science *262*, 563-566.

Aspenstrom, P., Richnau, N., and Johansson, A. S. (2006). The diaphanous-related formin DAAM1 collaborates with the Rho GTPases RhoA and Cdc42, CIP4 and Src in regulating cell morphogenesis and actin dynamics. Exp Cell Res *312*, 2180-2194.

Aspuria, P. J., and Tamanoi, F. (2004). The Rheb family of GTP-binding proteins. Cell Signal *16*, 1105-1112.

Atkey, M. R., Lachance, J. F., Walczak, M., Rebello, T., and Nilson, L. A. (2006). Capicua regulates follicle cell fate in the *Drosophila* ovary through repression of mirror. Development *133*, 2115-2123.

Aviv, T., Lin, Z., Lau, S., Rendl, L. M., Sicheri, F., and Smibert, C. A. (2003). The RNA-binding SAM domain of Smaug defines a new family of post-transcriptional regulators. Nat Struct Biol *10*, 614-621.

Bag, J. (2001). Feedback inhibition of poly(A)-binding protein mRNA translation. A possible mechanism of translation arrest by stalled 40 S ribosomal subunits. J Biol Chem *276*, 47352-47360.

Bagni, C., and Greenough, W. T. (2005). From mRNP trafficking to spine dysmorphogenesis: the roots of fragile X syndrome. Nat Rev Neurosci *6*, 376-387.

Bailey, T. L. a. E., C. (1994). Fitting a mixture model by expectation maximization to discover motifs in biopolymers, Paper presented at: Proceedings of the Second International Conference on Intelligent Systems for Molecular Biology (Menlo Park, California: AAAI Press).

Behm-Ansmant, I., Rehwinkel, J., Doerks, T., Stark, A., Bork, P., and Izaurralde, E. (2006). mRNA degradation by miRNAs and GW182 requires both CCR4:NOT deadenylase and DCP1:DCP2 decapping complexes. Genes Dev *20*, 1885-1898.

Benoit, B., Mitou, G., Chartier, A., Temme, C., Zaessinger, S., Wahle, E., Busseau, I., and Simonelig, M. (2005). An essential cytoplasmic function for the nuclear poly(A) binding protein, PABP2, in poly(A) tail length control and early development in *Drosophila*. Dev Cell *9*, 511-522.

Bergsten, S. E., and Gavis, E. R. (1999). Role for mRNA localization in translational activation but not spatial restriction of nanos RNA. Development *126*, 659-669.

Bethin, K. E., Nagai, Y., Sladek, R., Asada, M., Sadovsky, Y., Hudson, T. J., and Muglia, L. J. (2003). Microarray analysis of uterine gene expression in mouse and human pregnancy. Mol Endocrinol *17*, 1454-1469.

Bevilacqua, A., Ceriani, M. C., Canti, G., Asnaghi, L., Gherzi, R., Brewer, G., Papucci, L., Schiavone, N., Capaccioli, S., and Nicolin, A. (2003a). Bcl-2 protein is required for the adenine/uridine-rich element (ARE)-dependent degradation of its own messenger. J Biol Chem *278*, 23451-23459.

Bevilacqua, A., Ceriani, M. C., Capaccioli, S., and Nicolin, A. (2003b). Post-transcriptional regulation of gene expression by degradation of messenger RNAs. J Cell Physiol *195*, 356-372.

Bishop, A. L., and Hall, A. (2000). Rho GTPases and their effector proteins. Biochem J *348 Pt 2*, 241-255.

Blom, N., Gammeltoft, S., and Brunak, S. (1999). Sequence and structure-based prediction of eukaryotic protein phosphorylation sites. J Mol Biol *294*, 1351-1362.

Boag, P. R., Nakamura, A., and Blackwell, T. K. (2005). A conserved RNA-protein complex component involved in physiological germline apoptosis regulation in *C. elegans*. Development *132*, 4975-4986.

Bocca, S. N., Muzzopappa, M., Silberstein, S., and Wappner, P. (2001). Occurrence of a putative SCF ubiquitin ligase complex in *Drosophila*. Biochem Biophys Res Commun *286*, 357-364.

Bokel, C., Dass, S., Wilsch-Brauninger, M., and Roth, S. (2006). Drosophila Cornichon acts as cargo receptor for ER export of the TGFalpha-like growth factor Gurken. Development *133*, 459-470.

Bokel, C., Prokop, A., and Brown, N. H. (2005). Papillote and Piopio: *Drosophila* ZP-domain proteins required for cell adhesion to the apical extracellular matrix and microtubule organization. J Cell Sci *118*, 633-642.

Braat, A. K., Yan, N., Arn, E., Harrison, D., and Macdonald, P. M. (2004). Localization-dependent oskar protein accumulation; control after the initiation of translation. Dev Cell *7*, 125-131.

Brand, A. H., and Perrimon, N. (1993). Targeted gene expression as a means of altering cell fates and generating dominant phenotypes. Development *118*, 401-415.

Brendza, R. P., Serbus, L. R., Duffy, J. B., and Saxton, W. M. (2000). A function for kinesin I in the posterior transport of oskar mRNA and Staufen protein. Science *289*, 2120-2122.

Brengues, M., Teixeira, D., and Parker, R. (2005). Movement of eukaryotic mRNAs between polysomes and cytoplasmic processing bodies. Science *310*, 486-489.

Brooks, S. A., Connolly, J. E., and Rigby, W. F. (2004). The role of mRNA turnover in the regulation of tristetraprolin expression: evidence for an extracellular signal-regulated kinase-specific, AU-rich element-dependent, autoregulatory pathway. J Immunol *172*, 7263-7271.

Buckanovich, R. J., and Darnell, R. B. (1997). The neuronal RNA binding protein Nova-1 recognizes specific RNA targets in vitro and in vivo. Mol Cell Biol *17*, 3194-3201.

Burd, C. G., and Dreyfuss, G. (1994). Conserved structures and diversity of functions of RNA-binding proteins. Science *265*, 615-621.

Castagnetti, S., and Ephrussi, A. (2003). Orb and a long poly(A) tail are required for efficient oskar translation at the posterior pole of the *Drosophila* oocyte. Development *130*, 835-843.

Cha, B. J., Serbus, L. R., Koppetsch, B. S., and Theurkauf, W. E. (2002). Kinesin I-dependent cortical exclusion restricts pole plasm to the oocyte posterior. Nat Cell Biol *4*, 592-598.

Chang, J. S., Tan, L., and Schedl, P. (1999). The *Drosophila* CPEB homolog, orb, is required for oskar protein expression in oocytes. Dev Biol *215*, 91-106.

Chang, J. S., Tan, L., Wolf, M. R., and Schedl, P. (2001). Functioning of the Drosophila orb gene in gurken mRNA localization and translation. Development *128*, 3169-3177.

Chekulaeva, M., Hentze, M. W., and Ephrussi, A. (2006). Bruno acts as a dual repressor of oskar translation, promoting mRNA oligomerization and formation of silencing particles. Cell *124*, 521-533.

Chen, T., Damaj, B. B., Herrera, C., Lasko, P., and Richard, S. (1997). Self-association of the single-KH-domain family members Sam68, GRP33, GLD-1, and Qk1: role of the KH domain. Mol Cell Biol *17*, 5707-5718.

Cho, P. F., Gamberi, C., Cho-Park, Y. A., Cho-Park, I. B., Lasko, P., and Sonenberg, N. (2006). Cap-dependent translational inhibition establishes two opposing morphogen gradients in *Drosophila* embryos. Curr Biol *16*, 2035-2041.

Cho, P. F., Poulin, F., Cho-Park, Y. A., Cho-Park, I. B., Chicoine, J. D., Lasko, P., and Sonenberg, N. (2005). A new paradigm for translational control: inhibition via 5'-3' mRNA tethering by Bicoid and the eIF4E cognate 4EHP. Cell *121*, 411-423.

Christensen, A. K., Kahn, L. E., and Bourne, C. M. (1987). Circular polysomes predominate on the rough endoplasmic reticulum of somatotropes and mammotropes in the rat anterior pituitary. Am J Anat *178*, 1-10.

Christerson, L. B., and McKearin, D. M. (1994). orb is required for anteroposterior and dorsoventral patterning during Drosophila oogenesis. Genes Dev *8*, 614-628.

Clark, I., Giniger, E., Ruohola-Baker, H., Jan, L. Y., and Jan, Y. N. (1994). Transient posterior localization of a kinesin fusion protein reflects anteroposterior polarity of the *Drosophila* oocyte. Curr Biol *4*, 289-300.

Clark, I. E., Wyckoff, D., and Gavis, E. R. (2000). Synthesis of the posterior determinant Nanos is spatially restricted by a novel cotranslational regulatory mechanism. Curr Biol *10*, 1311-1314.

Cogswell, C., Price, S. J., Hou, X., Guay-Woodford, L. M., Flaherty, L., and Bryda, E. C. (2003). Positional cloning of jcpk/bpk locus of the mouse. Mamm Genome *14*, 242-249.

Coller, J. M., Tucker, M., Sheth, U., Valencia-Sanchez, M. A., and Parker, R. (2001). The DEAD box helicase, Dhh1p, functions in mRNA decapping and interacts with both the decapping and deadenylase complexes. RNA *7*, 1717-1727.

Comery, T. A., Harris, J. B., Willems, P. J., Oostra, B. A., Irwin, S. A., Weiler, I. J., and Greenough, W. T. (1997). Abnormal dendritic spines in fragile X knockout mice: maturation and pruning deficits. Proc Natl Acad Sci U S A *94*, 5401-5404.

Cook, H. A., Koppetsch, B. S., Wu, J., and Theurkauf, W. E. (2004). The *Drosophila* SDE3 homolog armitage is required for oskar mRNA silencing and embryonic axis specification. Cell *116*, 817-829.

Cougot, N., Babajko, S., and Seraphin, B. (2004). Cytoplasmic foci are sites of mRNA decay in human cells. J Cell Biol *165*, 31-40.

Dahanukar, A., Walker, J. A., and Wharton, R. P. (1999). Smaug, a novel RNA-binding protein that operates a translational switch in *Drosophila*. Mol Cell *4*, 209-218.

Dalmay, T., Horsefield, R., Braunstein, T. H., and Baulcombe, D. C. (2001). SDE3 encodes an RNA helicase required for post-transcriptional gene silencing in *Arabidopsis*. EMBO J *20*, 2069-2078.

Darnell, J. C., Jensen, K. B., Jin, P., Brown, V., Warren, S. T., and Darnell, R. B. (2001). Fragile X mental retardation protein targets G quartet mRNAs important for neuronal function. Cell *107*, 489-499.

Darnell, J. C., Mostovetsky, O., and Darnell, R. B. (2005). FMRP RNA targets: identification and validation. Genes Brain Behav *4*, 341-349.

Das, G., Jenny, A., Klein, T. J., Eaton, S., and Mlodzik, M. (2004). Diego interacts with Prickle and Strabismus/Van Gogh to localize planar cell polarity complexes. Development *131*, 4467-4476.

de Melo Neto, O. P., Standardt, N., Martins de Sa, M. (1995). Autoregulation of poly(a)-binding protein synthesis *in vitro*. Nucleic Acids Res *23*, 2198-2205.

de Moor, C. H., and Richter, J. D. (1999). Cytoplasmic polyadenylation elements mediate masking and unmasking of cyclin B1 mRNA. EMBO J *18*, 2294-2303.

de Valoir, T., Tucker, M. A., Belikoff, E. J., Camp, L. A., Bolduc, C., and Beckingham, K. (1991). A second maternally expressed *Drosophila* gene encodes a putative RNA helicase of the "DEAD box" family. Proc Natl Acad Sci U S A *88*, 2113-2117.

Decker, C. J., and Parker, R. (2002). mRNA decay enzymes: decappers conserved between yeast and mammals. Proc Natl Acad Sci U S A *99*, 12512-12514.

Dredge, B. K., and Darnell, R. B. (2003). Nova regulates GABA(A) receptor gamma2 alternative splicing via a distal downstream UCAU-rich intronic splicing enhancer. Mol Cell Biol *23*, 4687-4700.

Dredge, B. K., Stefani, G., Engelhard, C. C., and Darnell, R. B. (2005). Nova autoregulation reveals dual functions in neuronal splicing. EMBO J *24*, 1608-1620.

Drier, E. A., Huang, L. H., and Steward, R. (1999). Nuclear import of the *Drosophila* Rel protein Dorsal is regulated by phosphorylation. Genes Dev *13*, 556-568.

Driever, W., and Nusslein-Volhard, C. (1989). The bicoid protein is a positive regulator of hunchback transcription in the early *Drosophila* embryo. Nature *337*, 138-143.

Eckmann, C. R., Crittenden, S. L., Suh, N., and Kimble, J. (2004). GLD-3 and control of the mitosis/meiosis decision in the germline of *Caenorhabditis elegans*. Genetics *168*, 147-160.

Eckmann, C. R., Kraemer, B., Wickens, M., and Kimble, J. (2002). GLD-3, a bicaudal-C homolog that inhibits FBF to control germline sex determination in *C. elegans*. Dev Cell *3*, 697-710.

Edwards, K. A., and Kiehart, D. P. (1996). *Drosophila* nonmuscle myosin II has multiple essential roles in imaginal disc and egg chamber morphogenesis. Development *122*, 1499-1511.

Ephrussi, A., Dickinson, L. K., and Lehmann, R. (1991). Oskar organizes the germ plasm and directs localization of the posterior determinant nanos. Cell *66*, 37-50.

Ephrussi, A., and Lehmann, R. (1992). Induction of germ cell formation by oskar. Nature *358*, 387-392.

Ephrussi, A., and St Johnston, D. (2004). Seeing is believing: the bicoid morphogen gradient matures. Cell *116*, 143-152.

Erdelyi, M., Michon, A. M., Guichet, A., Glotzer, J. B., and Ephrussi, A. (1995). Requirement for *Drosophila* cytoplasmic tropomyosin in oskar mRNA localization. Nature *377*, 524-527.

Eystathioy, T., Jakymiw, A., Chan, E. K., Seraphin, B., Cougot, N., and Fritzler, M. J. (2003). The GW182 protein colocalizes with mRNA degradation associated proteins hDcp1 and hLSm4 in cytoplasmic GW bodies. RNA *9*, 1171-1173.

Fenger-Gron, M., Fillman, C., Norrild, B., and Lykke-Andersen, J. (2005). Multiple processing body factors and the ARE binding protein TTP activate mRNA decapping. Mol Cell *20*, 905-915.

Ferraiuolo, M. A., Basak, S., Dostie, J., Murray, E. L., Schoenberg, D. R., and Sonenberg, N. (2005). A role for the eIF4E-binding protein 4E-T in P-body formation and mRNA decay. J Cell Biol *170*, 913-924.

Findley, S. D., Tamanaha, M., Clegg, N. J., and Ruohola-Baker, H. (2003). Maelstrom, a *Drosophila* spindle-class gene, encodes a protein that colocalizes with Vasa and RDE1/AGO1 homolog, Aubergine, in nuage. Development *130*, 859-871.

Fischer, N., and Weis, K. (2002). The DEAD box protein Dhh1 stimulates the decapping enzyme Dcp1. Embo J *21*, 2788-2797.

Fourney, R. M., Miyakoshi, J., Paterson, M.C. (1988). Northern blotting: efficient RNA staining and transfer. Focus *10*, 5-6.

Frazer, K. A., Pachter, L., Poliakov, A., Rubin, E. M., and Dubchak, I. (2004). VISTA: computational tools for comparative genomics. Nucleic Acids Res *32*, W273-279.

Freeman, M. (1996). Reiterative use of the EGF receptor triggers differentiation of all cell types in the *Drosophila* eye. Cell *87*, 651-660.

Gallie, D. R. (1991). The cap and poly(A) tail function synergistically to regulate mRNA translational efficiency. Genes Dev *5*, 2108-2116.

Gao, F. B., Carson, C. C., Levine, T., and Keene, J. D. (1994). Selection of a subset of mRNAs from combinatorial 3' untranslated region libraries using neuronal RNA-binding protein Hel-N1. Proc Natl Acad Sci U S A *91*, 11207-11211.

Gavis, E. R., Lunsford, L., Bergsten, S. E., and Lehmann, R. (1996). A conserved 90 nucleotide element mediates translational repression of nanos RNA. Development *122*, 2791-2800.

Gerber, A. P., Herschlag, D., and Brown, P. O. (2004). Extensive association of functionally and cytotopically related mRNAs with Puf family RNA-binding proteins in yeast. PLoS Biol *2*, E79.

Gerber, A. P., Luschnig, S., Krasnow, M. A., Brown, P. O., and Herschlag, D. (2006). Genome-wide identification of mRNAs associated with the translational regulator PUMILIO in *Drosophila melanogaster*. Proc Natl Acad Sci U S A *103*, 4487-4492.

Ghiglione, C., Amundadottir, L., Andresdottir, M., Bilder, D., Diamonti, J. A., Noselli, S., Perrimon, N., and Carraway, I. K. (2003). Mechanism of inhibition of the *Drosophila* and mammalian EGF receptors by the transmembrane protein Kekkon 1. Development *130*, 4483-4493.

Ghiglione, C., Bach, E. A., Paraiso, Y., Carraway, K. L., 3rd, Noselli, S., and Perrimon, N. (2002). Mechanism of activation of the *Drosophila* EGF Receptor by the TGFalpha ligand Gurken during oogenesis. Development *129*, 175-186.

Ghiglione, C., Carraway, K. L., 3rd, Amundadottir, L. T., Boswell, R. E., Perrimon, N., and Duffy, J. B. (1999). The transmembrane molecule kekkon 1 acts in a feedback loop

to negatively regulate the activity of the *Drosophila* EGF receptor during oogenesis. Cell *96*, 847-856.

Gingras, A. C., Raught, B., Gygi, S. P., Niedzwiecka, A., Miron, M., Burley, S. K., Polakiewicz, R. D., Wyslouch-Cieszynska, A., Aebersold, R., and Sonenberg, N. (2001). Hierarchical phosphorylation of the translation inhibitor 4E-BP1. Genes Dev *15*, 2852-2864.

Gingras, A. C., Raught, B., and Sonenberg, N. (1999). eIF4 initiation factors: effectors of mRNA recruitment to ribosomes and regulators of translation. Annu Rev Biochem *68*, 913-963.

Glotzer, J. B., Saffrich, R., Glotzer, M., and Ephrussi, A. (1997). Cytoplasmic flows localize injected oskar RNA in *Drosophila* oocytes. Curr Biol *7*, 326-337.

Goff, D. J., Nilson, L. A., and Morisato, D. (2001). Establishment of dorsal-ventral polarity of the *Drosophila* egg requires capicua action in ovarian follicle cells. Development *128*, 4553-4562.

Gonzalez-Reyes, A., Elliott, H., and St Johnston, D. (1995). Polarization of both major body axes in *Drosophila* by gurken-torpedo signalling. Nature *375*, 654-658.

Green, J. B., Gardner, C. D., Wharton, R. P., and Aggarwal, A. K. (2003). RNA recognition via the SAM domain of Smaug. Mol Cell *11*, 1537-1548.

Guichard, A., Roark, M., Ronshaugen, M., and Bier, E. (2000). brother of rhomboid, a rhomboid-related gene expressed during early Drosophila oogenesis, promotes EGF-R/MAPK signaling. Dev Biol *226*, 255-266.

Gunkel, N., Yano, T., Markussen, F. H., Olsen, L. C., and Ephrussi, A. (1998). Localization-dependent translation requires a functional interaction between the 5' and 3' ends of oskar mRNA. Genes Dev *12*, 1652-1664.

Gygi, S. P., Rochon, Y., Franza, B. R., and Aebersold, R. (1999). Correlation between protein and mRNA abundance in yeast. Mol Cell Biol *19*, 1720-1730.

Habas, R., Kato, Y., and He, X. (2001). Wnt/Frizzled activation of Rho regulates vertebrate gastrulation and requires a novel Formin homology protein Daam1. Cell *107*, 843-854.

Hachet, O., and Ephrussi, A. (2001). Drosophila Y14 shuttles to the posterior of the oocyte and is required for oskar mRNA transport. Curr Biol *11*, 1666-1674.

Hake, L. E., and Richter, J. D. (1994). CPEB is a specificity factor that mediates cytoplasmic polyadenylation during Xenopus oocyte maturation. Cell *79*, 617-627.

Harris, A. N., and Macdonald, P. M. (2001). Aubergine encodes a *Drosophila* polar granule component required for pole cell formation and related to eIF2C. Development *128*, 2823-2832.

Hashimoto, C., Gerttula, S., and Anderson, K. V. (1991). Plasma membrane localization of the Toll protein in the syncytial *Drosophila* embryo: importance of transmembrane signaling for dorsal-ventral pattern formation. Development *111*, 1021-1028.

Hawkins, N. C., Van Buskirk, C., Grossniklaus, U., and Schupbach, T. (1997). Post-transcriptional regulation of gurken by encore is required for axis determination in Drosophila. Development *124*, 4801-4810.

Herpers, B., and Rabouille, C. (2004). mRNA localization and ER-based protein sorting mechanisms dictate the use of transitional endoplasmic reticulum-golgi units involved in gurken transport in *Drosophila* oocytes. Mol Biol Cell *15*, 5306-5317.

Hieronymus, H., and Silver, P. A. (2003). Genome-wide analysis of RNA-protein interactions illustrates specificity of the mRNA export machinery. Nat Genet *33*, 155-161.

Hieronymus, H., Yu, M. C., and Silver, P. A. (2004). Genome-wide mRNA surveillance is coupled to mRNA export. Genes Dev *18*, 2652-2662.

Hinton, T. M., Coldwell, M. J., Carpenter, G. A., Morley, S. J., and Pain, V. M. (2006). Functional analysis of individual binding activities of the scaffold protein eIF4G. J Biol Chem.

Hodgman, R., Tay, J., Mendez, R., and Richter, J. D. (2001). CPEB phosphorylation and cytoplasmic polyadenylation are catalyzed by the kinase IAK1/Eg2 in maturing mouse oocytes. Development *128*, 2815-2822.

Huang, Y. S., Jung, M. Y., Sarkissian, M., and Richter, J. D. (2002). N-methyl-D-aspartate receptor signaling results in Aurora kinase-catalyzed CPEB phosphorylation and alpha CaMKII mRNA polyadenylation at synapses. EMBO J *21*, 2139-2148.

Huttelmaier, S., Zenklusen, D., Lederer, M., Dictenberg, J., Lorenz, M., Meng, X., Bassell, G. J., Condeelis, J., and Singer, R. H. (2005). Spatial regulation of beta-actin translation by Src-dependent phosphorylation of ZBP1. Nature *438*, 512-515.

Ideker, T., Thorsson, V., Ranish, J. A., Christmas, R., Buhler, J., Eng, J. K., Bumgarner, R., Goodlett, D. R., Aebersold, R., and Hood, L. (2001). Integrated genomic and proteomic analyses of a systematically perturbed metabolic network. Science *292*, 929-934.

Iizuka, N., Najita, L., Franzusoff, A., and Sarnow, P. (1994). Cap-dependent and cap-independent translation by internal initiation of mRNAs in cell extracts prepared from *Saccharomyces cerevisiae*. Mol Cell Biol *14*, 7322-7330.

Imataka, H., Gradi, A., and Sonenberg, N. (1998). A newly identified N-terminal amino acid sequence of human eIF4G binds poly(A)-binding protein and functions in poly(A)-dependent translation. EMBO J *17*, 7480-7489.

Ingelfinger, D., Arndt-Jovin, D. J., Luhrmann, R., and Achsel, T. (2002). The human LSm1-7 proteins colocalize with the mRNA-degrading enzymes Dcp1/2 and Xrnl in distinct cytoplasmic foci. Rna *8*, 1489-1501.

Inoki, K., and Guan, K. L. (2006). Complexity of the TOR signaling network. Trends Cell Biol *16*, 206-212.

Intine, R. V., Tenenbaum, S. A., Sakulich, A. L., Keene, J. D., and Maraia, R. J. (2003). Differential phosphorylation and subcellular localization of La RNPs associated with precursor tRNAs and translation-related mRNAs. Mol Cell *12*, 1301-1307.

Irwin, S. A., Patel, B., Idupulapati, M., Harris, J. B., Crisostomo, R. A., Larsen, B. P., Kooy, F., Willems, P. J., Cras, P., Kozlowski, P. B., *et al.* (2001). Abnormal dendritic spine characteristics in the temporal and visual cortices of patients with fragile-X syndrome: a quantitative examination. Am J Med Genet *98*, 161-167.

Jankovics, F., Sinka, R., Lukacsovich, T., and Erdelyi, M. (2002). MOESIN crosslinks actin and cell membrane in *Drosophila* oocytes and is required for OSKAR anchoring. Curr Biol *12*, 2060-2065.

Jenny, A., Reynolds-Kenneally, J., Das, G., Burnett, M., and Mlodzik, M. (2005). Diego and Prickle regulate Frizzled planar cell polarity signalling by competing for Dishevelled binding. Nat Cell Biol *7*, 691-697.

Jensen, K. B., Dredge, B. K., Stefani, G., Zhong, R., Buckanovich, R. J., Okano, H. J., Yang, Y. Y., and Darnell, R. B. (2000). Nova-1 regulates neuron-specific alternative splicing and is essential for neuronal viability. Neuron *25*, 359-371.

Jiang, J., and Struhl, G. (1998). Regulation of the Hedgehog and Wingless signalling pathways by the F-box/WD40-repeat protein Slimb. Nature *391*, 493-496.

Jing, Q., Huang, S., Guth, S., Zarubin, T., Motoyama, A., Chen, J., Di Padova, F., Lin, S. C., Gram, H., and Han, J. (2005). Involvement of microRNA in AU-rich element-mediated mRNA instability. Cell *120*, 623-634.

Jordan, K. C., Clegg, N. J., Blasi, J. A., Morimoto, A. M., Sen, J., Stein, D., McNeill, H., Deng, W. M., Tworoger, M., and Ruohola-Baker, H. (2000). The homeobox gene mirror links EGF signalling to embryonic dorso-ventral axis formation through notch activation. Nat Genet *24*, 429-433.

Jordan, P., and Karess, R. (1997). Myosin light chain-activating phosphorylation sites are required for oogenesis in *Drosophila*. J Cell Biol *139*, 1805-1819.

Juge, F., Zaessinger, S., Temme, C., Wahle, E., and Simonelig, M. (2002). Control of poly(A) polymerase level is essential to cytoplasmic polyadenylation and early development in *Drosophila*. Embo J *21*, 6603-6613.

Kalifa, Y., Huang, T., Rosen, L. N., Chatterjee, S., and Gavis, E. R. (2006). Glorund, a *Drosophila* hnRNP F/H homolog, is an ovarian repressor of nanos translation. Dev Cell *10*, 291-301.

Kedersha, N., Stoecklin, G., Ayodele, M., Yacono, P., Lykke-Andersen, J., Fritzler, M. J., Scheuner, D., Kaufman, R. J., Golan, D. E., and Anderson, P. (2005). Stress granules and processing bodies are dynamically linked sites of mRNP remodeling. J Cell Biol *169*, 871-884.

Keene, J. D., and Lager, P. J. (2005). Post-transcriptional operons and regulons co-ordinating gene expression. Chromosome Res *13*, 327-337.

Keene, J. D., and Tenenbaum, S. A. (2002). Eukaryotic mRNPs may represent posttranscriptional operons. Mol Cell *9*, 1161-1167.

Kelley, R. L. (1993). Initial organization of the Drosophila dorsoventral axis depends on an RNA-binding protein encoded by the squid gene. Genes Dev *7*, 948-960.

Kennerdell, J. R., Yamaguchi, S., and Carthew, R. W. (2002). RNAi is activated during *Drosophila* oocyte maturation in a manner dependent on aubergine and spindle-E. Genes Dev *16*, 1884-1889.

Kim-Ha, J., Kerr, K., and Macdonald, P. M. (1995). Translational regulation of *oskar* mRNA by bruno, an ovarian RNA-binding protein, is essential. Cell *81*, 403-412.

Kim-Ha, J., Smith, J. L., and Macdonald, P. M. (1991). *oskar* mRNA is localized to the posterior pole of the *Drosophila* oocyte. Cell *66*, 23-35.

King, R. (1970). Ovarian development in *Drosophila melaogaster* (New York: Academic Press).

Kobayashi, S., Amikura, R., Nakamura, A., Lasko, P. (1999). Techniques for analyzing protein and RNA distribution in *Drosophila* ovaries and embryos at structural and ultrastructural resolution., In Advances in molecular biology: A comparative methods approach to the study of ovaries and embryos., J. Richter, ed. (Oxford: Oxford University Press), pp. 426-445.

Korner, C. G., Wormington, M., Muckenthaler, M., Schneider, S., Dehlin, E., and Wahle, E. (1998). The deadenylating nuclease (DAN) is involved in poly(A) tail removal during the meiotic maturation of *Xenopus* oocytes. Embo J *17*, 5427-5437.

Lachance, P. E., Miron, M., Raught, B., Sonenberg, N., and Lasko, P. (2002). Phosphorylation of eukaryotic translation initiation factor 4E is critical for growth. Mol Cell Biol *22*, 1656-1663.

Lantz, V., Chang, J. S., Horabin, J. I., Bopp, D., and Schedl, P. (1994). The *Drosophila* orb RNA-binding protein is required for the formation of the egg chamber and establishment of polarity. Genes Dev *8*, 598-613.

Lasko, P. F., and Ashburner, M. (1990). Posterior localization of vasa protein correlates with, but is not sufficient for, pole cell development. Genes Dev *4*, 905-921.

Lejeune, F., Li, X., and Maquat, L. E. (2003). Nonsense-mediated mRNA decay in mammalian cells involves decapping, deadenylating, and exonucleolytic activities. Mol Cell *12*, 675-687.

Lewis, H. A., Musunuru, K., Jensen, K. B., Edo, C., Chen, H., Darnell, R. B., and Burley, S. K. (2000). Sequence-specific RNA binding by a Nova KH domain: implications for paraneoplastic disease and the fragile X syndrome. Cell *100*, 323-332.

Lie, Y. S., and Macdonald, P. M. (1999). Translational regulation of oskar mRNA occurs independent of the cap and poly(A) tail in *Drosophila* ovarian extracts. Development *126*, 4989-4996.

Lin, M. D., Fan, S. J., Hsu, W. S., and Chou, T. B. (2006). *Drosophila* decapping protein 1, dDcp1, is a component of the oskar mRNP complex and directs its posterior localization in the oocyte. Dev Cell *10*, 601-613.

Liu, J., Rivas, F. V., Wohlschlegel, J., Yates, J. R., 3rd, Parker, R., and Hannon, G. J. (2005a). A role for the P-body component GW182 in microRNA function. Nat Cell Biol *7*, 1261-1266.

Liu, J., Valencia-Sanchez, M. A., Hannon, G. J., and Parker, R. (2005b). MicroRNA-dependent localization of targeted mRNAs to mammalian P-bodies. Nat Cell Biol *7*, 719-723.

Lukong, K. E., and Richard, S. (2003). Sam68, the KH domain-containing superSTAR. Biochim Biophys Acta *1653*, 73-86.

Mahone, M. (1994) The phenotypic and molecular characterization of teh *Bicaudal-C* locus in *Drosophila melaogaster*, McGill University, Montreal, Quebec.

Mahone, M., Saffman, E. E., and Lasko, P. F. (1995). Localized Bicaudal-C RNA encodes a protein containing a KH domain, the RNA binding motif of FMR1. EMBO J *14*, 2043-2055.

Manseau, L., Calley, J., and Phan, H. (1996). Profilin is required for posterior patterning of the *Drosophila* oocyte. Development *122*, 2109-2116.

Manseau, L. J., and Schupbach, T. (1989). *cappuccino* and *spire*: two unique maternal-effect loci required for both the anteroposterior and dorsoventral patterns of the *Drosophila* embryo. Genes Dev *3*, 1437-1452.

Mansfield, J. H., Wilhelm, J. E., and Hazelrigg, T. (2002). Ypsilon Schachtel, a *Drosophila* Y-box protein, acts antagonistically to Orb in the *oskar* mRNA localization and translation pathway. Development *129*, 197-209.

Markesich, D. C., Gajewski, K. M., Nazimiec, M. E., and Beckingham, K. (2000). Bicaudal encodes the *Drosophila* beta NAC homolog, a component of the ribosomal translational machinery*. Development *127*, 559-572.

Markussen, F. H., Breitwieser, W., and Ephrussi, A. (1997). Efficient translation and phosphorylation of Oskar require Oskar protein and the RNA helicase Vasa. Cold Spring Harb Symp Quant Biol *62*, 13-17.

Martin, S. G., Leclerc, V., Smith-Litiere, K., and St Johnston, D. (2003). The identification of novel genes required for *Drosophila* anteroposterior axis formation in a germline clone screen using GFP-Staufen. Development *130*, 4201-4215.

Matusek, T., Djiane, A., Jankovics, F., Brunner, D., Mlodzik, M., and Mihaly, J. (2006). The Drosophila formin DAAM regulates the tracheal cuticle pattern through organizing the actin cytoskeleton. Development *133*, 957-966.

Mendez, R., Hake, L. E., Andresson, T., Littlepage, L. E., Ruderman, J. V., and Richter, J. D. (2000a). Phosphorylation of CPE binding factor by Eg2 regulates translation of c-mos mRNA. Nature *404*, 302-307.

Mendez, R., Murthy, K. G., Ryan, K., Manley, J. L., and Richter, J. D. (2000b). Phosphorylation of CPEB by Eg2 mediates the recruitment of CPSF into an active cytoplasmic polyadenylation complex. Mol Cell *6*, 1253-1259.

Mendez, R., and Richter, J. D. (2001). Translational control by CPEB: a means to the end. Nat Rev Mol Cell Biol *2*, 521-529.

Micklem, D. R., Adams, J., Grunert, S., and St Johnston, D. (2000). Distinct roles of two conserved Staufen domains in *oskar* mRNA localization and translation. EMBO J *19*, 1366-1377.

Minshall, N., Thom, G., and Standart, N. (2001). A conserved role of a DEAD box helicase in mRNA masking. RNA *7*, 1728-1742.

Mohler, J., and Wieschaus, E. F. (1986). Dominant maternal-effect mutations of *Drosophila melanogaster* causing the production of double-abdomen embryos. Genetics *112*, 803-822.

Mohr, S. E., Dillon, S. T., and Boswell, R. E. (2001). The RNA-binding protein Tsunagi interacts with Mago Nashi to establish polarity and localize oskar mRNA during Drosophila oogenesis. Genes Dev *15*, 2886-2899.

Morisato, D., and Anderson, K. V. (1994). The spatzle gene encodes a component of the extracellular signaling pathway establishing the dorsal-ventral pattern of the *Drosophila* embryo. Cell *76*, 677-688.

Morris, J. Z., Hong, A., Lilly, M. A., and Lehmann, R. (2005). Twin, a CCR4 homolog, regulates cyclin poly(A) tail length to permit *Drosophila* oogenesis. Development *132*, 1165-1174.

Moussian, B., and Roth, S. (2005). Dorsoventral axis formation in the *Drosophila* embryo - shaping and transducing a morphogen gradient. Curr Biol *15*: R887-889.

Murata, T., Nagaso, H., Kashiwabara, S., Baba, T., Okano, H., and Yokoyama, K. K. (2001). The *hiiragi* gene encodes a poly(A) polymerase, which controls the formation of the wing margin in *Drosophila melanogaster*. Dev Biol *233*, 137-147.

Murthy, M., Garza, D., Scheller, R. H., and Schwarz, T. L. (2003). Mutations in the exocyst component Sec5 disrupt neuronal membrane traffic, but neurotransmitter release persists. Neuron *37*, 433-447.

Murthy, M., and Schwarz, T. L. (2004). The exocyst component Sec5 is required for membrane traffic and polarity in the *Drosophila* ovary. Development *131*, 377-388.

Muzzopappa, M., and Wappner, P. (2005). Multiple roles of the F-box protein Slimb in *Drosophila* egg chamber development. Development *132*, 2561-2571.

Myster, S. H., Wang, F., Cavallo, R., Christian, W., Bhotika, S., Anderson, C. T., and Peifer, M. (2004). Genetic and bioinformatic analysis of 41C and the 2R heterochromatin of Drosophila melanogaster: a window on the heterochromatin-euchromatin junction. Genetics *166*, 807-822.

Nagaso, H., Murata, T., Day, N., and Yokoyama, K. K. (2001). Simultaneous detection of RNA and protein by *in situ* hybridization and immunological staining. J Histochem Cytochem *49*, 1177-1182.

Nakamura, A., Amikura, R., Hanyu, K., and Kobayashi, S. (2001). Me31B silences translation of oocyte-localizing RNAs through the formation of cytoplasmic RNP complex during *Drosophila* oogenesis. Development *128*, 3233-3242.

Nakamura, A., Sato, K., and Hanyu-Nakamura, K. (2004). *Drosophila* Cup is an eIF4E binding protein that associates with Bruno and regulates *oskar* mRNA translation in oogenesis. Dev Cell *6*, 69-78.

Nelson, M. R., Leidal, A. M., and Smibert, C. A. (2004). *Drosophila* Cup is an eIF4E-binding protein that functions in Smaug-mediated translational repression. Embo J *23*, 150-159.

Neuman-Silberberg, F. S., and Schupbach, T. (1993). The *Drosophila* dorsoventral patterning gene gurken produces a dorsally localized RNA and encodes a TGF alpha-like protein. Cell *75*, 165-174.

Nilson, L. A., and Schupbach, T. (1998). Localized requirements for windbeutel and pipe reveal a dorsoventral prepattern within the follicular epithelium of the *Drosophila* ovary. Cell *93*, 253-262.

Olsen, P. H., and Ambros, V. (1999). The lin-4 regulatory RNA controls developmental timing in *Caenorhabditis elegans* by blocking LIN-14 protein synthesis after the initiation of translation. Dev Biol *216*, 671-680.

Ossipova, O., Dhawan, S., Sokol, S., and Green, J. B. (2005). Distinct PAR-1 proteins function in different branches of Wnt signaling during vertebrate development. Dev Cell *8*, 829-841.

Ostareck-Lederer, A., Ostareck, D. H., Cans, C., Neubauer, G., Bomsztyk, K., Superti-Furga, G., and Hentze, M. W. (2002). c-Src-mediated phosphorylation of hnRNP K drives translational activation of specifically silenced mRNAs. Mol Cell Biol *22*, 4535-4543.

Ostareck, D. H., Ostareck-Lederer, A., Shatsky, I. N., and Hentze, M. W. (2001). Lipoxygenase mRNA silencing in erythroid differentiation: The 3'UTR regulatory complex controls 60S ribosomal subunit joining. Cell *104*, 281-290.

Palacios, I. M., and St Johnston, D. (2002). Kinesin light chain-independent function of the Kinesin heavy chain in cytoplasmic streaming and posterior localisation in the *Drosophila* oocyte. Development *129*, 5473-5485.

Paliouras, M. (2005) Antimeros and Mile End, Two Bicaudal-C Interacting proteins, are required for *Drosophila* development, McGill University, Montreal, Quebec.

Parker, R., and Song, H. (2004). The enzymes and control of eukaryotic mRNA turnover. Nat Struct Mol Biol *11*, 121-127.

Paziewska, A., Wyrwicz, L. S., Bujnicki, J. M., Bomsztyk, K., and Ostrowski, J. (2004). Cooperative binding of the hnRNP K three KH domains to mRNA targets. FEBS Lett *577*, 134-140.

Penton, A., Wodarz, A., and Nusse, R. (2002). A mutational analysis of *dishevelled* in *Drosophila* defines novel domains in the dishevelled protein as well as novel suppressing alleles of axin. Genetics *161*, 747-762.

Peri, F., and Roth, S. (2000). Combined activities of Gurken and decapentaplegic specify dorsal chorion structures of the *Drosophila* egg. Development *127*, 841-850.

Puig, O., Caspary, F., Rigaut, G., Rutz, B., Bouveret, E., Bragado-Nilsson, E., Wilm, M., and Seraphin, B. (2001). The tandem affinity purification (TAP) method: a general procedure of protein complex purification. Methods *24*, 218-229.

Ramos, A., Hollingworth, D., Major, S. A., Adinolfi, S., Kelly, G., Muskett, F. W., and Pastore, A. (2002). Role of dimerization in KH/RNA complexes: the example of Nova KH3. Biochemistry *41*, 4193-4201.

Riechmann, V., Gutierrez, G. J., Filardo, P., Nebreda, A. R., and Ephrussi, A. (2002). Par-1 regulates stability of the posterior determinant Oskar by phosphorylation. Nat Cell Biol *4*, 337-342.

Rorth, P. (1998). Gal4 in the *Drosophila* female germline. Mech Dev *78*, 113-118.

Rosales-Nieves, A. E., Johndrow, J. E., Keller, L. C., Magie, C. R., Pinto-Santini, D. M., and Parkhurst, S. M. (2006). Coordination of microtubule and microfilament dynamics by *Drosophila* Rho1, Spire and Cappuccino. Nat Cell Biol *8*, 367-376.

Ross, A. F., Oleynikov, Y., Kislauskis, E. H., Taneja, K. L., and Singer, R. H. (1997). Characterization of a beta-actin mRNA zipcode-binding protein. Mol Cell Biol *17*, 2158-2165.

Roth, S., Neuman-Silberberg, F. S., Barcelo, G., and Schupbach, T. (1995). Cornichon and the EGF receptor signaling process are necessary for both anterior-posterior and dorsal-ventral pattern formation in *Drosophila*. Cell *81*, 967-978.

Rother, K. L. (1998) The KH domain protein *Bicaudal-C* regulates *oskar* expression during *Drosophila* mid-oogenesis, McGill University, Montreal, Quebec.

Saadi-Kheddouci, S., Berrebi, D., Romagnolo, B., Cluzeaud, F., Peuchmaur, M., Kahn, A., Vandewalle, A., and Perret, C. (2001). Early development of polycystic kidney disease in transgenic mice expressing an activated mutant of the beta-catenin gene. Oncogene *20*, 5972-5981.

Saffman, E. E., Styhler, S., Rother, K., Li, W., Richard, S., and Lasko, P. (1998). Premature translation of oskar in oocytes lacking the RNA-binding protein bicaudal-C. Mol Cell Biol *18*, 4855-4862.

Salles, F. J., Lieberfarb, M. E., Wreden, C., Gergen, J. P., and Strickland, S. (1994). Coordinate initiation of *Drosophila* development by regulated polyadenylation of maternal messenger RNAs. Science *266*, 1996-1999.

Sambrook, J., Russell, J., Maniatis., T. Molecular Cloning: A Laboratory Manual, 3 edn (Cold spring Harbor, New York: Cold Spring Harbor Laboratory Press).

Schaeffer, C., Bardoni, B., Mandel, J. L., Ehresmann, B., Ehresmann, C., and Moine, H. (2001). The fragile X mental retardation protein binds specifically to its mRNA via a purine quartet motif. Embo J *20*, 4803-4813.

Schultz, J., Ponting, C. P., Hofmann, K., and Bork, P. (1997). SAM as a protein interaction domain involved in developmental regulation. Protein Sci *6*, 249-253.

Schupbach, T., and Wieschaus, E. (1991). Female sterile mutations on the second chromosome of *Drosophila melanogaster*. II. Mutations blocking oogenesis or altering egg morphology. Genetics *129*, 1119-1136.

Searfoss, A., Dever, T. E., and Wickner, R. (2001). Linking the 3' poly(A) tail to the subunit joining step of translation initiation: relations of Pab1p, eukaryotic translation initiation factor 5b (Fun12p), and Ski2p-Slh1p. Mol Cell Biol *21*, 4900-4908.

Semotok, J. L., Cooperstock, R. L., Pinder, B. D., Vari, H. K., Lipshitz, H. D., and Smibert, C. A. (2005). Smaug recruits the CCR4/POP2/NOT deadenylase complex to trigger maternal transcript localization in the early *Drosophila* embryo. Curr Biol *15*, 284-294.

Sen, J., Goltz, J. S., Konsolaki, M., Schupbach, T., and Stein, D. (2000). Windbeutel is required for function and correct subcellular localization of the *Drosophila* patterning protein Pipe. Development *127*, 5541-5550.

Sen, J., Goltz, J. S., Stevens, L., and Stein, D. (1998). Spatially restricted expression of pipe in the *Drosophila* egg chamber defines embryonic dorsal-ventral polarity. Cell *95*, 471-481.

Serbus, L. R., Cha, B. J., Theurkauf, W. E., and Saxton, W. M. (2005). Dynein and the actin cytoskeleton control kinesin-driven cytoplasmic streaming in *Drosophila* oocytes. Development *132*, 3743-3752.

Shultz, L. D., Rajan, T. V., and Greiner, D. L. (1997). Severe defects in immunity and hematopoiesis caused by SHP-1 protein-tyrosine-phosphatase deficiency. Trends Biotechnol *15*, 302-307.

Simons, M., Gloy, J., Ganner, A., Bullerkotte, A., Bashkurov, M., Kronig, C., Schermer, B., Benzing, T., Cabello, O. A., Jenny, A., *et al.* (2005). Inversin, the gene product mutated in nephronophthisis type II, functions as a molecular switch between Wnt signaling pathways. Nat Genet *37*, 537-543.

Simons, M., and Walz, G. (2006). Polycystic kidney disease: cell division without a c(l)ue? Kidney Int *70*, 854-864.

Siomi, H., Matunis, M. J., Michael, W. M., and Dreyfuss, G. (1993). The pre-mRNA binding K protein contains a novel evolutionarily conserved motif. Nucleic Acids Res *21*, 1193-1198.

Smibert, C. A., Wilson, J. E., Kerr, K., and Macdonald, P. M. (1996). Smaug protein represses translation of unlocalized *nanos* mRNA in the *Drosophila* embryo. Genes Dev *10*, 2600-2609.

Sonoda, J., and Wharton, R. P. (1999). Recruitment of Nanos to *hunchback* mRNA by Pumilio. Genes Dev *13*, 2704-2712.

Spirin, A. (1986). Ribosome Structure and Protein Biosynthesis (Menlo Park, California: Benjamin / Cummings).

Spradling, A. C. (1986). P-element mediated transformation, In: *Drosophila*: A practical approach (Oxford: IRL Press).

St Johnston, D., Beuchle, D., and Nusslein-Volhard, C. (1991). *Staufen*, a gene required to localize maternal RNAs in the *Drosophila* egg. Cell *66*, 51-63.

Stathopoulos, A., and Levine, M. (2002). Dorsal gradient networks in the Drosophila embryo. Dev Biol *246*, 57-67.

Stein, E., Cerretti, D. P., and Daniel, T. O. (1996). Ligand activation of ELK receptor tyrosine kinase promotes its association with Grb10 and Grb2 in vascular endothelial cells. J Biol Chem *271*, 23588-23593.

Stocker, H., Radimerski, T., Schindelholz, B., Wittwer, F., Belawat, P., Daram, P., Breuer, S., Thomas, G., and Hafen, E. (2003). Rheb is an essential regulator of S6K in controlling cell growth in *Drosophila*. Nat Cell Biol *5*, 559-565.

Stoecklin, G., Mayo, T., and Anderson, P. (2006). ARE-mRNA degradation requires the 5'-3' decay pathway. EMBO Rep *7*, 72-77.

Strutt, D. (2003). Frizzled signalling and cell polarisation in *Drosophila* and vertebrates. Development *130*, 4501-4513.

Suh, N., Jedamzik, B., Eckmann, C. R., Wickens, M., and Kimble, J. (2006). The GLD-2 poly(A) polymerase activates gld-1 mRNA in the *Caenorhabditis elegans* germ line. Proc Natl Acad Sci U S A *103*, 15108-15112.

Sun, T. Q., Lu, B., Feng, J. J., Reinhard, C., Jan, Y. N., Fantl, W. J., and Williams, L. T. (2001). PAR-1 is a Dishevelled-associated kinase and a positive regulator of Wnt signalling. Nat Cell Biol *3*, 628-636.

Tadros, W., Houston, S. A., Bashirullah, A., Cooperstock, R. L., Semotok, J. L., Reed, B. H., and Lipshitz, H. D. (2003). Regulation of maternal transcript destabilization during egg activation in *Drosophila*. Genetics *164*, 989-1001.

Takahashi, M., Takahashi, F., Ui-Tei, K., Kojima, T., and Saigo, K. (2005). Requirements of genetic interactions between Src42A, armadillo and shotgun, a gene encoding E-cadherin, for normal development in *Drosophila*. Development *132*, 2547-2559.

Tan, L., Chang, J. S., Costa, A., and Schedl, P. (2001). An autoregulatory feedback loop directs the localized expression of the *Drosophila* CPEB protein Orb in the developing oocyte. Development *128*, 1159-1169.

Tarun, S. Z., Jr., and Sachs, A. B. (1996). Association of the yeast poly(A) tail binding protein with translation initiation factor eIF-4G. Embo J *15*, 7168-7177.

Temme, C., Zaessinger, S., Meyer, S., Simonelig, M., and Wahle, E. (2004). A complex containing the CCR4 and CAF1 proteins is involved in mRNA deadenylation in *Drosophila*. EMBO J *23*, 2862-2871.

Tenenbaum, S. A., Carson, C. C., Lager, P. J., and Keene, J. D. (2000). Identifying mRNA subsets in messenger ribonucleoprotein complexes by using cDNA arrays. Proc Natl Acad Sci U S A *97*, 14085-14090.

Theurkauf, W. E. (1994a). Microtubules and cytoplasm organization during *Drosophila* oogenesis. Dev Biol *165*, 352-360.

Theurkauf, W. E. (1994b). Premature microtubule-dependent cytoplasmic streaming in *cappuccino* and *spire* mutant oocytes. Science *265*, 2093-2096.

Thio, G. L., Ray, R. P., Barcelo, G., and Schupbach, T. (2000). Localization of *gurken* RNA in *Drosophila* oogenesis requires elements in the 5' and 3' regions of the transcript. Dev Biol *221*, 435-446.

Tirronen, M., Lahti, V. P., Heino, T. I., and Roos, C. (1995). Two *otu* transcripts are selectively localised in *Drosophila* oogenesis by a mechanism that requires a function of the otu protein. Mech Dev *52*, 65-75.

Tsuji, E., Tsuji, Y., Fujiwara, T., Ogata, S., Tsukamoto, K., and Saku, K. (2006). Splicing variant of Cdc42 interacting protein-4 disrupts beta-catenin-mediated cell-cell adhesion: expression and function in renal cell carcinoma. Biochem Biophys Res Commun *339*, 1083-1088.

Twombly, V., Blackman, R. K., Jin, H., Graff, J. M., Padgett, R. W., and Gelbart, W. M. (1996). The TGF-beta signaling pathway is essential for *Drosophila* oogenesis. Development *122*, 1555-1565.

Uchida, N., Hoshino, S., and Katada, T. (2004). Identification of a human cytoplasmic poly(A) nuclease complex stimulated by poly(A)-binding protein. J Biol Chem *279*, 1383-1391.

Ule, J., Jensen, K. B., Ruggiu, M., Mele, A., Ule, A., and Darnell, R. B. (2003). CLIP identifies Nova-regulated RNA networks in the brain. Science *302*, 1212-1215.

van der Geer, P., and Hunter, T. (1994). Phosphopeptide mapping and phosphoamino acid analysis by electrophoresis and chromatography on thin-layer cellulose plates. Electrophoresis *15*, 544-554.

Van Doren, M., Williamson, A. L., and Lehmann, R. (1998). Regulation of zygotic gene expression in *Drosophila* primordial germ cells. Curr Biol *8*, 243-246.

van Eeden, F. J., Palacios, I. M., Petronczki, M., Weston, M. J., and St Johnston, D. (2001). Barentsz is essential for the posterior localization of *oskar* mRNA and colocalizes with it to the posterior pole. J Cell Biol *154*, 511-523.

van Hoof, A., and Parker, R. (2002). Messenger RNA degradation: beginning at the end. Curr Biol *12*, R285-287.

Voas, M. G., and Rebay, I. (2004). Signal integration during development: insights from the *Drosophila* eye. Dev Dyn *229*, 162-175.

Waggoner, S. A., and Liebhaber, S. A. (2003). Identification of mRNAs associated with alphaCP2-containing RNP complexes. Mol Cell Biol *23*, 7055-7067.

Wang, L., Eckmann, C. R., Kadyk, L. C., Wickens, M., and Kimble, J. (2002). A regulatory cytoplasmic poly(A) polymerase in *Caenorhabditis elegans*. Nature *419*, 312-316.

Wasserman, J. D., and Freeman, M. (1998). An autoregulatory cascade of EGF receptor signaling patterns the *Drosophila* egg. Cell *95*, 355-364.

Webster, P. J., Liang, L., Berg, C. A., Lasko, P., and Macdonald, P. M. (1997). Translational repressor bruno plays multiple roles in development and is widely conserved. Genes Dev *11*, 2510-2521.

Wei, C. C., Balasta, M. L., Ren, J., and Goss, D. J. (1998). Wheat germ poly(A) binding protein enhances the binding affinity of eukaryotic initiation factor 4F and (iso)4F for cap analogues. Biochemistry *37*, 1910-1916.

Wessely, O., and De Robertis, E. M. (2000). The *Xenopus* homologue of Bicaudal-C is a localized maternal mRNA that can induce endoderm formation. Development *127*, 2053-2062.

Wessely, O., Tran, U., Zakin, L., and De Robertis, E. M. (2001). Identification and expression of the mammalian homologue of Bicaudal-C. Mech Dev *101*, 267-270.

Weston, A., and Sommerville, J. (2006). Xp54 and related (DDX6-like) RNA helicases: roles in messenger RNP assembly, translation regulation and RNA degradation. Nucleic Acids Res *34*, 3082-3094.

Wheatley, S., Kulkarni, S., and Karess, R. (1995). *Drosophila* nonmuscle myosin II is required for rapid cytoplasmic transport during oogenesis and for axial nuclear migration in early embryos. Development *121*, 1937-1946.

Wilhelm, J. E., Buszczak, M., and Sayles, S. (2005). Efficient protein trafficking requires trailer hitch, a component of a ribonucleoprotein complex localized to the ER in Drosophila. Dev Cell *9*, 675-685.

Wilhelm, J. E., Hilton, M., Amos, Q., and Henzel, W. J. (2003). Cup is an eIF4E binding protein required for both the translational repression of oskar and the recruitment of Barentsz. J Cell Biol *163*, 1197-1204.

Wilhelm, J. E., and Smibert, C. A. (2005). Mechanisms of translational regulation in *Drosophila*. Biol Cell *97*, 235-252.

Winter, C. G., Wang, B., Ballew, A., Royou, A., Karess, R., Axelrod, J. D., and Luo, L. (2001). *Drosophila* Rho-associated kinase (Drok) links Frizzled-mediated planar cell polarity signaling to the actin cytoskeleton. Cell *105*, 81-91.

Wreden, C., Verrotti, A. C., Schisa, J. A., Lieberfarb, M. E., and Strickland, S. (1997). Nanos and pumilio establish embryonic polarity in *Drosophila* by promoting posterior deadenylation of *hunchback* mRNA. Development *124*, 3015-3023.

Wu, L., Wells, D., Tay, J., Mendis, D., Abbott, M. A., Barnitt, A., Quinlan, E., Heynen, A., Fallon, J. R., and Richter, J. D. (1998). CPEB-mediated cytoplasmic polyadenylation and the regulation of experience-dependent translation of alpha-CaMKII mRNA at synapses. Neuron *21*, 1129-1139.

Yang, W. H., Yu, J. H., Gulick, T., Bloch, K. D., and Bloch, D. B. (2006). RNA-associated protein 55 (RAP55) localizes to mRNA processing bodies and stress granules. Rna *12*, 547-554.

Yano, T., Lopez de Quinto, S., Matsui, Y., Shevchenko, A., and Ephrussi, A. (2004). Hrp48, a *Drosophila* hnRNPA/B homolog, binds and regulates translation of *oskar* mRNA. Dev Cell *6*, 637-648.

Zaessinger, S., Busseau, I., and Simonelig, M. (2006). Oskar allows *nanos* mRNA translation in *Drosophila* embryos by preventing its deadenylation by Smaug/CCR4. Development *133*, 4573-4583.

Zhang, B., Gallegos, M., Puoti, A., Durkin, E., Fields, S., Kimble, J., and Wickens, M. P. (1997). A conserved RNA-binding protein that regulates sexual fates in the *C. elegans* hermaphrodite germ line. Nature *390*, 477-484.

Zhang, Y. Q., Bailey, A. M., Matthies, H. J., Renden, R. B., Smith, M. A., Speese, S. D., Rubin, G. M., and Broadie, K. (2001). *Drosophila* fragile X-related gene regulates the MAP1B homolog Futsch to control synaptic structure and function. Cell *107*, 591-603.

Zhang, Y. Q., Matthies, H. J., Mancuso, J., Andrews, H. K., Woodruff, E., 3rd, Friedman, D., and Broadie, K. (2004). The *Drosophila* fragile X-related gene regulates axoneme differentiation during spermatogenesis. Dev Biol *270*, 290-307.

Zhao, D., Woolner, S., and Bownes, M. (2000). The Mirror transcription factor links signalling pathways in *Drosophila* oogenesis. Dev Genes Evol *210*, 449-457.

Zhong, S., Li, C., and Wong, W. H. (2003). ChipInfo: Software for extracting gene annotation and gene ontology information for microarray analysis. Nucleic Acids Res *31*, 3483-3486.

Appendix